

EXHIBIT G



Final Report

Anderson Law Offices LLC
Mr. Benjamin H. Anderson

Date: 05/20/2014

Released by:
Dr. Howard Jordi
Founder
Jordi Labs LLC

Report Number: J8689

Anderson Law Offices LLC - Confidential



WEB: www.jordilabs.com

EMAIL: info@jordilabs.com



May 20, 2014

Benjamin H. Anderson
Anderson Law Offices LLC

P: 216.589.0256
E: ben@andersonlawoffices.net

Dear Mr. Anderson,

Please find enclosed the test results for your samples.

I. Background and Qualifications

I, Dr. Howard Jordi received my undergraduate degree in Chemistry from Northern Illinois University in 1967 and my Ph.D. in biochemistry from the same university in 1974.

From 1973-1977, I served in the United States Army Institute of Dental Research where I characterized various drugs contained in biodegradable copolymers of polylactic and polyglycolic acid. I then worked at Water's Associates from 1977-1980. Water's is a world leader in the sale of a wide range of analytical technologies including liquid chromatography, mass spectrometry, rheometry and microcalorimetry. At Waters, I progressed from a Biological Applications chemist to the laboratory manager for the life science division and finally to the Chemicals Applications Manager for the Chromatography Supplies Division.

I am the founder of Jordi Labs and served as president and CEO from 1980-2008. Jordi Labs was founded to provide high quality analytical services to the polymer and plastics industries. In my role as President and CEO, I developed hundreds of analytical methods and have analyzed all of the major polymer systems (polypropylene, polyethylene, urethanes, styrenics, etc.). The first services offered by Jordi Labs included high temperature GPC for polyolefins (polyethylene and polypropylene) and polymer additives identification and quantification (antioxidants, slip agents, etc.) In this capacity, I have been analyzing polypropylenes for over 25 years. I have reformulated numerous polypropylene samples including identifying and quantifying their additive packages and have been aiding clients for over 25 years in the identification of the root cause of failure in polypropylene systems. I have served extensively as a consultant on polymer related failures for a wide range of industrial clients and have over 40 years of practical experience in the analytical chemistry of polymers. I have in-depth knowledge of a wide range of analytical techniques including FTIR, NMR, DSC, TGA, HPLC, SEM, GPC, DMS, LCMS, GCMS, H-GCMS and PYMS

among others. Jordi Labs currently offers over 20 different analytical techniques. I have developed a range of polymeric chromatography columns for polymer molecular weight determination, some of which are patented.

(Attached as Exhibit "A" to this report is a true and accurate copy of my current curriculum vitae.)

II. Summary of Opinions

A series of fiber mesh control and explant samples were received by Jordi Labs. Upon handling, it was observed that the explant samples showed decreased elasticity as compared to the control fiber mesh samples. Analysis by Scanning Electron microscopy showed no cracking for a series of control samples even when subjected to treatment in formalin at elevated temperature. In contrast, severe cracking was observed for 18 of 24 explant samples. Four more of the remaining samples showed modest cracking and 2 showed no signs of cracking.

The cracking in the explant samples was observed to propagate in a direction perpendicular to the fiber draw direction and was noted to be primarily on the fiber surface. When significantly advanced, this resulted in flaking off of shards or platelets of polypropylene from the fiber. The chemical identity of these shards was verified by FTIR-microscopy and by SEM-EDX. Optical microscopy work conducted during the FTIR analysis demonstrated that the application of gentle force could be used to remove cracked surface material. The elemental composition of the cracked surface regions was found to show increased intensity for oxygen, phosphorous, sulfur and sodium as compared to the non-cracked regions. FTIR microscopy analysis of the shards showed a carbonyl band at $\sim 1760\text{ cm}^{-1}$ and 1044 cm^{-1} which is consistent with surface oxidation of the polymer (degradation). Analysis of the explanted fiber mesh by GPC-HT indicated that large scale molecular weight degradation had not occurred in the samples. The large scale surface cracking observed would suggest that we would have expected to see molecular weight degradation. The fact that we did not observe changes in the molecular weight is consistent with the observed surface cracking. The majority of the observed cracking was on the surface of the fibers and thus when the entire fiber was dissolved to run the molecular weight analysis, the concentration of degraded material was greatly reduced in relation to the non-degraded internal fiber material. GPC is a bulk technique which analyzes all of the fiber and not just the cracked surface material. As a result no overall changes in the molecular weight were observed. However we did observe marked surface cracking and degradation of many of the surface regions of the explant materials. Differential scanning calorimetry analyses of the explant fiber mesh and control samples showed a general trend of decreasing crystallinity for the cracked samples demonstrating a larger portion of amorphous material in the cracked samples relative to the controls. As such, an increasing amount of amorphous material is consistent with degradation leading to loss of mechanical strength and stress cracking.

Therefore, based on my review of the scientific literature, my review of Ethicon's internal documents, my knowledge, training and experience as a polymer scientist, and the review of the data discussed herein, it is my opinion, to a reasonable degree of scientific certainty that

the Prolene mesh in TVT and TVT-O ("TVT Products") degrades in the human body due to oxidation of the polypropylene. This oxidation process results from the body's normal reaction to a foreign body (polypropylene mesh) in the tissues, causing a chemical reaction (as part of the inflammatory process) similar to that of known oxidizers acting upon the polypropylene like hypochlorous acid, peroxides and superoxides, to name a few.

Characterization of the additives package in the samples was conducted using pyrolysis mass spectroscopy and quadrupole time of flight liquid chromatography mass spectroscopy. Two antioxidants were identified including Santonox-R and Dilauryl thiodipropionate in addition to a series of ethoxylated spin finishes. A relative quantitation was performed to determine the amount in the control samples as compared to the explant samples by QTOF-LCMS. It was found that the explant samples showed significantly less signal for the antioxidant as compared to the control lots (Santonox-R, 3.0% of control lot value and Dilauryl thiodipropionate, 1.8% of the control lot value).

Therefore, it is my opinion to a reasonable degree of scientific certainty that antioxidants that are claimed by Ethicon to be added to their Prolene mesh products leach away from the surface of the raw polypropylene fiber into the body, leaving the polypropylene unprotected from the inflammatory mediators and chemical oxidizers, increasing the risk of oxidation and degradation in the tissues.

III. List of Abbreviations

List of Abbreviations	
DSC	Differential Scanning Calorimetry
DMS	Desorption Mass Spectroscopy
FTIR	Fourier Transform Infrared Spectroscopy
FTIR-Micro	Fourier Transform Infrared Spectroscopy Microscopy
GCMS	Gas Chromatography Mass Spectroscopy
GPC	Gel Permeation Chromatography
GPC-HT	High Temperature Gel Permeation Chromatography
H-GCMS	Headspace Gas Chromatography Mass Spectroscopy
HPLC	High Performance Liquid Chromatography
LCMS	Liquid Chromatography Mass Spectroscopy
NMR	Nuclear Magnetic Resonance
OM	Optical Microscopy
PYMS	Pyrolysis Mass Spectroscopy
QTOF-LCMS	Quadrupole Time of Flight Liquid Chromatography Mass Spectroscopy
SEM	Scanning Electron Microscopy
SEM-EDX	Scanning Electron Microscopy - Energy Dispersive X-ray Spectroscopy
TEM	Transmission Electron Microscopy
TGA	Thermogravimetric Analysis
~	Approximately

IV. Sample Identification

Control Samples - TVT and TVT-O*

Jordi Number/Lot Number

1. 13158 Lot 3436364
2. 13159 Lot 3405405
3. 13160 Lot 3405460
4. 13161 Lot 3422128
5. 13162 Lot 3398135
6. 13163 Lot 3405474

*According to Ethicon documents, the mesh material in the TVT & TVT-O products is Prolene Old Construction 6 mil mesh.^{1,2,3} Further, these documents state that TVT was first sold in 1998 in the United States.

Explant Samples

Jordi Number/Patient Name

1. 13400 Oiler, Jennell
2. 13401 Simpson, Cynthia Ann
3. 13402 Valentino, Gloria
4. 13403 Herman, Sheryl
5. 13404 Phillips, Amy Nicole
6. 13405 Smith, Eva
7. 13406 Wilson, Virginia
8. 13407 Dowden, Ann Marie
9. 13408 Johnston Williams, Shari
10. 13409 Sharp, Jaqueline D.
11. 13410 Ioannov, Stella
12. 13411 McNamara, Eve
13. 13412 Thomas, Theresa
14. 13413 Pankey, Tina
15. 13414 Keller, Linda
16. 13415 Harden, Terri L
17. 13416 Phyllis, Long
18. 13417 Garcia, Alma L
19. 13418 Bonee, Dorothy Sara
20. 13419 Robinson, Tasha R.
21. 13420 Gomez, Flor
22. 13421 Shaw, Ava
23. 13674 Lewis, Carolyn
24. 13675 Batiste, Linda

¹ ETH.MESH.02219202 - Material Specification for TVT Prolene Polypropylene Mesh Roll Stock

² ETH.MESH.09479067 - TVT PROLENE Polypropylene Mesh Roll Stock Appendix II Digital Photograph of 050166

³ ETH.MESH.01816988 - Mesh Timeline

V. Degradation

Degradation Pathways of Polypropylene

Most polymers undergo degradation when exposed to appropriate conditions. Polymer degradation may refer to change in the polymeric properties such as structural integrity, color, shape or tensile strength, to name a few. The degradation process involves several physical and/or chemical processes which are accompanied by structural changes in the polymer leading to significant deterioration of the quality of the polymer.^{4,5,6} There are several different types of degradation mechanisms:

1. Photochemical degradation: Exposure to UV and/or visible light
2. High-energy radiation induced degradation: Exposure to X-rays, γ -rays, etc.
3. Mechanical degradation: Stress forces, abrasive forces during processing or application
4. Thermal degradation: Exposure to heat
5. Chemical degradation: Hydrolysis or exposure to acids, alkalis, salts, reactive gases, etc.
6. Oxidation: Reaction with oxygen, ozone, peroxides, etc.
7. Biodegradation: Interaction with enzymes and microbes
8. Combination of two or more of the above mechanisms

The physiological environment in the human body does not involve many of these conditions such as exposure to light. For a non-hydrolyzable hydrophobic polymer such as polypropylene, oxidation and biodegradation pathways are the most pertinent and will be discussed in detail below.

Oxidative degradation: Polypropylene is highly susceptible to attack by oxidants such as atmospheric oxygen, ozone or peroxides.^{7,8,9,10} Oxidative degradation can alter its molecular weight and polydispersity index (PDI) through cleavage of the long polypropylene chains into smaller fragments. The process of oxidative degradation of polypropylene and the steps involved are described in Scheme 1.^{11,12}

⁴ Cornelia Vasile, Degradation and decomposition, in *Handbook of Polyolefin*, eds. Cornelia Vasile and Raymond B. Seymour (Marcel Dekker Inc, New York, USA) 1993, 479-552.

⁵ A. Ravve, Degradation of Polymers, in *Principles of Polymer Chemistry 2nd Ed.*, (Kluwer Academic/Plenum Publishers, New York, USA) 2000, 581-616.

⁶ Devesh Tripathi, *Practical Guide to Polypropylene*, (Rapra Technology Ltd. Shropshire, UK) 2002.

⁷ Cornelia Vasile, Degradation and decomposition, in *Handbook of Polyolefin*, eds. Cornelia Vasile and Raymond B. Seymour (Marcel Dekker Inc, New York, USA) 1993, 479-552.

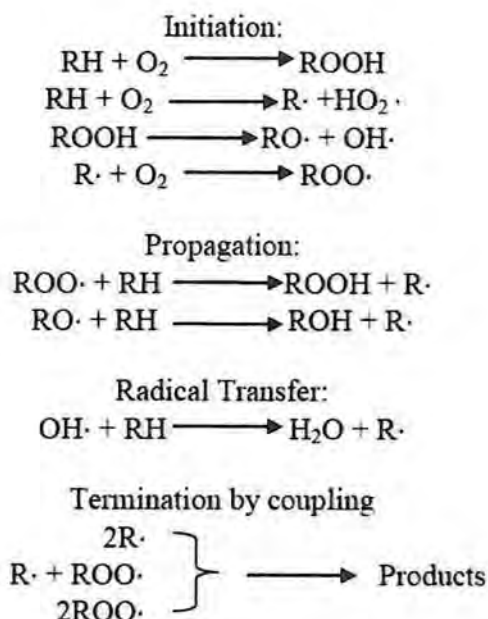
⁸ A. Ravve, Degradation of Polymers, in *Principles of Polymer Chemistry 2nd Ed.*, (Kluwer Academic/Plenum Publishers, New York, USA) 2000, 581-616.

⁹ Denis Bertin, Marie Leblanc, Sylvain R. A. Marque and Didier Siri, *Polymer Degradation and Stability* 95 (2010) 782-791.

¹⁰ R. A. Silva, P. A. Silva and M. E. Carvalho, *Materials Science Forum* 539-543 (2007) 573-576.

¹¹ Cornelia Vasile, Degradation and decomposition, in *Handbook of Polyolefin*, eds. Cornelia Vasile and Raymond B. Seymour (Marcel Dekker Inc, New York, USA) 1993, 479-552.

¹² Timothy C Liebert, Richard P. Chartoff, Stanley L. Cosgrove and Roberts S. McCuskey *Journal of Biomedical Materials Research* 10 (1976) 939-951.



Scheme 1. Mechanism of Oxidative Degradation of Polypropylene (RH = polypropylene)

As a result, polypropylene is an incompatible material under oxidative conditions.^{13,14} While oxidants such as ozone are not present in a biological system, the presence of oxygen (O₂) and its other forms such as superoxides, peroxides and free radicals makes the human body a powerful oxidizing environment to polymers and oxidation occurs via similar processes.¹⁵

Biodegradation: There is ample evidence in the literature that indicates that polypropylene undergoes degradation in the biological system.^{16,17,18,19} The physiological environment of the polymer can critically control its function and performance. Biodegradation is the ability of the microorganisms, fungi and bacteria to influence degradation through physical, chemical or enzymatic action.²⁰ The mechanism of biodegradation of a polymer involves attachment of a microorganism to the surface of a polymer, growth of the microorganism utilizing the polymer as the carbon source, primary degradation of the polymer and ultimate degradation.²¹

¹³ R. A. Silva, P. A. Silva and M. E. Carvalho, *Materials Science Forum* 539-543 (2007) 573-576.

¹⁴ Kurt Schwarzenbach, Antioxidants, in *Plastics Additives 2nd Ed.*, R. Gächter and H. Müller (Hanser Publishers, Munich Germany) 1987, 18.

¹⁵ Timothy C Liebert, Richard P. Chartoff, Stanley L. Cosgrove and Roberts S. McCuskey *Journal of Biomedical Materials Research* 10 (1976) 939-951.

¹⁶ Timothy C Liebert, Richard P. Chartoff, Stanley L. Cosgrove and Roberts S. McCuskey *Journal of Biomedical Materials Research* 10 (1976) 939-951.

¹⁷ Donald R. Ostegard, *International Urogynecology Journal* 22 (2011) 771-774.

¹⁸ D. F. Williams, *Journal of Materials Science* 17 (1982) 1233-1246 and references therein.

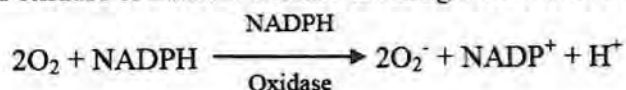
¹⁹ C. D. Klink, K. Junge, M. Binnebösel, H. P. Alizai, J. Otto, U. P. Neumann and U. Klinge, *Journal of Investigative Surgery* 24 (2011) 292-299.

²⁰ Cornelia Vasile, Degradation and decomposition, in *Handbook of Polyolefin*, eds. Cornelia Vasile and Raymond B. Seymour (Marcel Dekker Inc, New York, USA) 1993, 479-552.

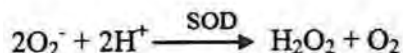
²¹ J. Arutchevi, M. Sudhakar, Ambika Arkatkar, Mukesh Doble, Sumit Bhaduri and Parasu Veera Uppara, *Indian Journal of Biotechnology* 7 (2008) 9-22.

Upon implantation of polypropylene in the body, white blood cells begin to produce oxidants such as hydrogen peroxide and hypochlorous acid that continue the oxidation induced during sterilization or manufacturing. Oxidation of polypropylene produces more free radicals which causes depolymerization, oxidative degradation, hydrolysis and stress cracking. Enzymes present in the body are able to catalyze these reactions at body temperature. Breakdown of the polymeric chains can then cause the surface of a polymeric implant to crack.²²

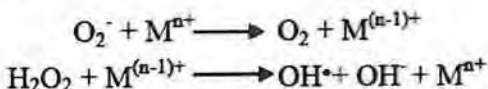
Macrophages in the body produce large amounts of both superoxide (O_2^-) and hydrogen peroxide (H_2O_2) when faced with infectious agents or other foreign materials.²³ This process known as the oxidative burst is the one electron reduction of oxygen (O_2) to O_2^- and is catalyzed by NADPH oxidase or NADH oxidase utilizing NADPH or NADH as substrates.



Superoxide radicals react to produce hydrogen peroxide with the reaction being catalyzed by superoxide dismutase (SOD).



While both superoxide and hydrogen peroxide can react with polypropylene, the presence of metal ions such as Fe(II) and Cu(I) leads to the generation of hydroxyl radicals which are even more reactive towards polypropylene.



Net Reaction:



The overall net reaction shown above is usually referred to as metal catalyzed Haber-Weiss reaction. Most of the hydroxyl radicals generated in vivo are formed from the metal ion dependent breakdown of hydrogen peroxide.

Mechanical degradation: Mechanical degradation or stress-induced cracking of polymers is a degradation pathway which involves irreversible breakdown (cracking, fracture, deformation etc.) of the polymeric material under mechanical stress.^{24,25} Environmental stress cracking (ESC) is cracking of a polymer due to the combined action of a stress and a fluid. It is associated with the phenomenon of crazing and solvent plasticization of the

²² Gina Sternschuss, Donald R. Ostergard and Hiren Patel, *The Journal of Urology* 188 (2012) 27-32.

²³ S. A. M. Ali, S. -P. Zhong, P. J. Doherty and D. F. Williams, *Biomaterials* 14 (1993) 648-656.

²⁴ Cornelia Vasile, Degradation and decomposition, in *Handbook of Polyolefin*, eds. Cornelia Vasile and Raymond B. Seymour (Marcel Dekker Inc, New York, USA) 1993, 479-552.

²⁵ Tibor Kelen, *Mechanical Deformation, in Polymer Degradation*, (Van Nostrand Reinhold Company, New York, USA) 1983, 157-172.

polymer.²⁶ As mentioned earlier, the environment of a polymer can have a significant effect on the polymer. The polymer can absorb the fluid surrounding it and the polymer swells causing compressive stress at the surface. This initiates a phenomenon known as crazing which is the mechanical separation of the entangled chains of the polymer. Solvent induced crazes grow more quickly and to greater dimensions than those in inert environments. The crazes that are under the influence of stress act as initiation sites for cracks. Other factors influencing cracking in crazed polymers include time, temperature, molecular weight of the polymer, its structure and thermal history. The stressed chains become mechanically excited. Deexcitation of these chains occurs via various phenomena such as conformational changes, or bond scission/breakage causing the polymer to crack. The ultimate response is a fractured polymeric material. In the conclusion of a 2010 study where polypropylene explants from the human body were characterized, Clave et al. state that "The diffusion of organic molecules into the polymer (especially esterified fatty acids or cholesterol) may be a cause of the polymer structure degradation."²⁷ Molecules like fatty acids and cholesterol are hydrophobic and have similar chemistries and would be expected to be compatible with polypropylene chains. These molecules would easily diffuse into the amorphous regions of polypropylene polymers initiating the formation of crazing.

There is over 45 years of literature and studies related to degradation.
28,29,30,31,32,33,34,35,36,37,38,39,40

²⁶ R. Chatten, D. Vesely, "Environmental stress cracking of polypropylene" in *Polypropylene An A-Z Reference Polymer Science and Technology Series 2* Ed. J. Karger-Kocsis (1999) 206-214. (ISBN: 978-94-010-5899-5)

²⁷ Arnaud Clave, Hanna Yah, Jean-Claude Hammou, Suzelei Montanari, Pierre Gounon and Henri Clave, "Polypropylene as a reinforcement in pelvic surgery is not inert: comparative analysis of 100 explants" *International Urogynecology Journal and Pelvic Floor Dysfunction* 21 (2010) 261-270.

²⁸ H.J. Oswald, E. Tun, The Deterioration of Polypropylene By Oxidative Degradation, *Polymer Engineering and Science*, 5 (1965) 152-158.

²⁹ Timothy C. Liebert, Richard P. Chertoff, Stanley L. Cosgrove, Robert S. McCuskey, Subcutaneous Implants of Polypropylene Filaments, *J. Biomed. Mater. Res.*, 10 (1976) 939-951.

³⁰ Williams, Review Biodegradation of surgical polymers, *Journal of Materials Science*, 17 (1982) 1233-1246

³¹ Williams and Sheng P. Zhong, Are Free Radicals Involved in Biodegradation of Implanted Polymers?, *Adv. Matter*, 3 (1991) 623-626.

³² S.A.M. Ali, S.-P. Zhong, P.J. Doherty and D.F. Williams, Mechanisms of polymer degradation in implantable devices, *Biomaterials*, 14 (1993) 648-656

³³ Celine Mary, Yves Marois, Martin W. King, Gaetan Laroche, Yvan Douville, Louisette Martin, Robert Guidoin, Comparison of the In Vivo Behaviour of Polyvinylidene Fluoride and Polypropylene Sutures Used in Vascular Surgery, *ASAIO Journal*, 44 (1998) 199-206.

³⁴ Costello, S. L. Bachman, B. J. Ramshaw and S. A. Grant, "Materials characterization of explanted polypropylene hernia meshes" *Journal of Biomedical Materials Research Part B: Applied Biomaterials* 83B (2007) 44-49.

³⁵ Costello, C.R., Bachman S.L., Grant S.A. and others, "Characterization of Heavyweight and Lightweight Polypropylene Prosthetic Mesh Explants From a Single Patient" *Surgical Innovation* 14 (2007) 168-176.

³⁶ Matthew J. Cozad, David A. Grant, Sharon L. Bachman, Daniel N. Grant, Bruce J. Ramshaw, Sheila A. Grant, Materials characterization of explanted polypropylene, polyethylene terephthalate, and expanded polytetrafluoroethylene composites: Spectral and thermal analysis, *J Biomed Mater Res B Appl Biomater*, 94 (2010) 455-462.

³⁷ Arnaud Clave, Hanna Yah, Jean-Claude Hammou, Suzelei Montanari, Pierre Gounon and Henri Clave, "Polypropylene as a reinforcement in pelvic surgery is not inert: comparative analysis of 100 explants" *International Urogynecology Journal and Pelvic Floor Dysfunction* 21 (2010) 261-270.

³⁸ Donald Ostergard, Degradation, infection and heat effects on polypropylene mesh for pelvic implantation: what was known and when it was known, *Int Urogynecol J*, 22 (2011) 771-774.

³⁹ C.D. Klink, K. Junge, M. Binnebosel, H. P. Alizai, J. Otto, U. P. Neumann, U. Klinge, Comparison of Long-Term Biocompatibility of PVDF and PP Meshes, *Journal of Investigative Surgery*, 24 (2011) 292-299.

⁴⁰ Gina Sternschuss, Donald R. Ostergard, Hiren Patel, Post-Implantation Alterations of Polypropylene in the Human, *The Journal of Urology*, 188 (2012) 27-32.

VI. Deposition of Daniel F. Burkley, MS

I have studied the deposition of Mr. Daniel F. Burkley, an Analytical Chemist employed by Ethicon/Johnson & Johnson and we feel qualified to express my opinion to a reasonable degree of scientific certainty on certain aspects of his deposition. Specifically, we would like to comment on the following topics:

a. GPC analysis of the 7 year dog study and comparison with Jordi GPC analysis

The Jordi GPC analysis of both control and explant samples tends to confirm "The 7 Year Dog Study" performed at Ethicon referred to as Exhibit T-282 in his deposition of May 22, 2013, in that little to no macro Mw degradation was noted. This might be due to the solubilization of the total sample when perhaps only the surface polymer (as shown by SEM images) was in fact degraded. This behavior might indicate that degradation is only a surface and not a bulk phenomenon. This would tend to be expected as macrophages attack the exposed surface of the polypropylene material.⁴¹ Therefore, even if no gross Mw degradation was observed in either study, it cannot be stated to a reasonable degree of scientific certainty that the polypropylene suture did not degrade. In other words, the dissolution of non-cracked polypropylene during the GPC analysis would render the cracked polypropylene portion insignificant in terms of relative quantities. Based on my review of the scientific literature, my review of Ethicon's internal documents, including the data from the 7 year dog study, my knowledge, training and experience as polymer scientists, and the review of the data discussed herein, it is my opinion to a reasonable degree of scientific certainty that the cracked surface of Ethicon's Prolene suture in Burkley's 7-year dog study was indeed due to degradation and oxidation and that the conclusion by Ethicon that "degradation in PROLENE is still increasing and PVDF, even though a few cracks were found, is still by far the most surface resistant in-house made suture in terms of cracking" should have caused Ethicon to do further explant degradation studies. This is especially true given that the mesh material made of Prolene was intended to be permanently implanted in a woman's pelvic tissue. Of note, Ethicon's SEM images of the dog suture showed similar degradation and cracks as my own images. [See image below]⁴²

⁴¹ S. A. M. Ali, S. -P. Zhong, P. J. Doherty and D. F. Williams, *Biomaterials* 14 (1993) 648-656.

⁴² ETH.MESH.09557798 – Seven Year Dog Study images

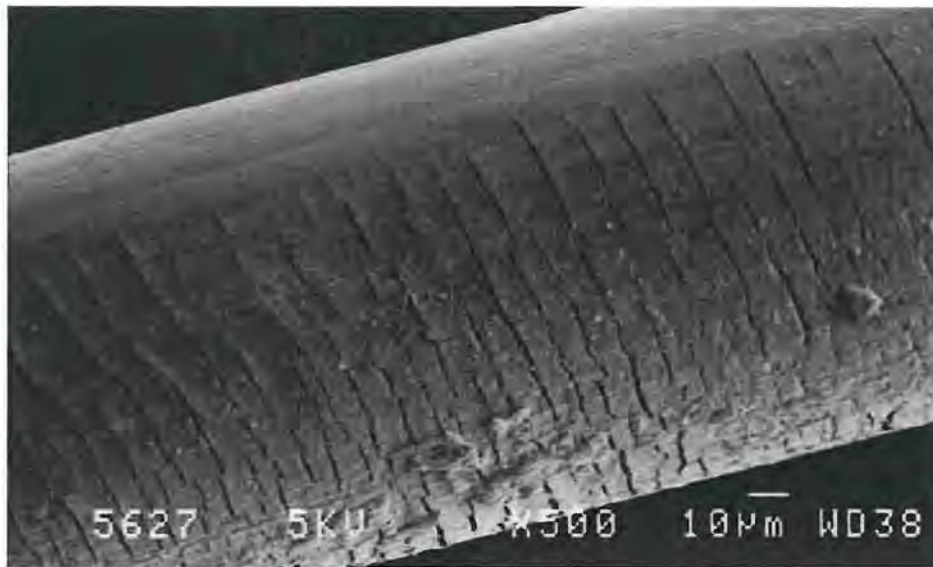


Image 1: SEM image of suture explanted from a dog by Ethicon

b. IR analysis

We would like to comment on the presence of a carbonyl band at 1650 cm^{-1} in the infrared spectrum of explanted material in the Ethicon 7 year dog study as described by Mr. Burkley on pages 300-301 of his deposition. The 1650 cm^{-1} and 1540 cm^{-1} bands are typically indicative of what are known as the amide-I and amide-II bands respectively of the polyamides.⁴³ Since proteins are polyamides, they should contain both bands. This is clearly shown in Figure 87 on page 76 of this report which is an overlay of infrared spectra of explant sample 13413, albumin (a protein) and control fiber lot 3422128. The bottom line would seem to be the lack of major carbonyl oxidation bands, which would be expected to be present in the $1650\text{-}1760\text{ cm}^{-1}$ range in the 7-year dog study explants if the polypropylene had undergone major oxidation. Figure 84 of this report clearly shows the presence of a carbonyl band at 1761 cm^{-1} in the explanted mesh sample 13413. Thus, it would appear that the explanted suture material from the 7 year dog study did not show significant oxidation while the explanted mesh samples in my current work did show significant oxidation. This is most probably due to the different environments in which the sutures were placed relative to where the mesh was placed (i.e., a more aseptic environment in the dog study versus a relatively more septic environment in which the explanted mesh samples were placed). Numerous studies in the scientific literature discuss the highly-septic, bacteria laden environment of the pelvis and specifically, the vagina.^{44,45,46,47,48,49}

⁴³ *The Infrared Spectra Atlas of Monomers and Polymers*, Sadtler Research Laboratories, Philadelphia, PA 1983, page 471.

⁴⁴ Shah, K., Nikolavsky D., Flynn, B. "Bacteriological Analysis of Explanted Transvaginal Meshes" Infections/Inflammation of the Genitourinary Tract: Kidney & Bladder (II): 2013. http://www.nua2013.org/abstracts/archive/abstracts_MP42.cfm

⁴⁵ Boulanger L, Boukerrou M, Rubod C, Collinet P, Fruchard A, Courcol RJ, Cosson M. Bacteriological analysis of meshes removed for complications after surgical management of urinary incontinence or pelvic organ prolapse. *Int Urogynecol J Pelvic Floor Dysfunct*. 2008 Jun;19(6):827-31.

⁴⁶ A. Vollebregt, A. Troelstra, and C. H. van der Vaart, "Bacterial colonisation of collagen-coated polypropylene vaginal mesh: are additional intraoperative sterility procedures useful?," *International urogynecology journal and pelvic floor dysfunction*, vol. 20, no. 11, pp. 1345-51, Nov. 2009

⁴⁷ R. de Tayrac and V. Letouzey, "Basic science and clinical aspects of mesh infection in pelvic floor reconstructive surgery.," *International urogynecology journal*, vol. 22, no. 7, pp. 775-80, Jul. 2011

It is probably also due to a higher surface area of the mesh samples relative to the suture samples. The higher surface area in the mesh implant leads to greater foreign body reaction, greater inflammatory response and thus, higher amounts of inflammatory mediators attacking the surface of the fibers leading to greater amounts of degradation and oxidation. These are the most scientifically probable explanations for the discrepancy between carbonyl bands of the suture from the healthy dog heart and the explanted mesh from a woman's vaginal or pelvic tissues.

c. Cracking of polypropylene fibers as observed on SEM

Mr. Burkley mentioned two main reasons for cracking of SEM fibers: desiccation and abrasion during sample preparation. Jordi SEM Analysis avoided this by using variable pressure mode SEM. This type of SEM allows for analysis of the specimen at an elevated pressure as compared to a standard SEM instrument. This, in turn reduces the vacuum requirements, thus minimizing the desiccation of the samples. Additionally, the samples did not need to be sputter coated because of the utilization of variable pressure mode SEM. Samples were prepared for variable pressure mode SEM analysis by simply cutting a portion of the sample and removing enough tissue to expose the fiber surface. This was done carefully to avoid direct contact with the fibers and to minimize mechanical abrasion of the fibers. It is therefore my opinion to a reasonable degree of scientific certainty that the cracks observed in the SEM images of the explants are not artifacts but indeed signs of polypropylene degradation when implanted inside the human body. This is supported by the fact that the control samples analyzed in this report did not crack even after exposure to similar conditions. Visually, it was also noted that control and explant fibers did not behave the same when handled (i.e., the explant fibers were found to be less elastic).

Another observation that supports this hypothesis is that this report revealed a large decrease in the levels of antioxidants in the explanted samples relative to control sample. On the basis of the LCMS analysis, Jordi Labs found only 1.8% and 3.0% of the original levels of dilauryl thiodipropionate and Santonox R respectively, relative to the amounts found in the control sample. Literature suggests that a decrease in the levels of antioxidants in polypropylene is closely tied to the degradation of polypropylene.^{50,51}

Therefore, to a reasonable degree of scientific certainty, over time, subsequent layers of the implanted Prolene fibers will degrade in vivo. As such, and over time, one would reasonably expect to observe oxidation even in the currently non-cracked regions of the explant fibers. In fact, the SEM-EDX results in this report show a uniformly higher presence of oxygen in non-cracked regions of all the explant samples tested relative to the control sample, further supporting my opinions in this regard.

⁴⁸ Berrocal J., Clave H., Cosson M., Debodinance Ph., Garbin O., Jacquetin B., Rosenthal C., Salet-Lizee D., Villet R., Conceptual advances in the surgical management of genital prolapse The TVM Technique, *J Gynecol Obstet Biol Reprod* (2004) 33, 577-587.

⁴⁹ Choi, J et al. *Use of Mesh During Ventral Hernia Repair in Clean-Contaminated and Contaminated Cases*. *Annals of Surgery* (2012) 255:1

⁵⁰ Moore, E., (1996) *Polypropylene Handbook. Polymerization, Characterization, Properties, Processing and Applications*, Hanser Publishing, New York, Page 182-188.

⁵¹ Timothy C Liebert, Richard P. Chertoff, Stanley L. Cosgrove and Roberts S. McCuskey *Journal of Biomedical Materials Research* 10 (1976) 939-951.

d. Duration of implantation studies of polypropylene

While the issue of physiological conditions in a dog heart versus a human pelvis is outside the scope of this report, it is imperative to mention that the degradation of polypropylene continues to occur when inside the human body and that studies for samples implanted longer than 7 years would answer more questions about the longer-term degradation characteristics of polypropylene.⁵² Mr. Burkley testified that he was unaware of any further studies by Ethicon following the dog study in which Ethicon studied the degradation of its explanted TVT products.

VII. Test Results

A summary of the individual test results from 24 TVT and TVT-O explants is provided below. All accompanying data, including spectra, have been included in the data section of this report and attached as Exhibits "C-I".

Sample Storage

Samples were stored in a temperature controlled (25°C) storage room when not in immediate use. This room was locked and was accessible only to authorized personnel.

Sample Preparation

Control Samples

Control samples were received for analysis in sealed packaging. An example is shown in **Figure 1**. Each sample was then photographed and logged into a database system which assigns an auto-generated sample identification number (Jordi Sample Number as listed in **Table 1**). The packaging was opened and the device was removed. The device consisted of a white plastic handle with a plastic coated metal tool. Attached to the plastic coated metal tool was a fiber mesh inside of a plastic sleeve. The plastic sleeve was removed and the fiber mesh was collected for analysis. For the remainder of this report, all designations regarding the sample are intended to refer to the *fiber mesh*, as no other portion of the samples was analyzed. Individual test procedures require the use of specific sample preparation techniques. The summary of results for each method indicates how the samples were prepared for that analysis. Analyses performed on the fiber mesh taken from the control samples are summarized in **Table 1** for each sample.

Control Experiment

The control samples were also used as part of a control experiment designed to provide an indication as to the effects of formalin storage. Formalin was used as the storage solvent for

⁵² Moore, E., (1996) Polypropylene Handbook. Polymerization, Characterization, Properties, Processing and Applications, Hanser Publishing, New York, Page 182-188.

transport of the explant samples following surgery prior to their delivery to Jordi Labs. To that end, a sample of each control material (~100 mg) was placed in formalin (90 ml) and heated at 60°C for 48 hours. In my experience, this temperature would be expected to provide an accelerated rate of aging and is consistent with other published methods for this purpose.^{53,54} Following aging, these samples were analyzed in a fashion similar to the explant samples to provide an indication whether or not formalin storage had affected the samples. These samples are referred to as "formalin treated" samples throughout the remainder of this report.

Table 1 Control Samples - Analysis Chart								
Sample Lot Number	OM	SEM	SEM EDX	FTIR Micro	DSC	GPC HT	QTOF LCMS	PYMS
3436364	X, F	X, F	X, F		X	X, F	X	X
3405405	X, F	X, F			X	X, F	X, F	X
3405460	X, F	X, F			X	X, F	X	X
3422128	X, F	X, F	F	X	X, F	X, F	X, F	X
3398135	X, F	X, F			X	X, F	X	X
3405474	X, F	X, F			X	X, F	X	X

X indicates that this test was performed on the control sample

F indicates that this test was performed on the control sample following accelerated aging in formalin.

⁵³ ASTM D3045: <http://www.astm.org/Standards/D3045.htm>

⁵⁴ Inoue, M. (1961), *J. Polym. Sci.*, 55: 443-450.



Figure 1: Example of sample preparation process and sampling location for control samples for Control sample Lot# 3405460. Left (sample as received exterior packaging), right (sample as received interior packaging).

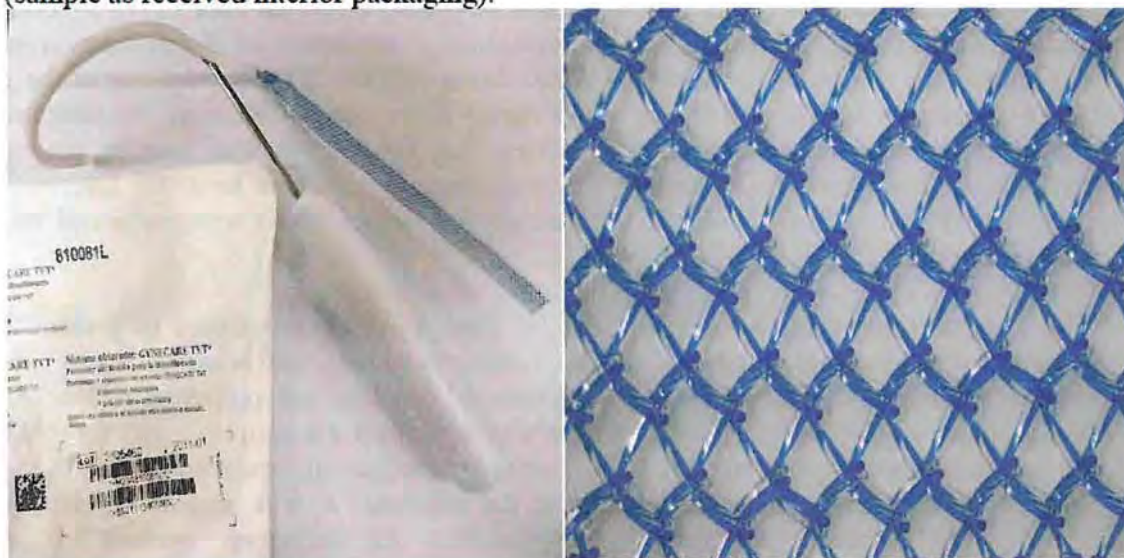


Figure 1 Continued: Example of sample preparation process and sampling location for control samples for Control sample Lot# 3405460. Left (sample device removed from interior packaging), right (fiber mesh used for analysis)

Explant Samples

The explant samples were received for analysis in sealed containers which contained formalin. Each sample was then photographed and logged into a database system which assigns an auto-generated sample identification number (Jordi Sample Number as shown in **Table 2**). The containers were opened and the samples were initially separated into two portions of approximately equal length. The first half was returned to Steelgate. The second half was then sectioned again to prepare an approximately .5cm x .5cm portion which was returned to a legal representative. The remaining portion was used for analysis at Jordi Labs.

The preparation of each sample included weighing the original sample following blotting with a kim wipe to remove excess formalin. The samples were then sectioned for OM, SEM, SEM-EDX and FTIR-microscopy analysis. These tests are non-destructive and thus it was possible to analyze a single portion of sample by all of these methods. The samples were sectioned using a fresh disposable scalpel to cut off a portion of the explant which was approximately 2-3mm in length. A small amount of tissue was carefully removed using forceps to uncover the fibers present underneath. The minimum amount of tissue required was removed so as to avoid disturbing the fibers. In all ways, care was taken to minimize any impact on the fibers. An example of the portion analyzed by OM, SEM, SEM-EDX and FTIR-microscopy is shown in **Figure 2**.

The fiber mesh was then freed from the tissue matrix using forceps. The fibers and tissue were then collected in separate vials and weights of each were recorded. OM images of each fraction were then taken. **Figure 2** shows an image of the fibers and tissue following separation. The fibers were placed under reduced pressure for one hour to ensure complete removal of the traces of formalin. For the remainder of this report, all designations regarding the sample are intended to refer to the *Fiber Mesh (Figure 2 bottom left)* or to the *Fiber Mesh Embedded in Tissue (Figure 2 top right)* as no other portion of the samples was analyzed. Individual test procedures require the use of specific sample preparation techniques. The summary of results for each method indicates how the samples were prepared for that analysis. **Table 2** summarizes the testing which was performed on each explant sample.

The sample preparation methods utilized by Jordi Labs were selected to protect the integrity and scientific reliability of the results obtained, and were necessary so that we could understand if the cracks were evidence of degraded polypropylene and/or biofilm. The methods applied represent the optimum way to prepare the samples given the totality of the tests which were to be performed, the limited sample quantity and the potential for testing artifacts following chemical treatments on the explants. It is a general principle in investigative chemistry and forensic science that the minimum amount of sample preparation required is preferred. The reason this is true is that all sample preparation no matter how carefully performed increases the risk of contamination, loss or otherwise adulterating the sample. Therefore, we believe to a reasonable degree of scientific certainty that the sample cleaning method utilized in the Jordi Analysis is superior to the use of any chemicals to dissolve the tissue.

Table 2 Explant Sample - Analysis Chart									
Sample Ident.	Weight Fibers	OM	SEM	SEM EDX	DSC	FTIR Micros.	GPC HT	QTOF LCMS	PYMS
13400	12.536	T, FM	T	T	FM	FM	FM	FM	FM
13401	18.464	T, FM	T		FM			FM	FM
13402	22.482	T, FM	T		FM		FM	FM	FM
13403	2.128	T, FM	T	T					FM
13404	4.292	T, FM	T				FM		
13405	7.302	T, FM	T			FM		FM	FM
13406	1.428	T, FM	T						
13407	14.512	T, FM	T		FM		FM	FM	FM
13408	6.322	T, FM	T	T	FM			FM	FM
13409	8.984	T, FM	T	T	FM		FM	FM	FM
13410	5.324	T, FM	T				FM	FM	
13411	34.68	T, FM	T		FM		FM	FM	FM
13412	7.06	T, FM	T			FM	FM	FM	FM
13413	8.26	T, FM	T			FM	FM	FM	FM
13414	7.162	T, FM	T		FM		FM	FM	FM
13415	11.534	T, FM	T		FM		FM	FM	FM
13416	8.068	T, FM	T		FM		FM	FM	FM
13417	1.772	T, FM	T						
13418	19.45	T, FM	T	T	FM		FM	FM	FM
13419	3.932	T, FM	T		FM				FM
13420	9.044	T, FM	T		FM				FM
13421	8.188	T, FM	T		FM		FM	FM	FM
13674	7.620	T, FM	T	T	FM	FM	FM	FM	FM
13675	5.258	T, FM	T	T	FM	FM	FM	FM	FM

T - indicates that this test was performed on Fiber Mesh Embedded in Tissue

FM - indicates that this test was performed on Fiber Mesh

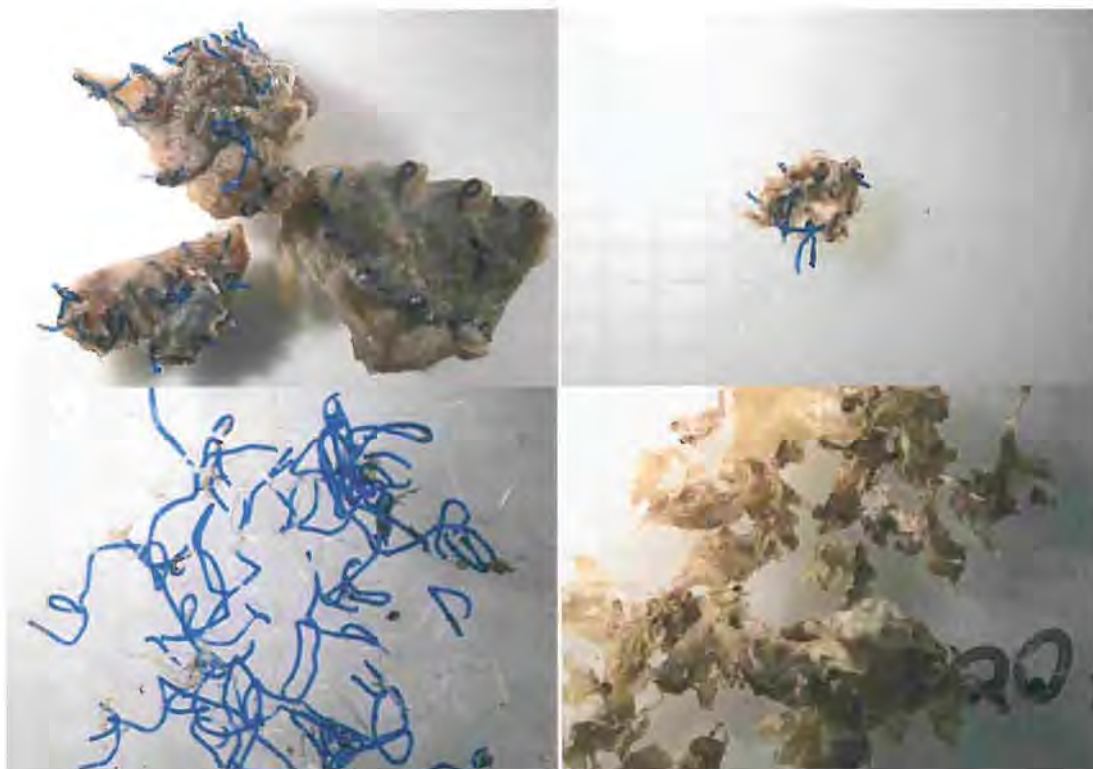


Figure 2: Example explant sample showing the sample preparation process. Top Left (sample as received), Top Right (sample as prepared for OM, SEM, SEM-EDX and FTIR-microscopy), bottom left (fibers removed from tissue matrix), bottom right (tissue matrix after fiber removal)

Observations

It was noted during sample preparation that a readily apparent difference in fiber stiffness existed between the control samples and the explanted fiber mesh. The control samples were observed to be highly flexible and were noted to have flexibility similar to that of fishing line (a typical polypropylene fiber). The explant samples were observed to be much stiffer and to break when bent sufficiently. In contrast, the control samples showed greater flexibility and elasticity and tended to return to their original shape following distortion. When intentionally subjected to strong force, the explant samples were observed to crack completely in some instances and to form two pieces. Similar force applied to the control fibers did not result in cracking.

It is therefore my opinion, to a reasonable degree of scientific certainty, that based upon these observations the mesh hardens, stiffens and becomes markedly less pliable once implanted and subjected to the environmental factors of the tissue in which it was implanted.

SEM and OM

Background and Method

Scanning Electron Microscopy (SEM)^{55,56,57,58} is a technique which utilizes a scanned electron beam to provide high resolution images of the specimen. The method is preferred for materials which are too small for traditional light microscopy. The current analysis was performed using variable pressure SEM. This type of SEM allows for analysis of the specimen at an elevated pressure as compared to a standard SEM instrument which requires that the sample be under vacuum. This in turn allows for analysis of wet samples and reduces the vacuum requirements.

Optical Microscopy (OM) was performed using a reflection microscope. This technique was used to provide images of the specimens for comparison with SEM and to aid in identification of sample locations and image features.

Sample Preparation

Samples were prepared for variable pressure SEM analysis by simply cutting a portion of the sample and removing enough tissue to expose the fiber surface. This was done carefully to avoid direct contact with the fibers. No sputter coating or other sample pretreatment was required due to the use of environmental SEM. The samples were mounted on 12 mm diameter Al stubs that were partially covered with carbon tape. In order to avoid any cracking during mounting, the samples were laid down gently onto the C tape without pressing them on. The samples were analyzed by optical microscopy prior to SEM to show a larger image and to aid in identification of sample features.

Results

Individual SEM and OM images are provided below for each control sample and the explant samples. Additional images are provided for each sample in the data section of this report. **Figures 3-14** show the results for the control samples. **Figures 15-62** show the results for the explant samples. The control samples were observed to show very smooth surfaces with relatively few imperfections. No cracking was observed in the control samples. A very small amount of particulate matter was observed attached to the surface of the control fibers.

In contrast, the explant samples showed three distinct morphologies (textures/shapes). Some portions of the fibers appeared smooth similar to that in the control samples. Other portions showed cracking and peeling of the surface layer. Finally, some regions were consistent with

⁵⁵ A. S. Vaughan, *Polymer Microscopy in Polymer Characterization*, Eds. B. J. Hunt and M. I. James, (Blackie Academic & Professional, Glasgow, UK), 1993, 306-313.

⁵⁶ D. Campbell and J. R. White, *Polymer Characterization: Physical Techniques*, (Chapman & Hall, London, UK), 1989, 242-270.

⁵⁷ Nicholas P. Cheremisinoff, *Polymer Characterization: Laboratory Techniques and Analysis*, (Noyes Publications, Westwood, NJ, USA) 1996, 25-41.

⁵⁸ Jan W. Gooch, *Analysis and Deformation of Polymeric Materials: Paints, Plastics, Adhesives and Inks*, (Plenum Press, New York, USA) 1997, 17-21.

adhesion of a foreign material to the fiber surface. A comparison of this adhered foreign material with the surrounding tissue showed that this material had a consistent morphology with the tissue. **Figure 28** shows a good example of all three textures with each region highlighted for clarity.

The explant samples can be readily grouped into three categories. Two of the samples (13419 and 13421) showed no visible indications of cracking. Four of the samples showed moderate cracking (13401, 13408, 13411 and 13420). The remaining eighteen samples showed extensive cracking. The nature of the cracking in these later samples was often very substantial. **Figures 22, 30, 34 and 52** are good examples of this. The cracks were observed to occur generally in a direction perpendicular to the fiber draw direction. When cracking became extensive, the cracked material was also observed to begin to peel away from the remainder of the underlying fiber.

Control Experiment

A control experiment was conducted to confirm that the cracking observed was not related to storage of the fibers in formalin. This fluid was used for transport of the specimens following surgery prior to their delivery to Jordi Labs. Following aging of the samples in formalin, the samples were analyzed in a fashion similar to the explant samples. SEM results for all six control lots are shown in the data section, but one example is presented in **Figures 63 and 64**. The surface of the fibers was found to remain smooth. It is my opinion to a reasonable degree of scientific certainty that this supports that the cracking observed in the explants occurred prior to storage of the fibers in formalin.

Scientific Opinion

Based on numerous scientific literature, my knowledge, training and experience, and my examination of the data, it is my opinion to a reasonable degree of scientific certainty that the SEM results are consistent with cracking of the polypropylene fiber. The images support that the polypropylene itself is cracking as in **Figures 34 and 62** where the fiber extrusion lines can be seen to extend through the cracked region. The fiber cracking process appears to be generally localized to the surface layers of the fibers; however, in some explant samples, the cracking passes through the entire fiber. Cracking through the fiber was most commonly observed where a fiber was highly bent. The fibers show clear indications of crack propagation forming circular rings perpendicular to the fiber draw direction. As the degree of cracking increases, the fibers show peeling of the top most surface layer such that the thickness of the fiber is reduced. The cracked material is not biofilm or protein crosslinked with formaldehyde but was identified using an independent technique (FTIR-Microscopy) to be oxidized polypropylene shards along with some protein from the surrounding tissue.

The smooth images obtained for all control samples demonstrate that cracking is not a test artifact but a feature of the explanted fiber material. The control experiment which submerged the control samples in formalin further demonstrates that this damage is not a result of storage of the samples in the formalin solution.

It is my opinion to a reasonable degree of scientific certainty, based on the review of the scientific literature and my knowledge, training and experience in polymer science, this level of degradation will have a *strong impact* on fiber mechanical properties including stiffness, elasticity and resistance to break. It is also my opinion that the cracking seen by SEM is consistent with the observed increase in stiffness and the decreased elasticity experienced when handling the explant samples. These observations, when taken together, would suggest that the explanted fibers would be expected to show reduced flexibility, elasticity and an increased propensity to break when subjected to deformation (bending). Sharp or protruding surfaces could result, and if present in the patient, would be likely to cause discomfort and irritation. A smooth surface area of a prosthetic implant will cause less irritation and less inflammatory response than a rough, cracked surface. Also, by shedding particles of polypropylene into the surrounding tissues, the surface area of the mesh increases, as will the foreign body reaction and inflammatory response. The more material and the more particles in tissue, the greater the inflammatory response will be. Therefore, to a reasonable degree of scientific certainty, the Prolene mesh in the TVT products degrades, cracks, and releases polypropylene particulates into the surrounding tissue after implantation, causing an increased inflammatory response.

Control Samples

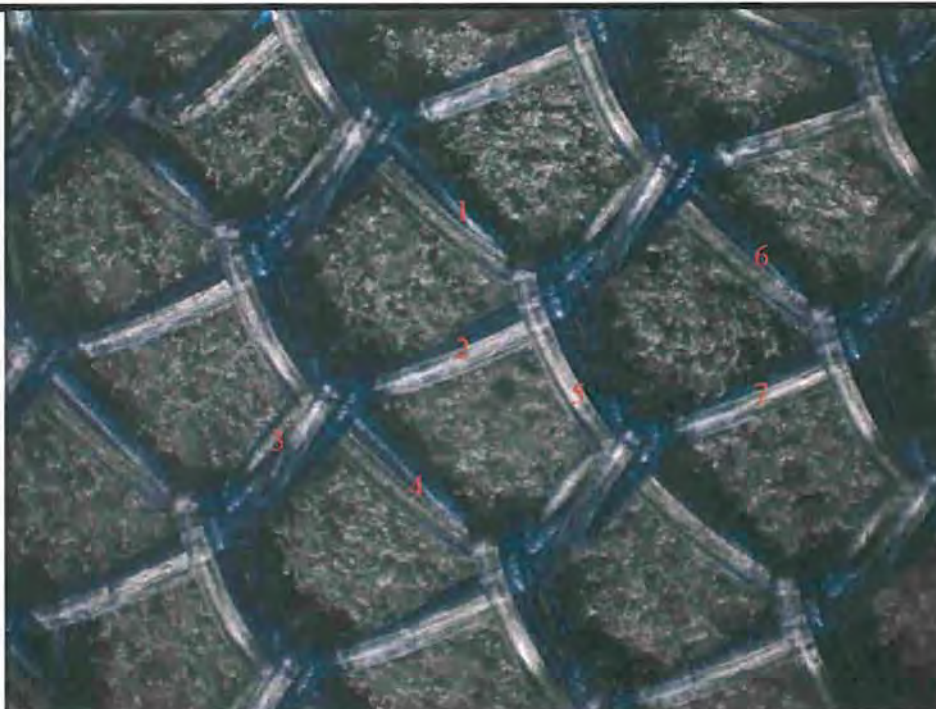


Figure 3

Optical Image

Comment:

Sample 13158
Lot#3436364

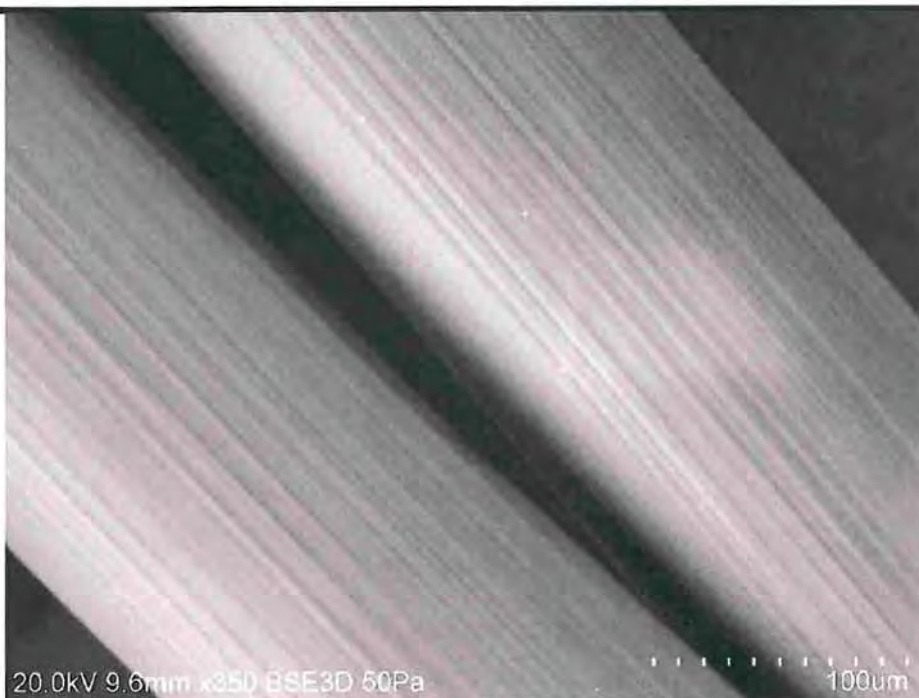


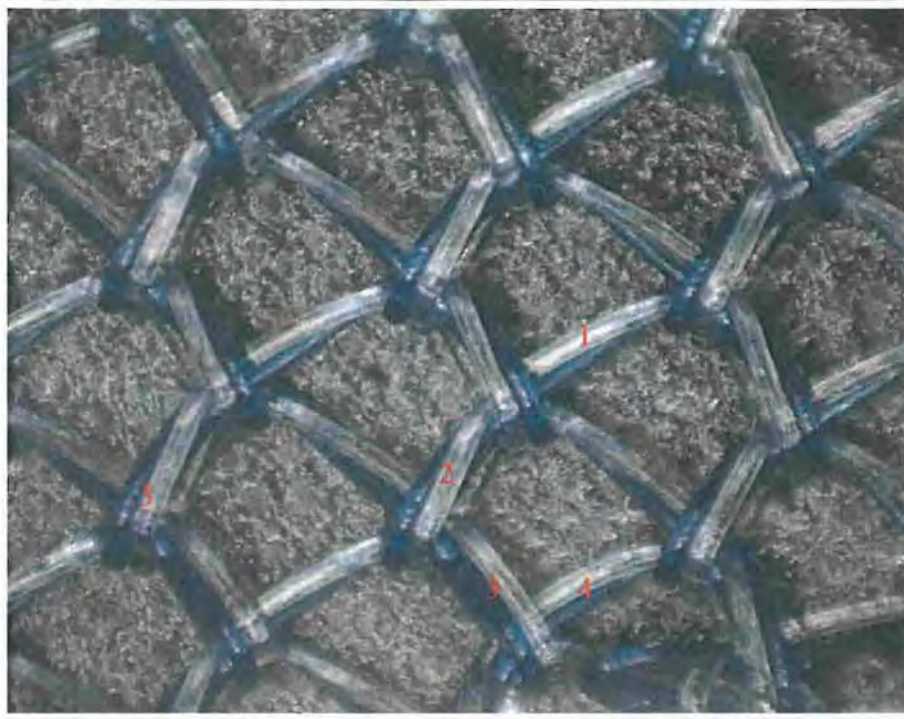
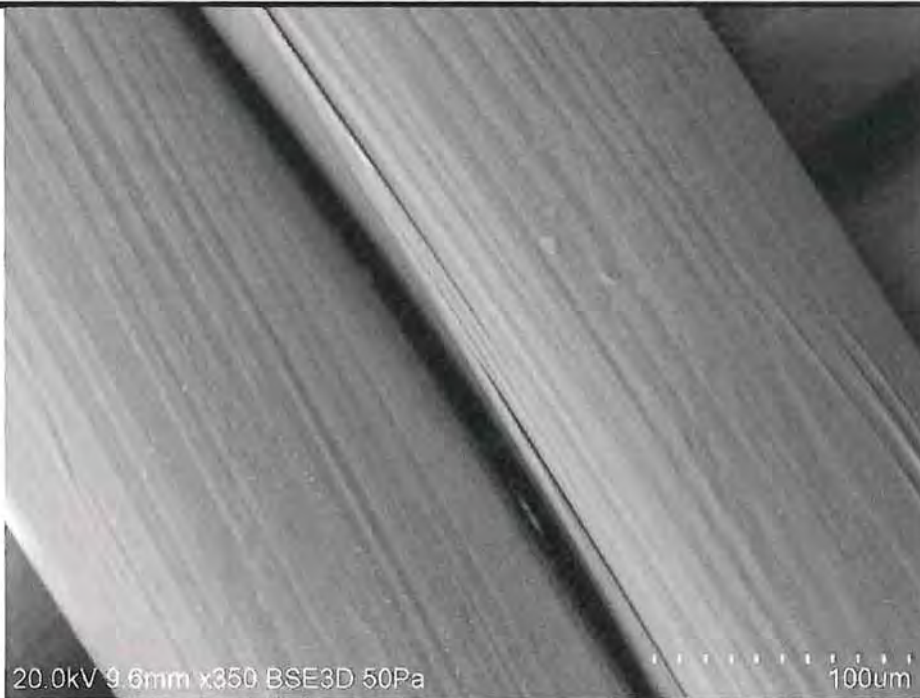
Figure 4

Mag = 350X

Voltage = 20kV

Comment:

Sample 13158
Lot#3436364

	<table><tr><td>Figure 5</td></tr><tr><td>Optical Image</td></tr><tr><td>Comment: Sample 13159 Lot#3405405</td></tr></table>	Figure 5	Optical Image	Comment: Sample 13159 Lot#3405405	
Figure 5					
Optical Image					
Comment: Sample 13159 Lot#3405405					
	<table><tr><td>Figure 6</td></tr><tr><td>Mag = 350X</td></tr><tr><td>Voltage = 20kV</td></tr><tr><td>Comment: Sample 13159 Lot#3405405</td></tr></table>	Figure 6	Mag = 350X	Voltage = 20kV	Comment: Sample 13159 Lot#3405405
Figure 6					
Mag = 350X					
Voltage = 20kV					
Comment: Sample 13159 Lot#3405405					

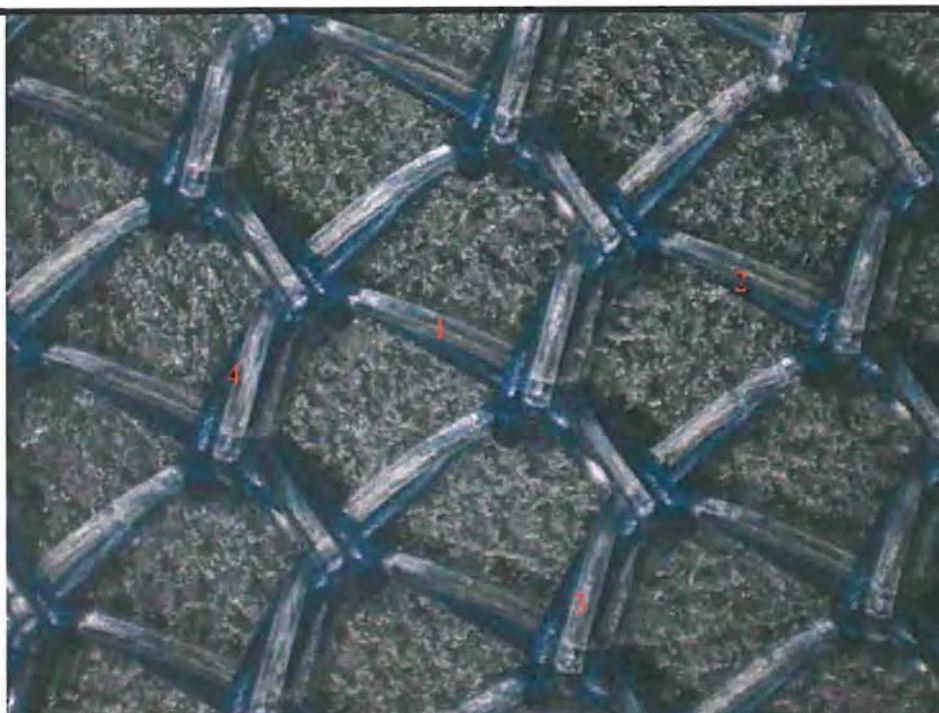


Figure 7

Optical Image

Comment:

Sample 13160
Lot#3405460

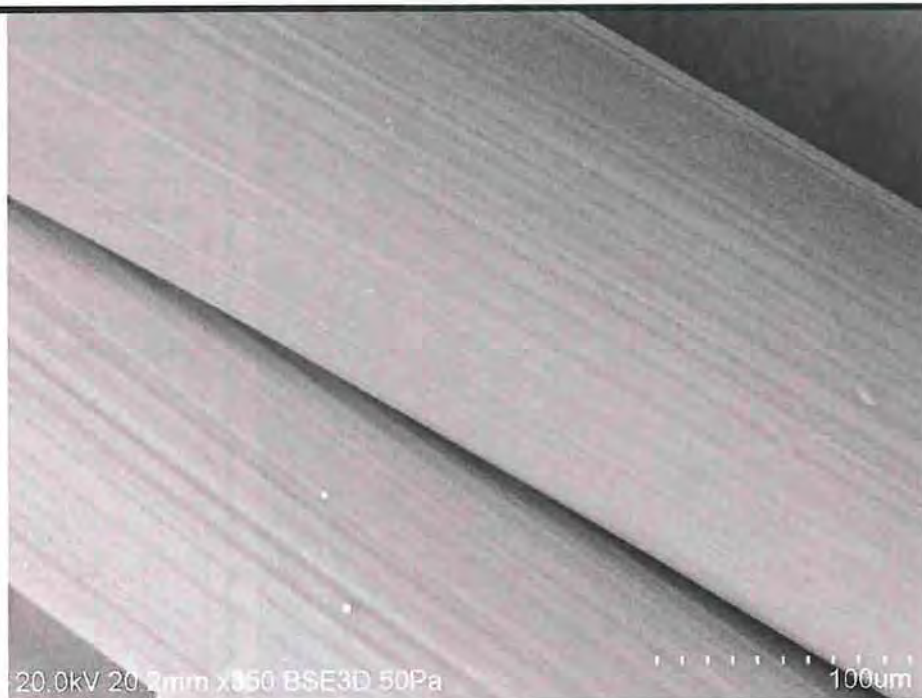


Figure 8

Mag = 350X

Voltage = 20kV

Comment:

Sample 13160
Lot#3405460



Figure 9

Optical Image

Comment:

Sample 13161
Lot#3422128

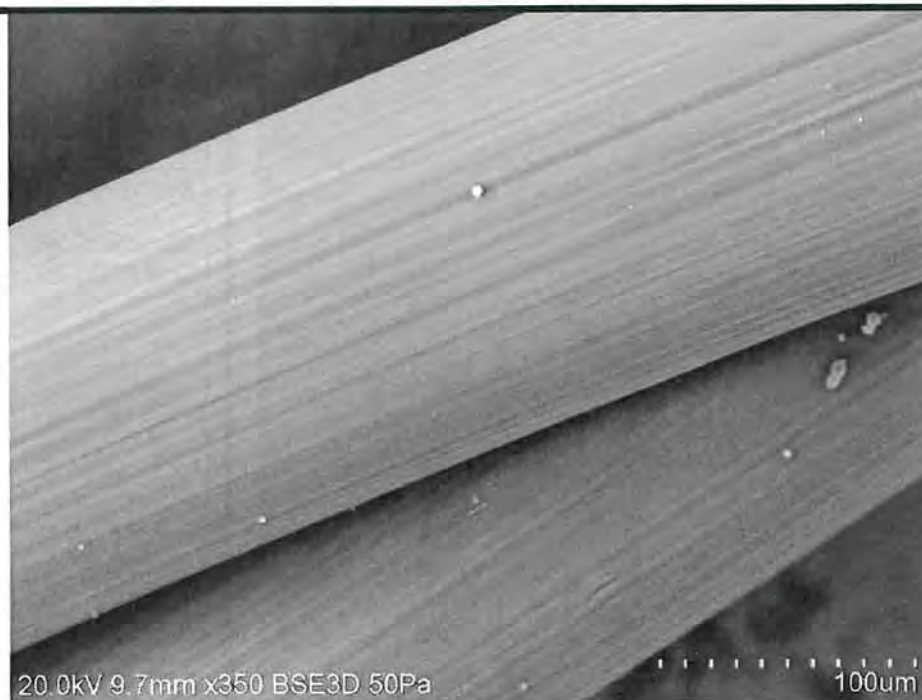


Figure 10

Mag = 350X

Voltage = 20kV

Comment:

Sample 13161
Lot#3422128



Figure 11

Optical Image

Comment:

Sample 13162
Lot#3398135



Figure 12

Mag = 350X

Voltage = 20kV

Comment:

Sample 13162
Lot#3398135

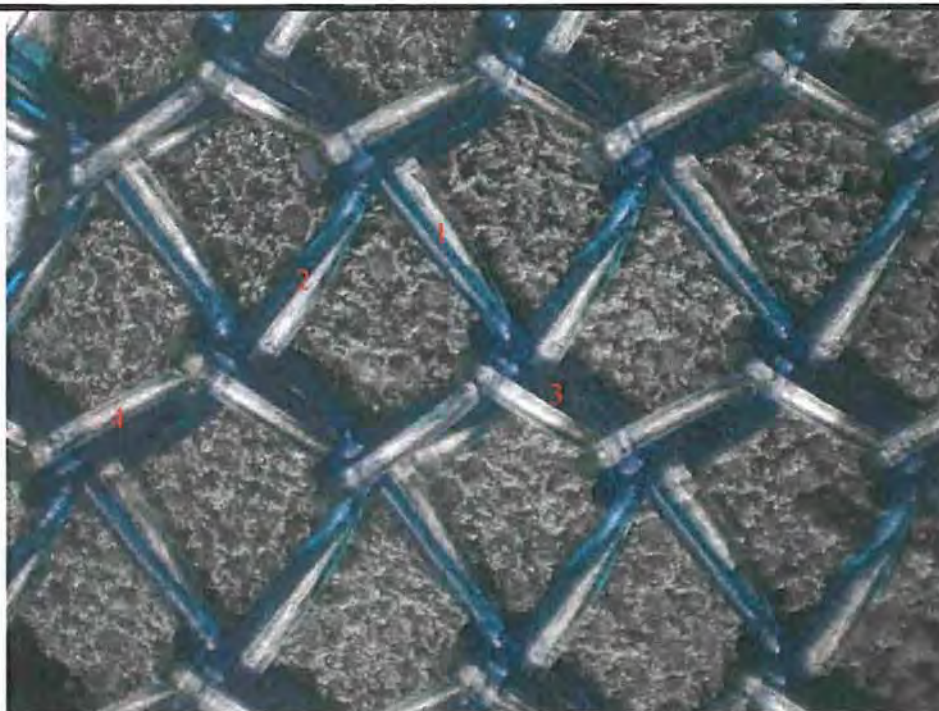


Figure 13

Optical Image

Comment:

Sample 13163
Lot#3405474

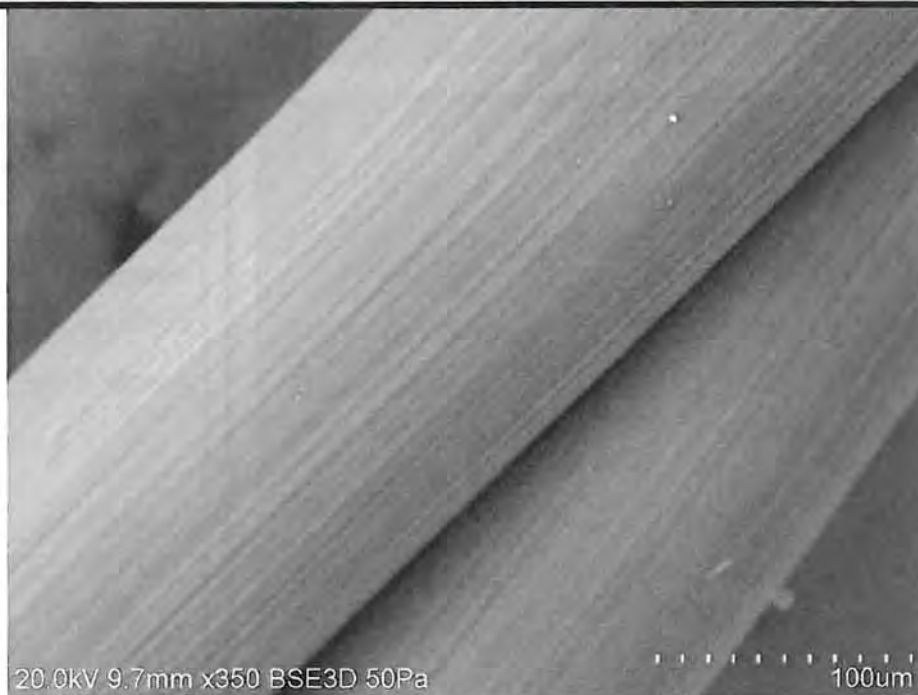


Figure 14

Mag = 350X

Voltage = 20kV

Comment:

Sample 13163
Lot#3405474

Explant Samples



Figure 15

Optical Image

Comment:

Sample J7959
13400



Figure 16

Mag = 350X

Voltage = 20kV

Comment:

Sample J7959
13400

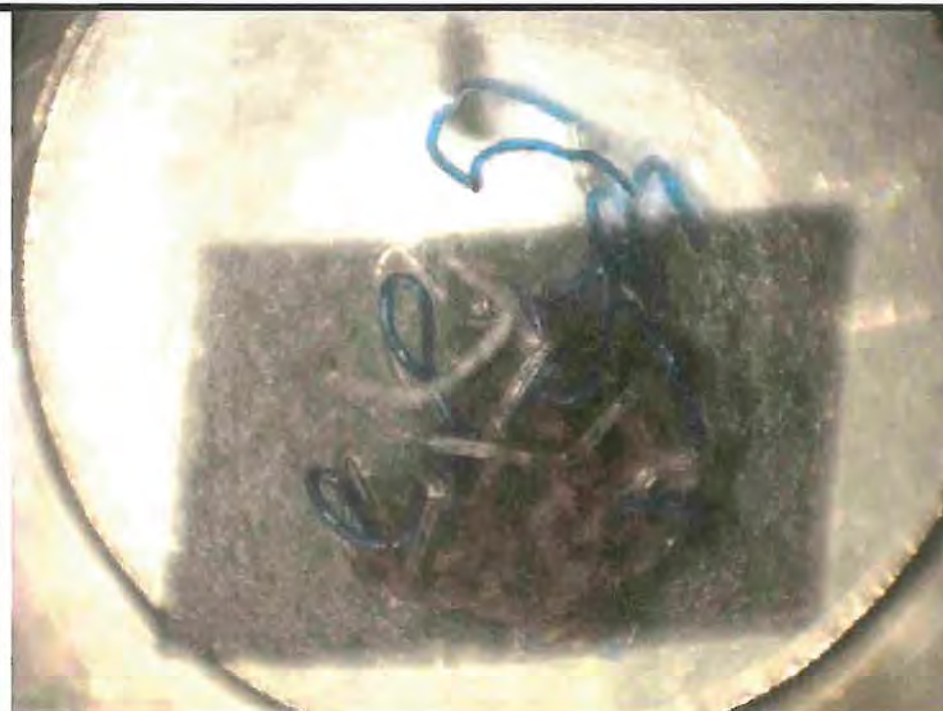


Figure 17

Optical Image

Comment:

Sample J7959
13401



Figure 18

Mag = 350X

Voltage = 20kV

Comment:

Sample J7959
13401

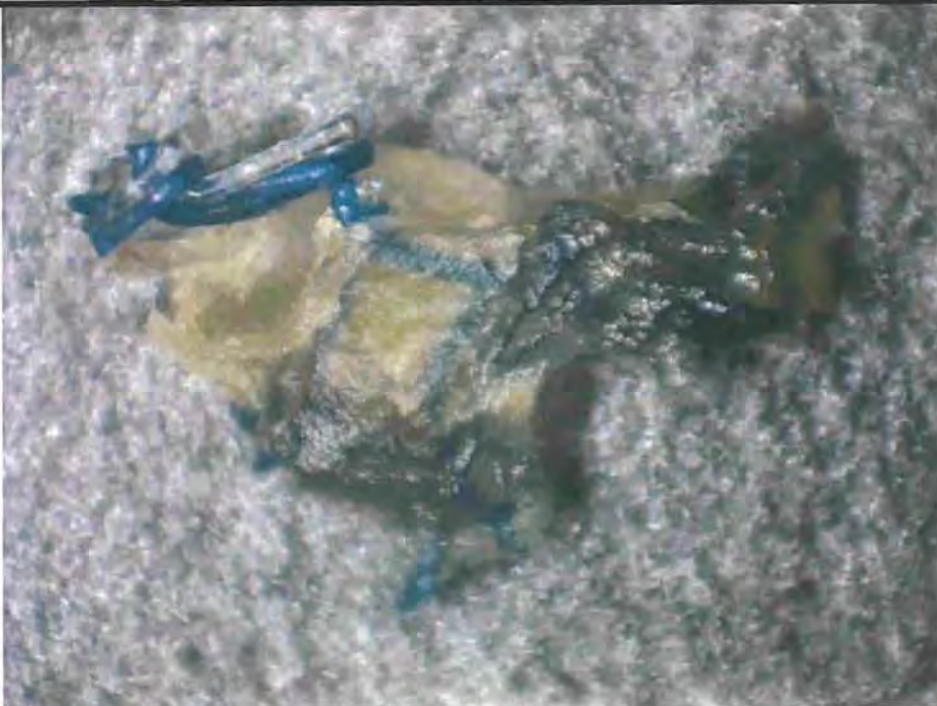


Figure 19

Optical Image

Comment:

Sample J7959
13402

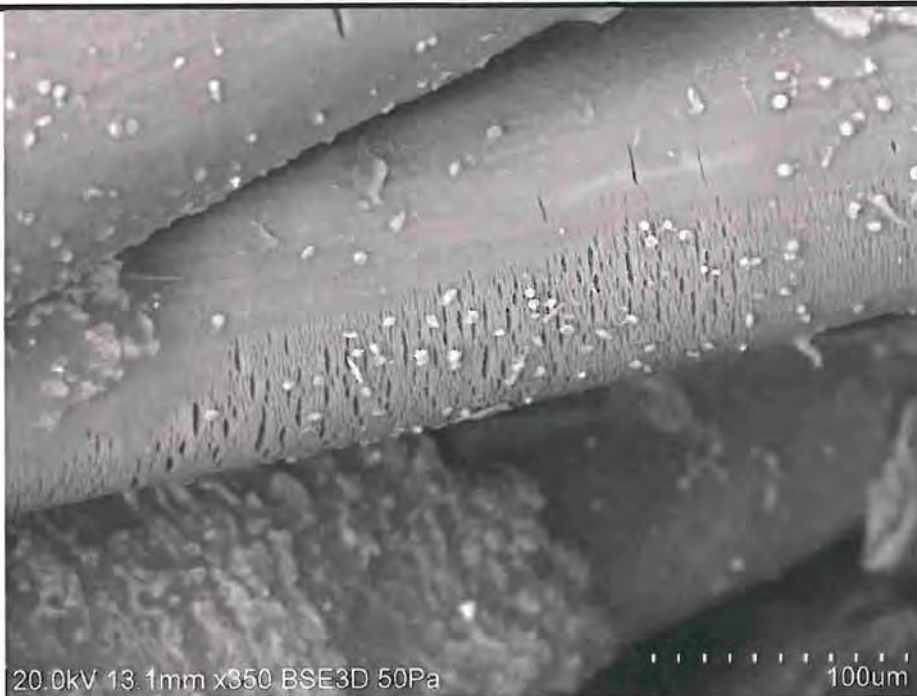


Figure 20

Mag = 350X

Voltage = 20kV

Comment:

Sample J7959
13402



Figure 21

Optical Image

Comment:

Sample J7959
13403



Figure 22

Mag = 350X

Voltage = 20kV

Comment:

Sample J7959
13403

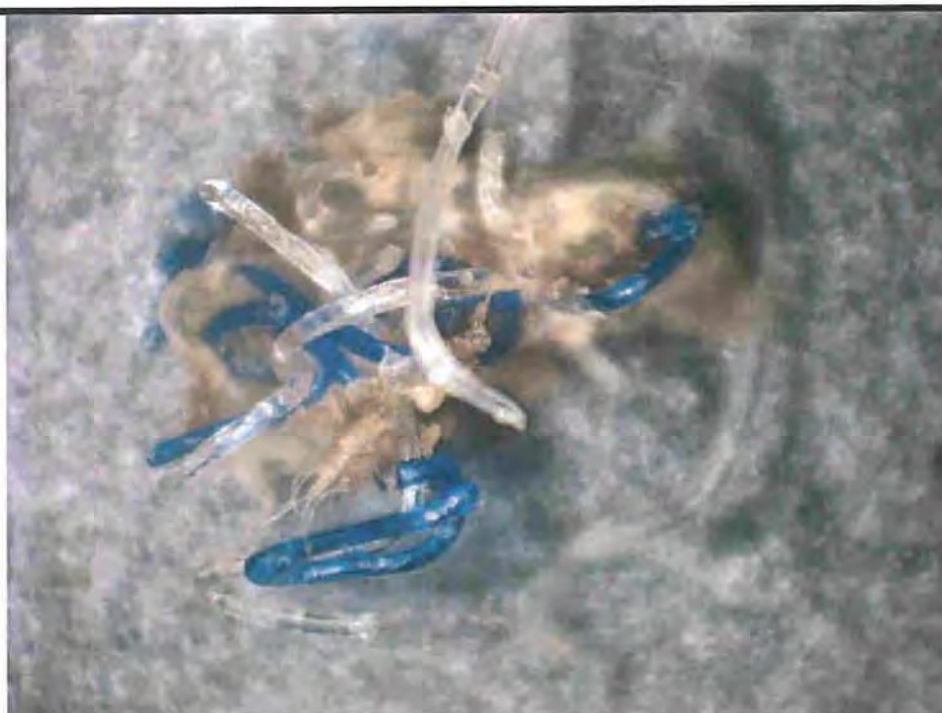


Figure 23

Optical Image

Comment:

Sample J7959
13404



Figure 24

Mag = 350X

Voltage = 20kV

Comment:

Sample J7959
13404

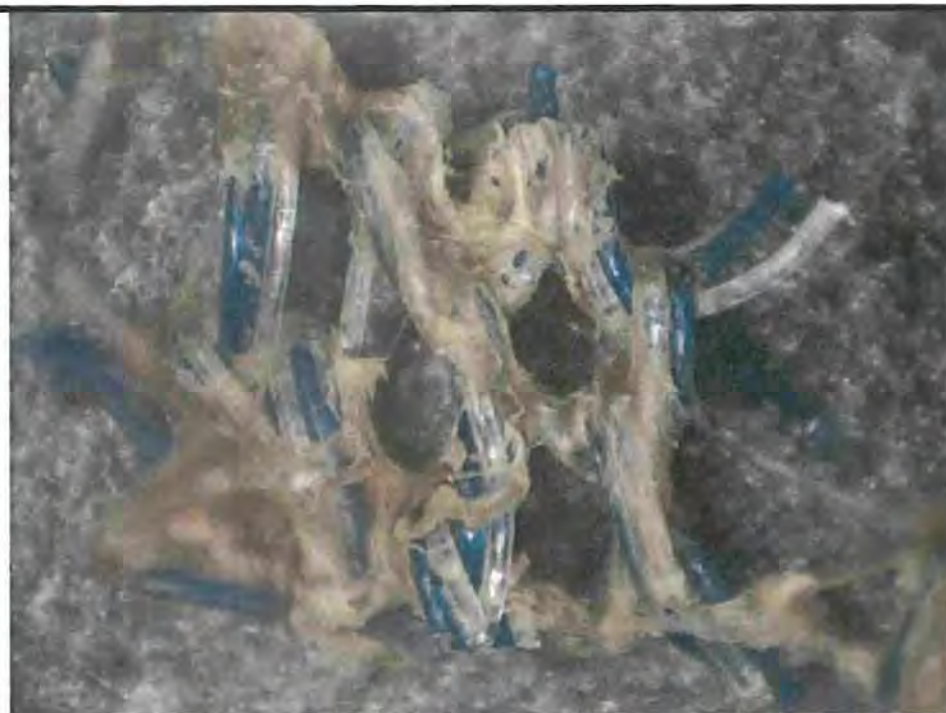


Figure 25

Optical Image

Comment:

Sample J7959
13405

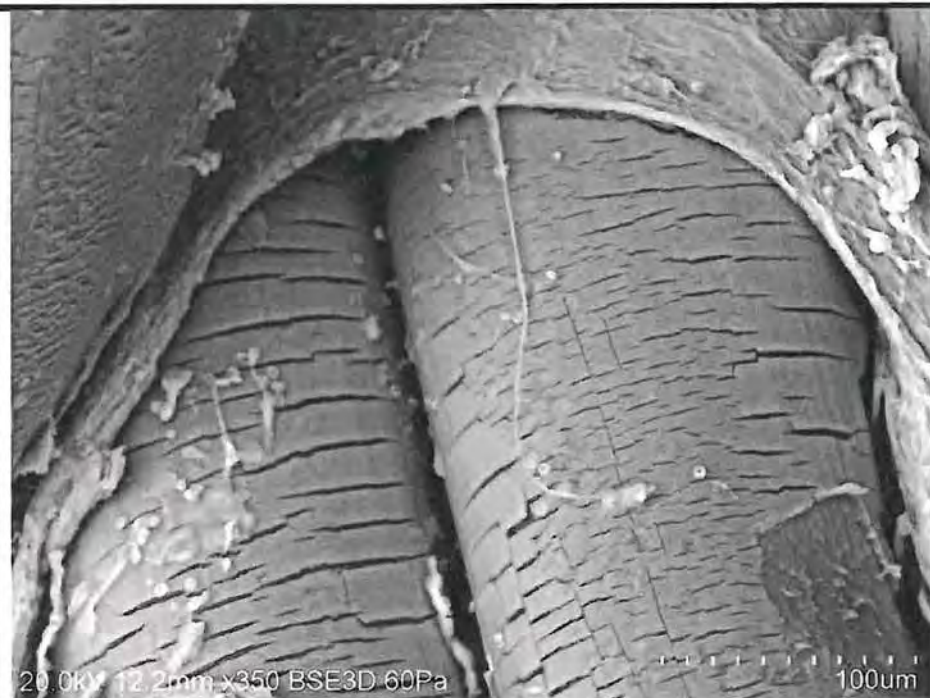


Figure 26

Mag = 350X

Voltage = 20kV

Comment:

Sample J7959
13405



Figure 27

Optical Image

Comment:

Sample J7959
13406



Figure 28

Mag = 350X

Voltage = 20kV

Comment:

Sample J7959
13406

Key:

----- Undamaged
Region
----- Cracked
Region
----- Adhered
Material

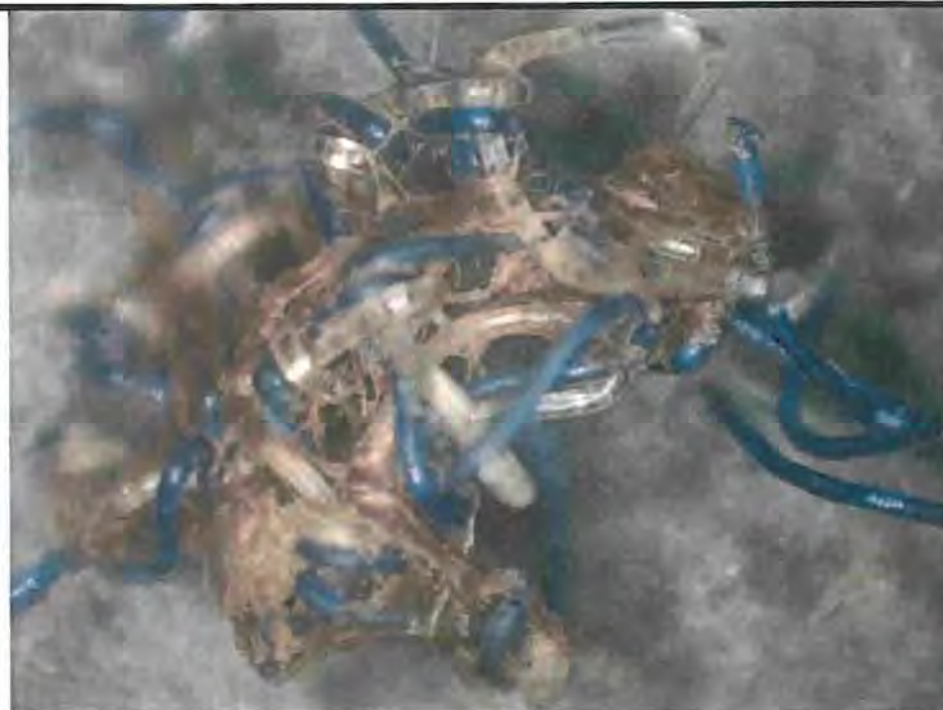


Figure 29

Optical Image

Comment:

Sample J7959
13407

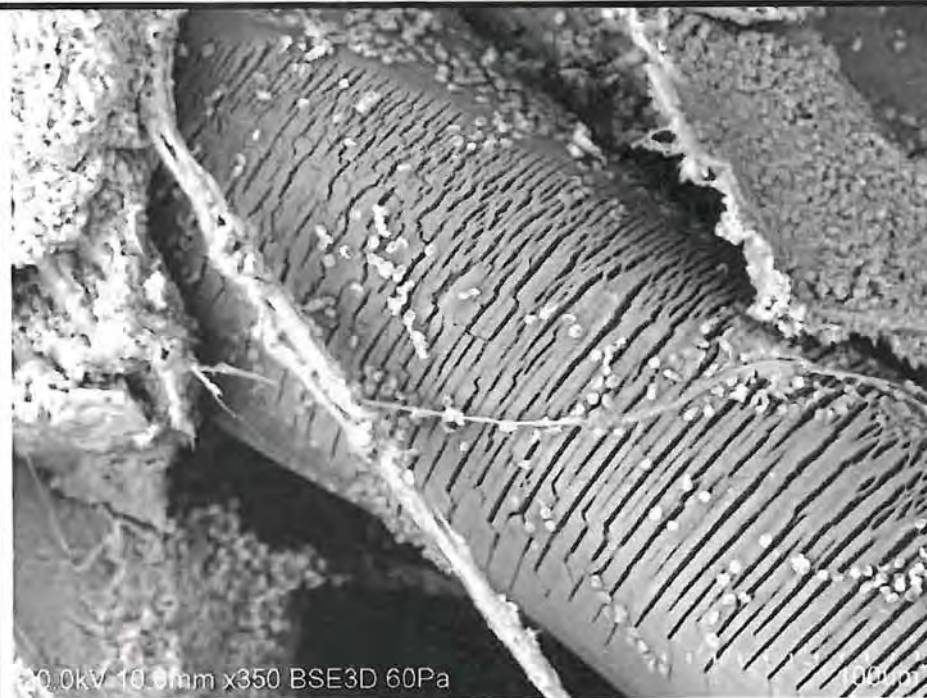


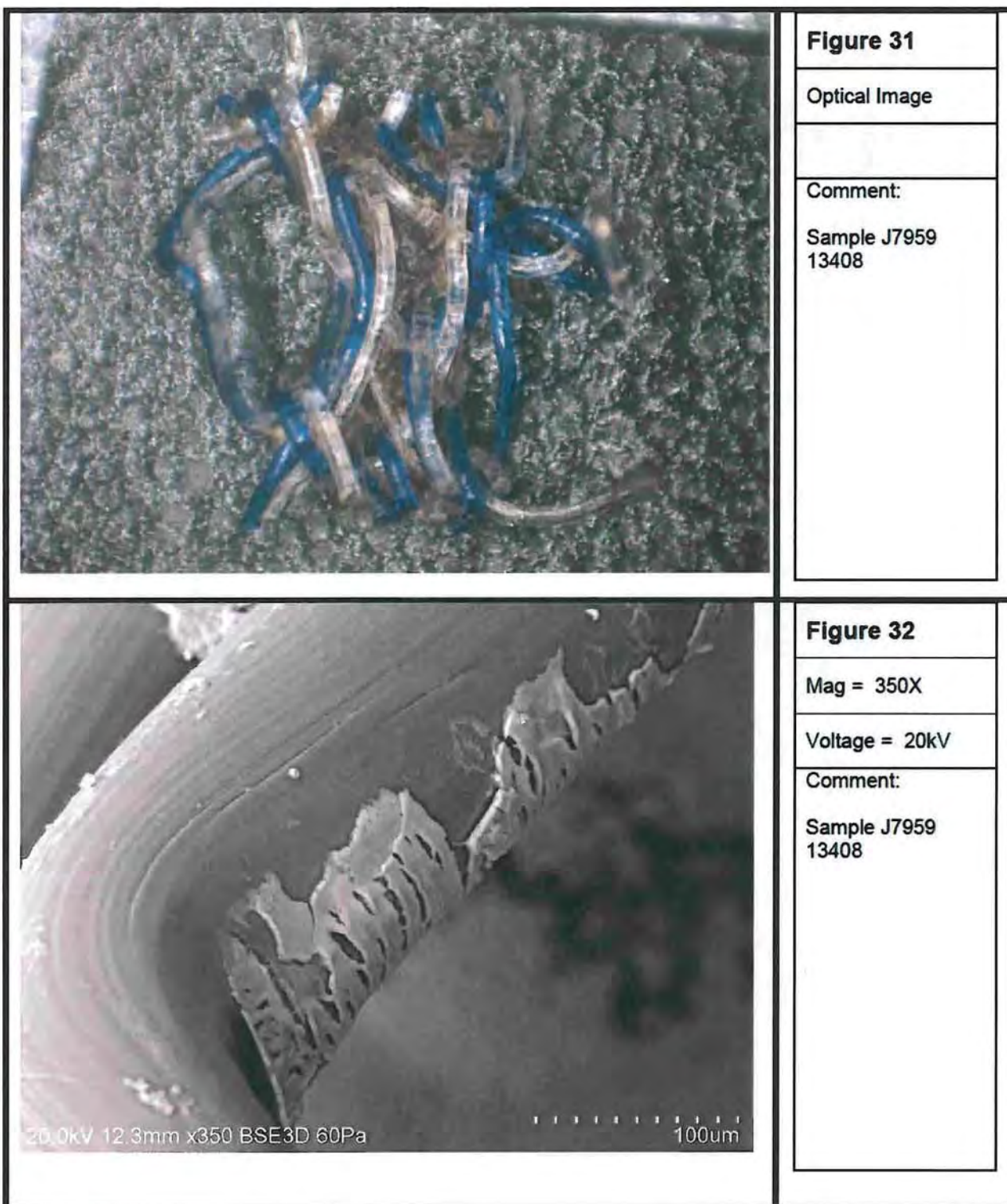
Figure 30

Mag = 350X

Voltage = 20kV

Comment:

Sample J7959
13407



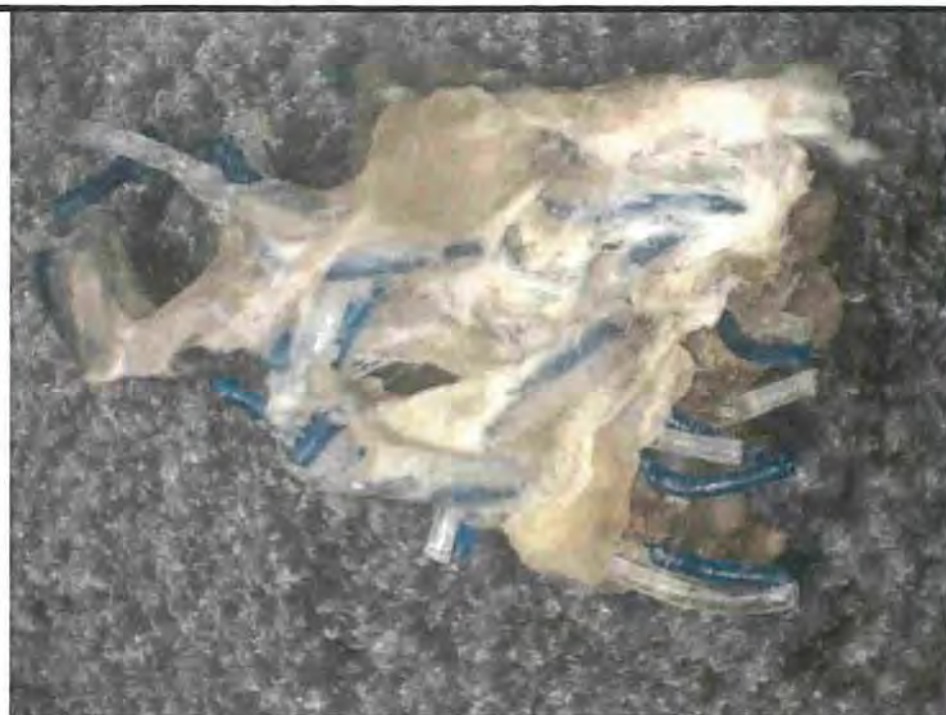


Figure 33

Optical Image

Comment:

Sample J7959
13409



Figure 34

Mag = 350X

Voltage = 20kV

Comment:

Sample J7959
13409



Figure 35

Optical Image

Comment:

Sample J7959
13410

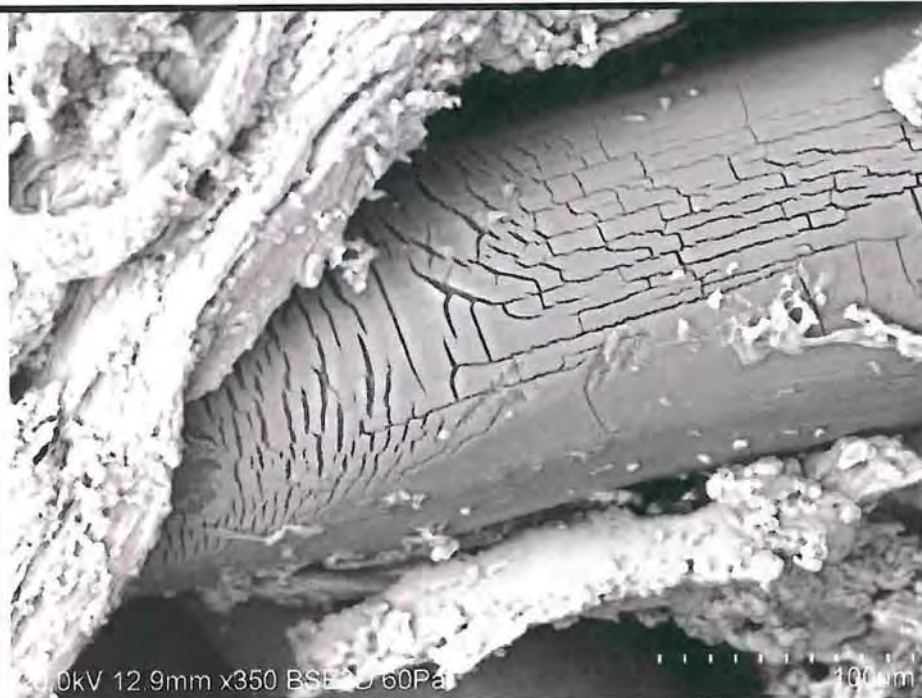


Figure 36

Mag = 350X

Voltage = 20kV

Comment:

Sample J7959
13410

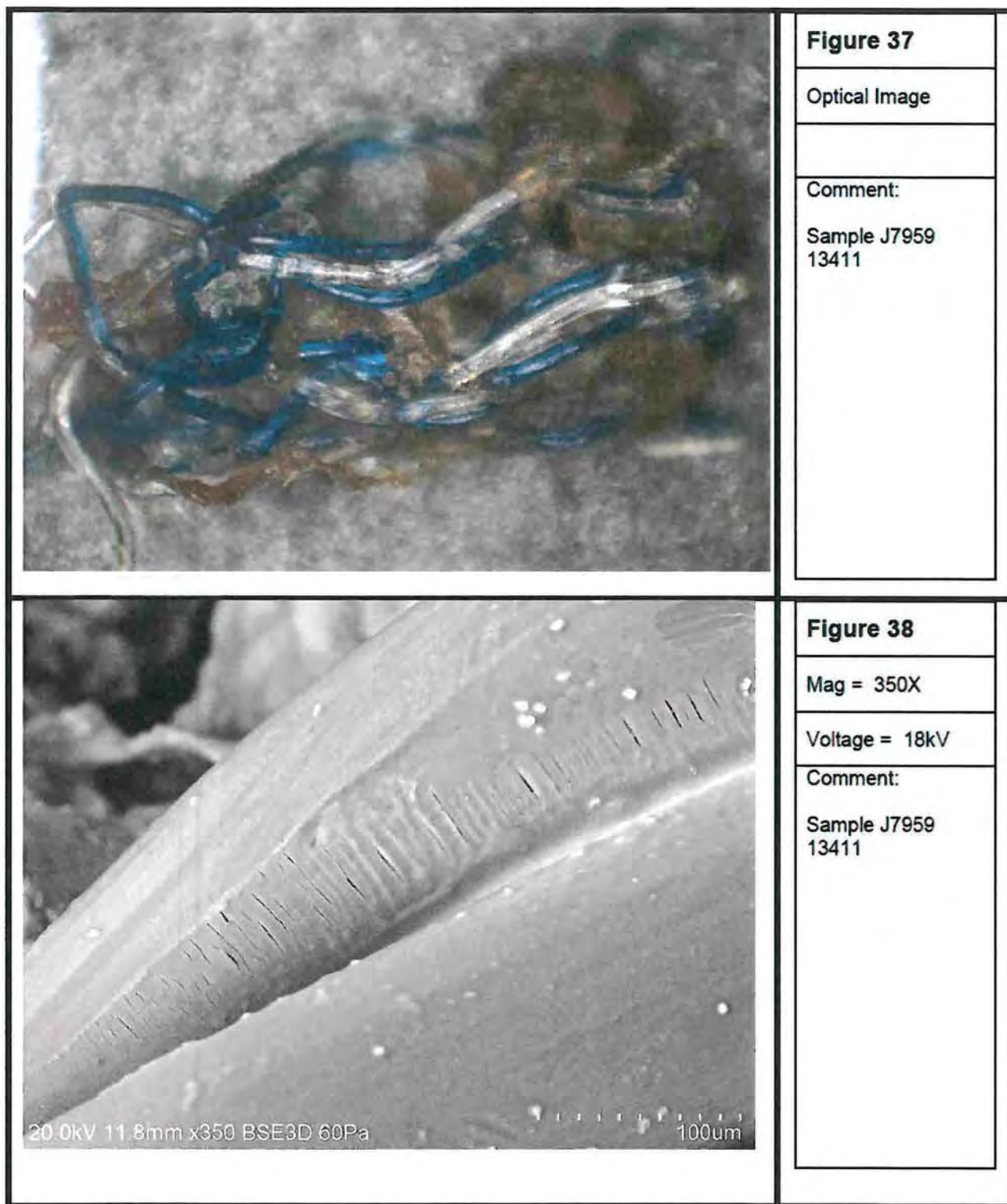




Figure 39

Optical Image

Comment:

Sample J7959
13412

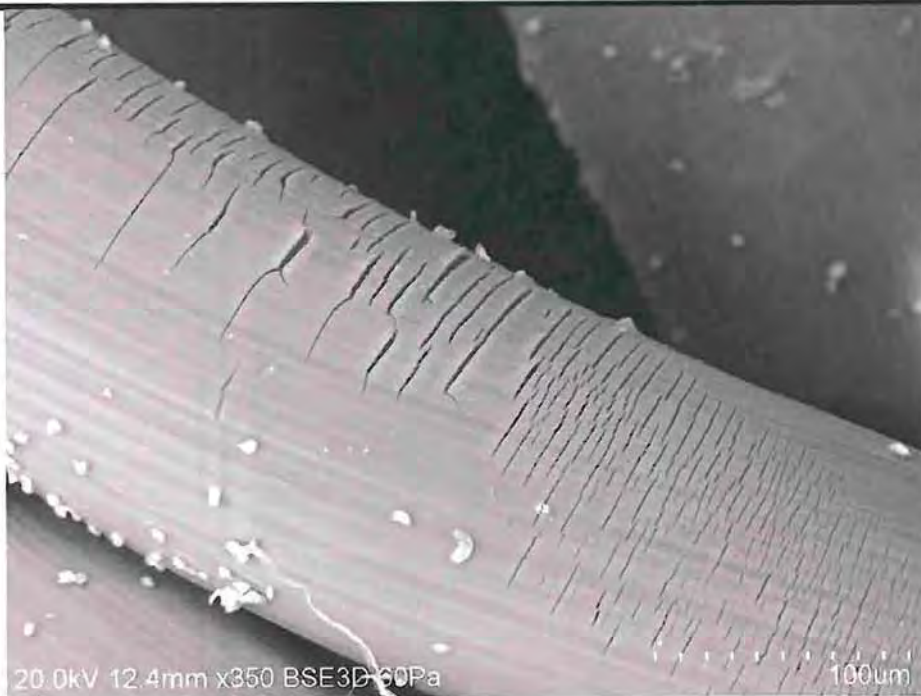


Figure 40

Mag = 350X

Voltage = 20kV

Comment:

Sample J7959
13412

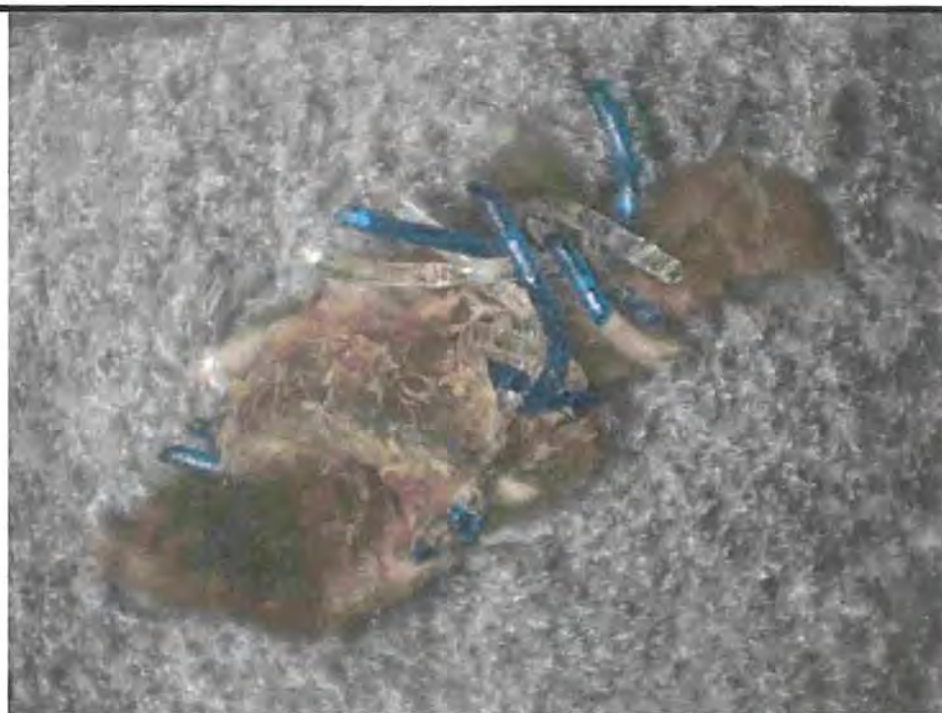


Figure 41

Optical Image

Comment:

Sample J7959
13413

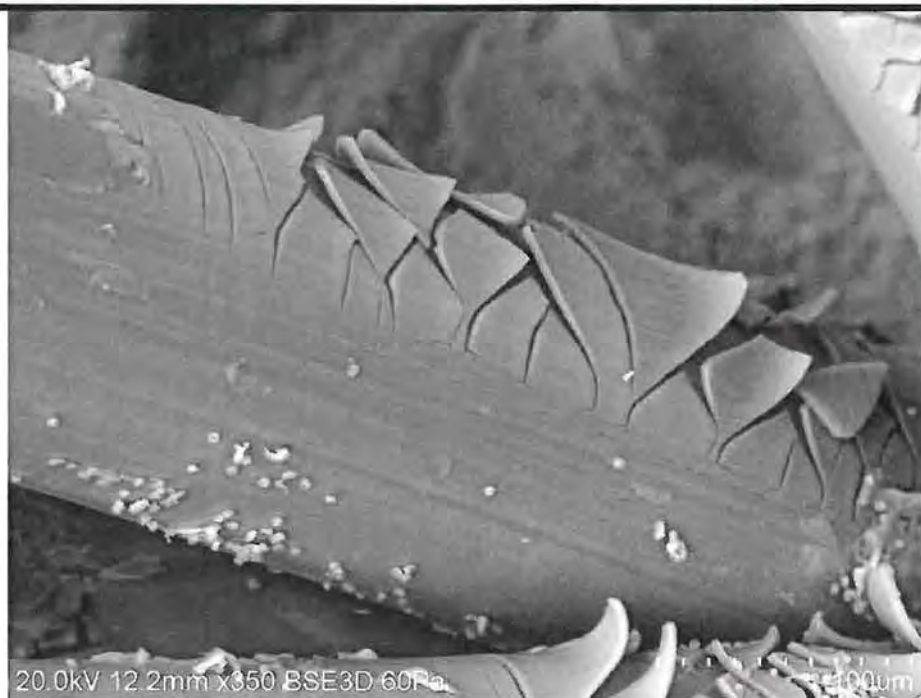


Figure 42

Mag = 350X

Voltage = 20kV

Comment:

Sample J7959
13413



Figure 43

Optical Image

Comment:

Sample J7959
13414



Figure 44

Mag = 350X

Voltage = 20kV

Comment:

Sample J7959
13414

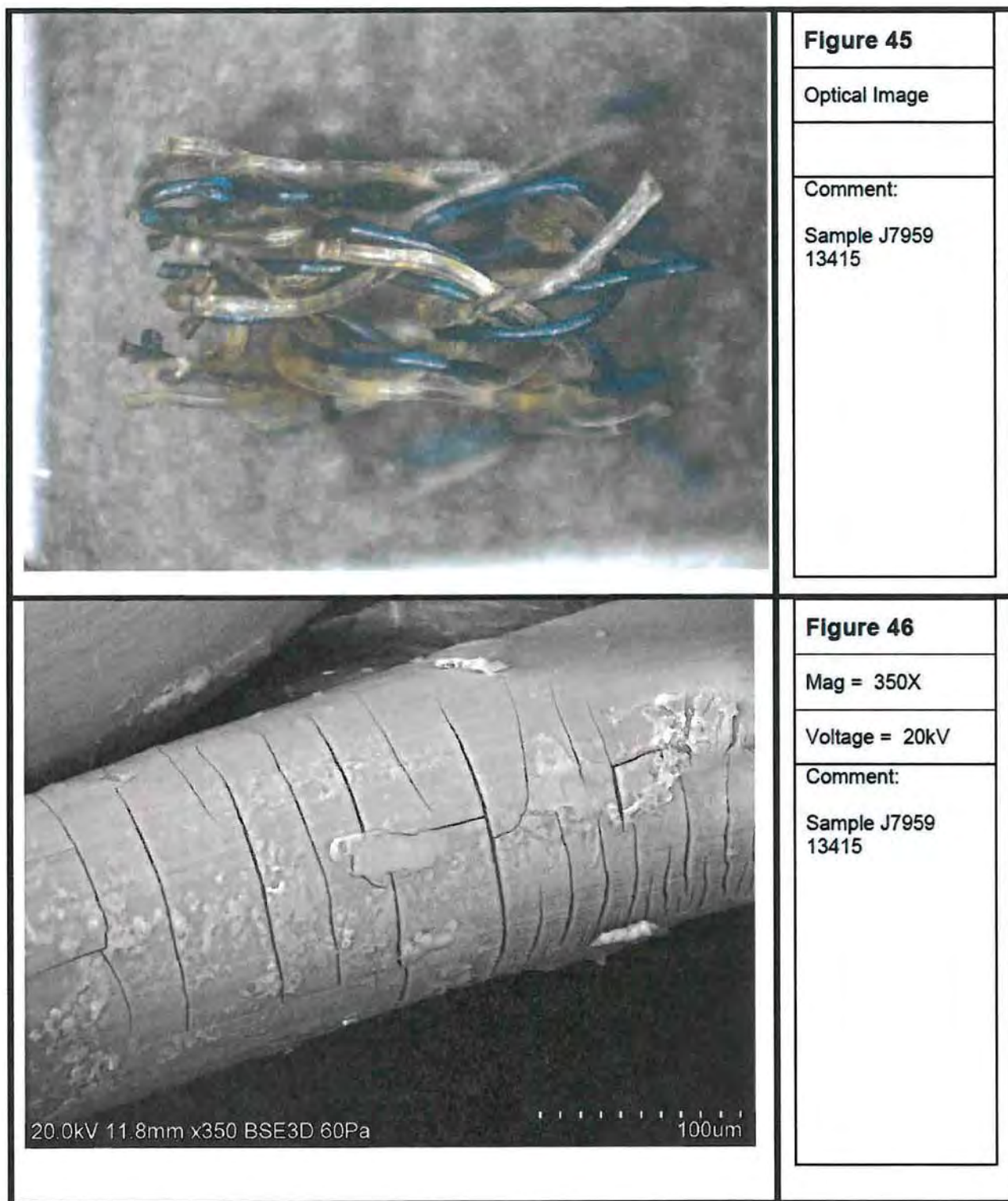




Figure 47

Optical Image

Comment:

Sample J7959
13416

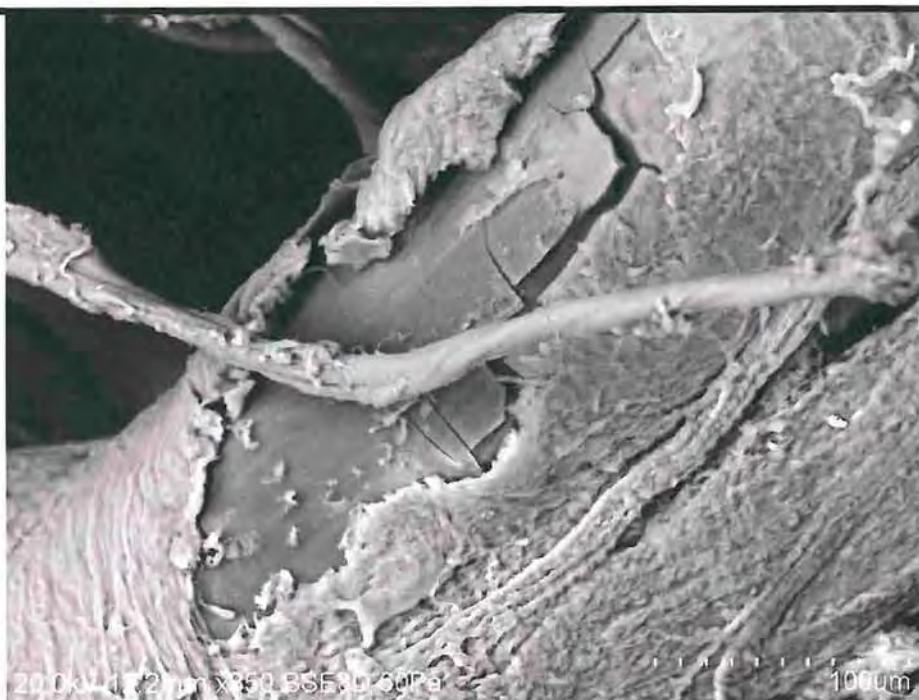


Figure 48

Mag = 350X

Voltage = 20kV

Comment:

Sample J7959
13416



Figure 49

Optical Image

Comment:

Sample J7959
13417

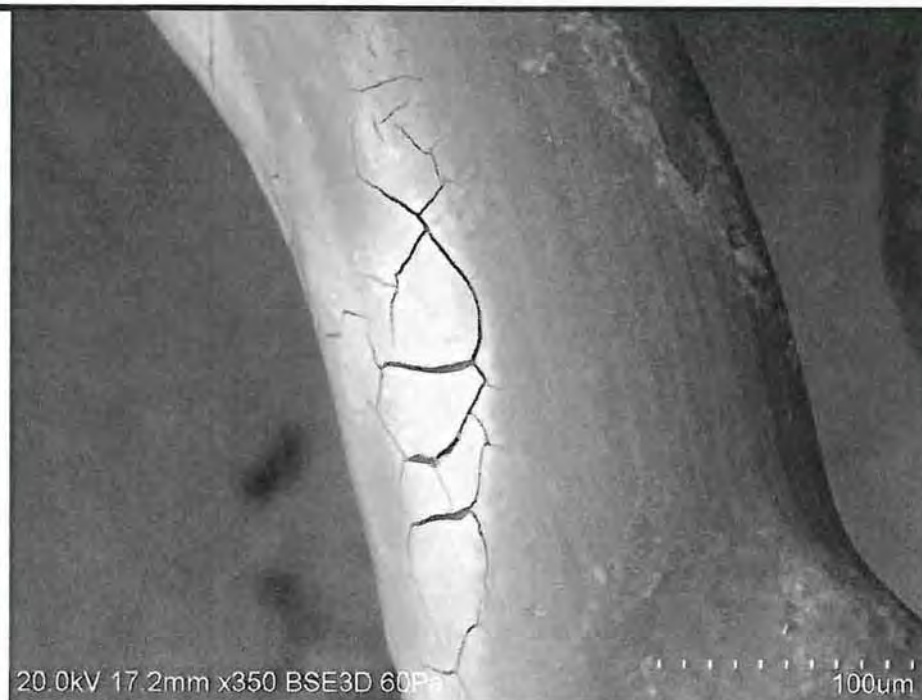


Figure 50

Mag = 350X

Voltage = 20kV

Comment:

Sample J7959
13417



Figure 51

Optical Image

Comment:

Sample J7959
13418

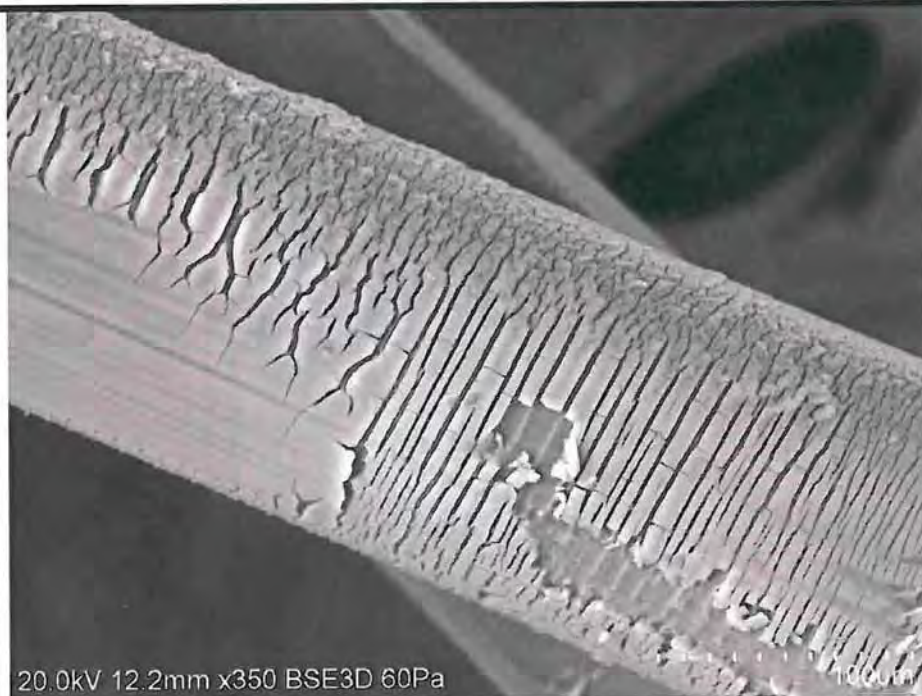


Figure 52

Mag = 350X

Voltage = 20kV

Comment:

Sample J7959
13418



Figure 53

Optical Image

Comment:

Sample J7959
13419

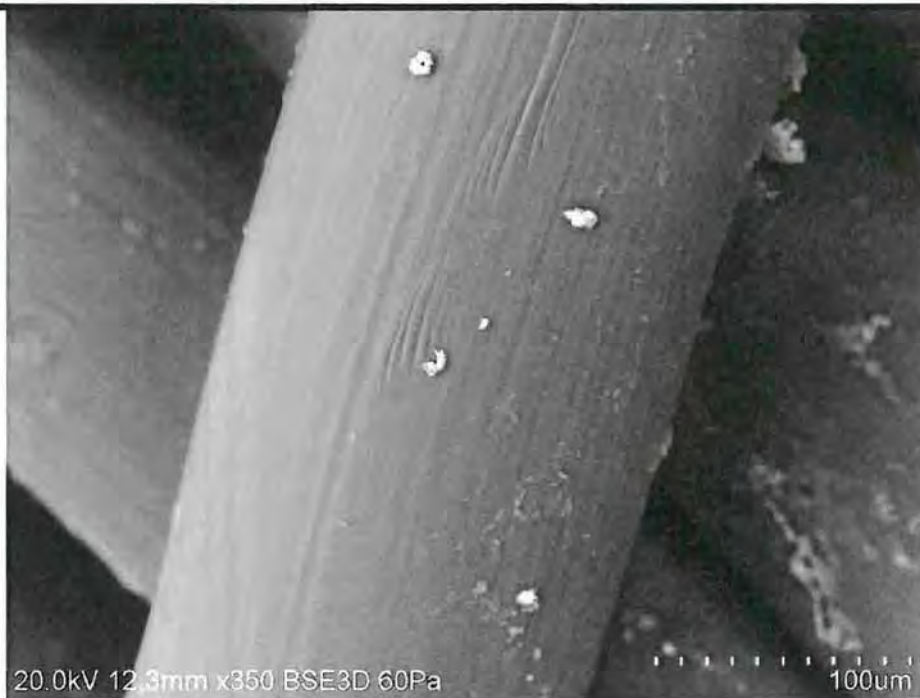


Figure 54

Mag = 350X

Voltage = 20kV

Comment:

Sample J7959
13419

20.0kV 12.3mm x350 BSE3D 60Pa

100um



Figure 55

Optical Image

Comment:

Sample J7959
13420

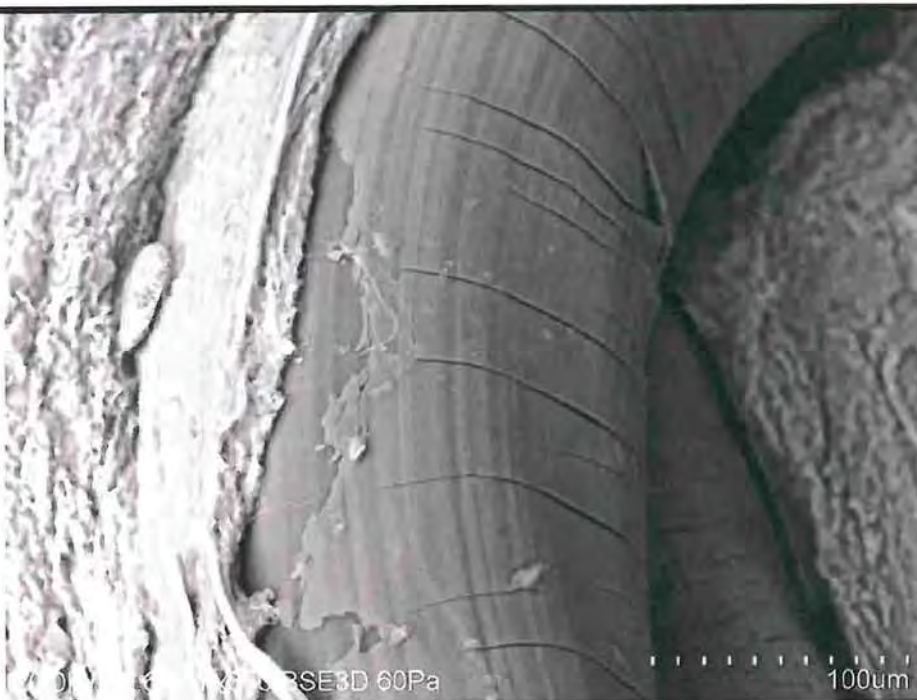


Figure 56

Mag = 350X

Voltage = 20kV

Comment:

Sample J7959
13420



Figure 57

Optical Image

Comment:

Sample J7959
13421

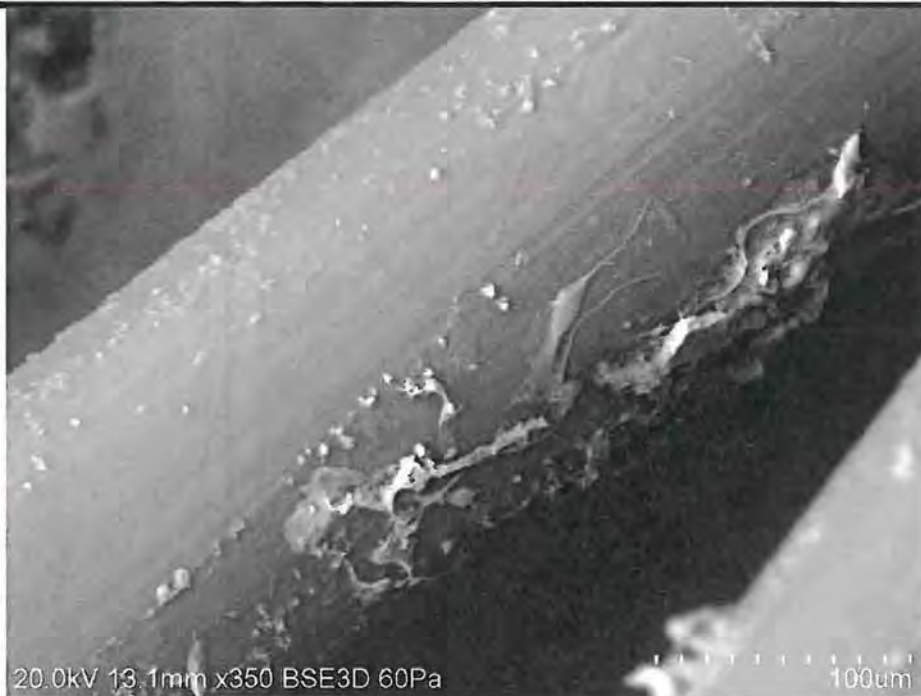


Figure 58

Mag = 25X

Voltage = 20kV

Comment:

Sample J7959
13421

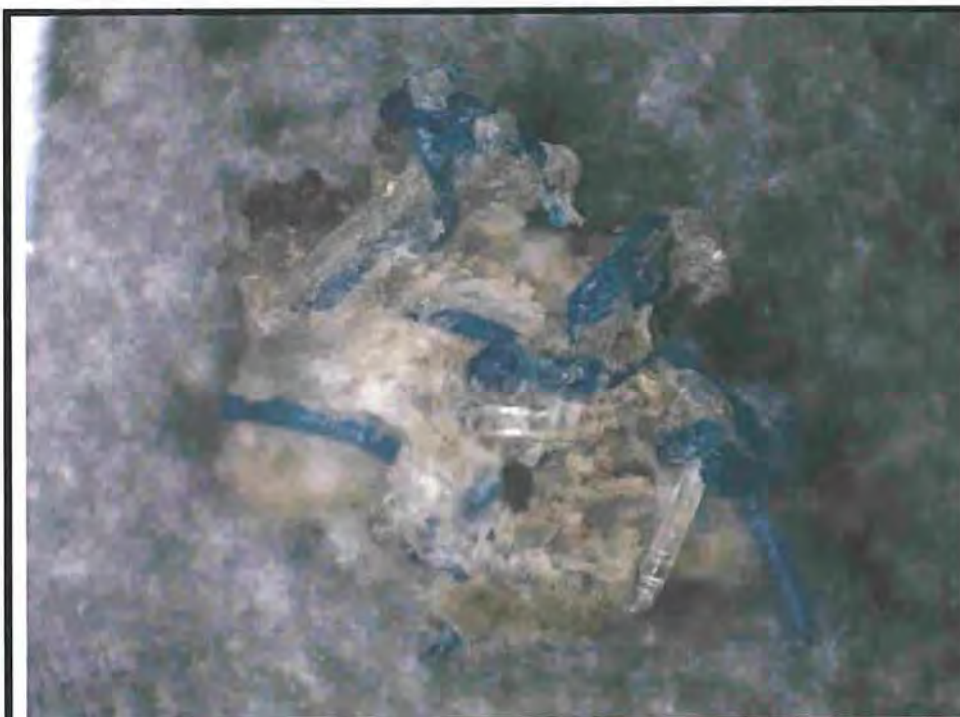


Figure 59

Optical

Comment:

J8041-13674



Figure 60

Mag = 300X

Voltage = 20kV

Comment:

J8041-13674

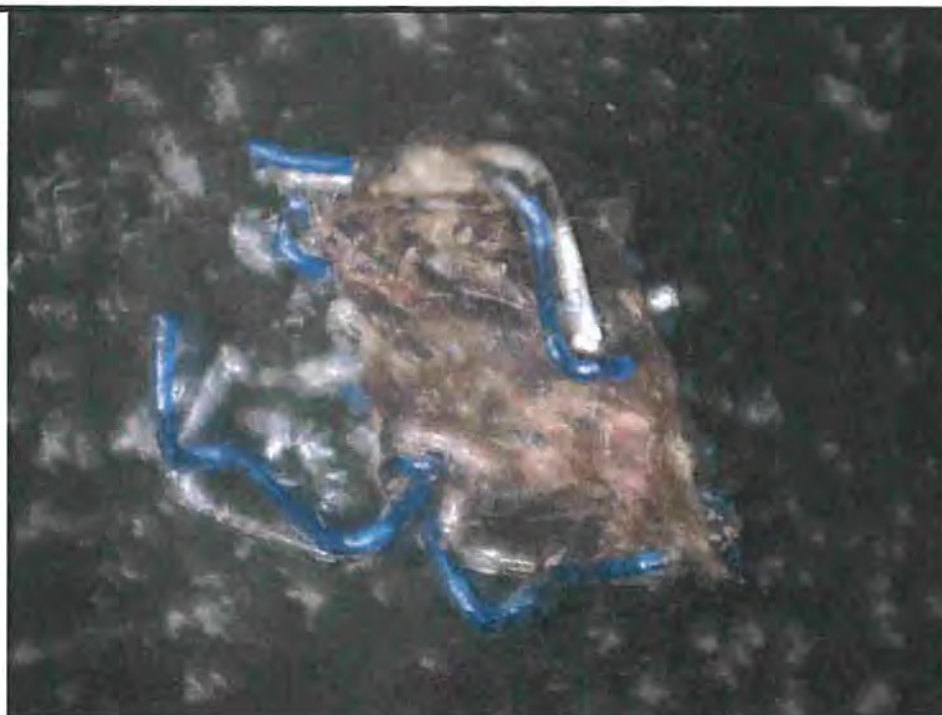


Figure 61

Optical

Comment:

J8041-13675

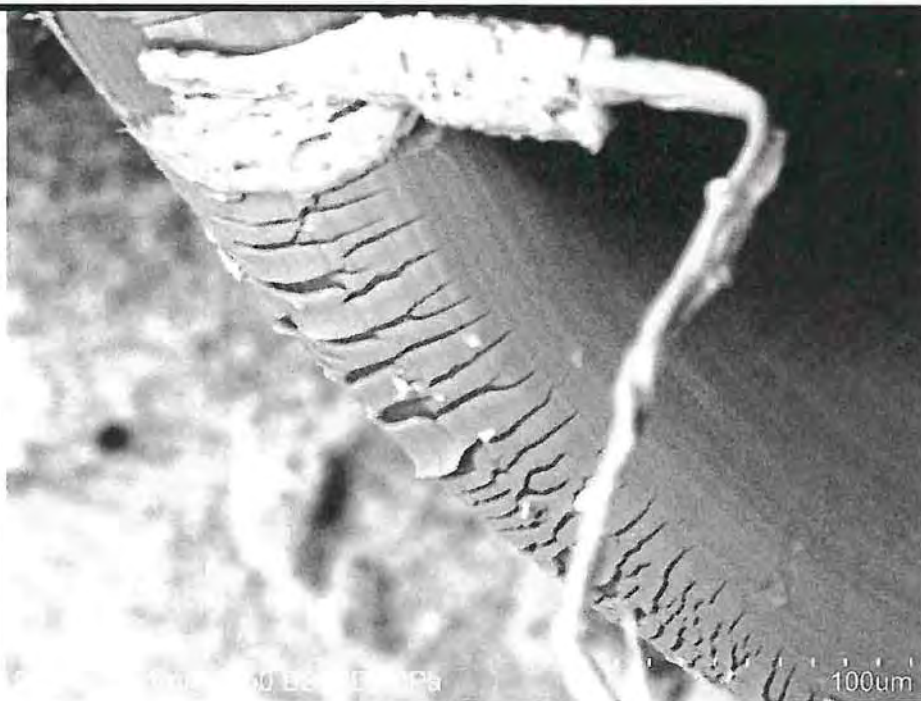


Figure 62

Mag = 450X

Voltage = 20kV

Comment:

J8041-13675

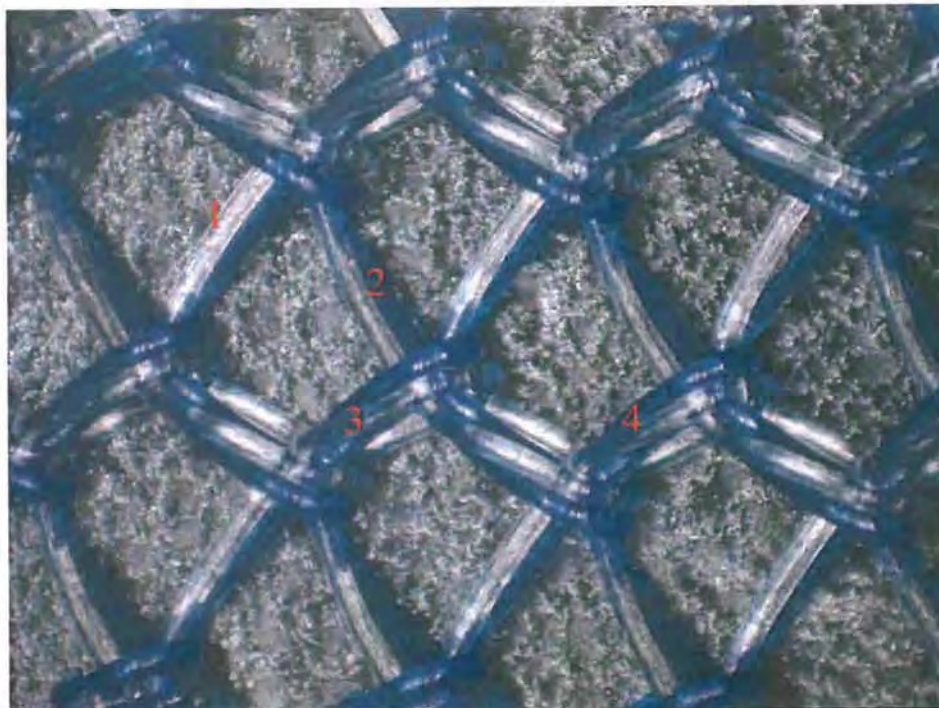


Figure 63

Optical Image

Comment:

Sample 13444
Lot# 3436364
Formalin Treated



Figure 64

Mag = 350X

Voltage = 20kV

Comment:

Sample 13444
Lot# 3436364
Formalin Treated

SEM-EDX

Background and Method

Scanning Electron Microscopy with Energy Dispersive X-ray Spectroscopy (SEM-EDX) is similar to SEM as described above, but with the addition of an Energy Dispersive X-ray Spectrometer (EDX). The purpose of the EDX is to identify the elemental composition of the sample. It does this by using an electron beam to excite the electrons in the various atoms of the sample. The return of the electrons from the excited state to the ground state is associated with the release of a characteristic X-ray which can be used to identify the elements present. All elements from atomic number 4 (Be) to 92 (U) can be detected including light elements such as oxygen and nitrogen.^{59,60} It is also possible to scan the beam in a television-like raster and display the X-ray line intensity producing element distribution images or maps. Detection limits for SEM-EDX typically are in the 1000 ppm range (.1%).

It is generally observed that EDX is not as precise for lighter elements due to the small corresponding change in percent weight associated with changes in concentration for lighter elements. This makes the detector less sensitive for these elements and requires a larger change in concentration to obtain a measurable signal. In the current work, a silicon drifts detector was utilized which shows improved performance for lighter elements as compared to older technologies.^{61,62,63}

Sample Preparation

The same portion of sample used for SEM was also applied for SEM-EDX. Please see the SEM sample preparation section for additional details. Five explant samples, one control sample and two formalin treated control samples were analyzed (See Tables 1 and 2).

Results

SEM-EDX results are shown for the control sample in **Figures 65-66**. The location sampled is indicated in the figure by a pink box. Only carbon and a very small signal for oxygen were observed in the control samples.

Example analysis results for the explant samples are shown in **Figures 67-76**. Spectra were acquired on the explant samples in both the cracked regions, which were attached to the fiber surface, and on exposed non-cracked regions of the fiber surface.

⁵⁹ Andrew R. Barron, *An Introduction to Energy Dispersive X-ray Spectroscopy* <http://cnx.org/content/m43555/1.1/>

⁶⁰ Jan W. Gooch, *Analysis and Deformation of Polymeric Materials: Paints, Plastics, Adhesives and Inks*, (Plenum Press, New York, USA) 1997, 19-21

⁶¹ Dale E. Newbury and Nicholas W. M. Ritchie "Elemental mapping of microstructures by scanning electron microscopy-energy dispersive X-ray spectrometry (SEM-EDS): extraordinary advances with the silicon drift detector (SDD)" *J. Anal. At. Spectrom.*, 2013, 28, 973-988

⁶² Ralf Terborg and Martin Rohde(2003). *Microscopy and Microanalysis*, 9 (Suppl. 02), pp 120-121.

⁶³ Fiorini, C.; Kemmer, J.; Lechner, P.; Kromer, K.; Rohde, M.; Schulein, T., *Review of Scientific Instruments*, vol.68, no.6, pp.2461,2465, Jun 1997.

The explant samples were found to be primarily carbon in both the cracked and non-cracked regions. Additional elements detected are shown in **Table 3**. A comparison is provided with the control sample. The location from which the spectrum was acquired is indicated in the figures by pink boxes. A comparison of the two regions shows that the cracked regions showed increased intensity for the elements other than carbon. This included increased intensity for oxygen.

An analysis was also performed on two of the control samples which were treated with formalin. These samples showed similar results as compared to the control samples prior to formalin exposure with the exception that some white spots were infrequently observed. **Figure 77** shows an example of this type of morphology. When examined, these white spots were shown to contain high concentrations of sodium and oxygen with some weak signals for chlorine.

The presence of aluminum in the sample results is due to the specimen holder used to fix the sample for analysis and is not considered significant.

Table 3 New Elemental Composition as Determined by SEM-EDX																
Element	Sample Identification Non-Cracked Region							Sample Identification Cracked Region							Control Sample	
	13400	13403	13409	13408	13418	13674	13675	13400	13403	13409	13408	13418	13674	13675		
Carbon	x	x	x	x	x	x	x	x	x	x	x	x	x	x	Lot# 3436364	
Nitrogen									X		X					
Oxygen	x	x	x	x	x	x	x	X	X	X	X	X	X	X		x
Sodium	x		x			x		X	X	X	X	X	X	X		
Phosphorus	x		x					X		X	X	X	X	X		
Sulfur	x		x		x			X		X	X	X	X	X		
Aluminum	x	x		x	x	x		x	x		x	x	x			
Calcium											X					

x = Detected

X = Element detected at a higher level in the cracked region

Scientific Opinion

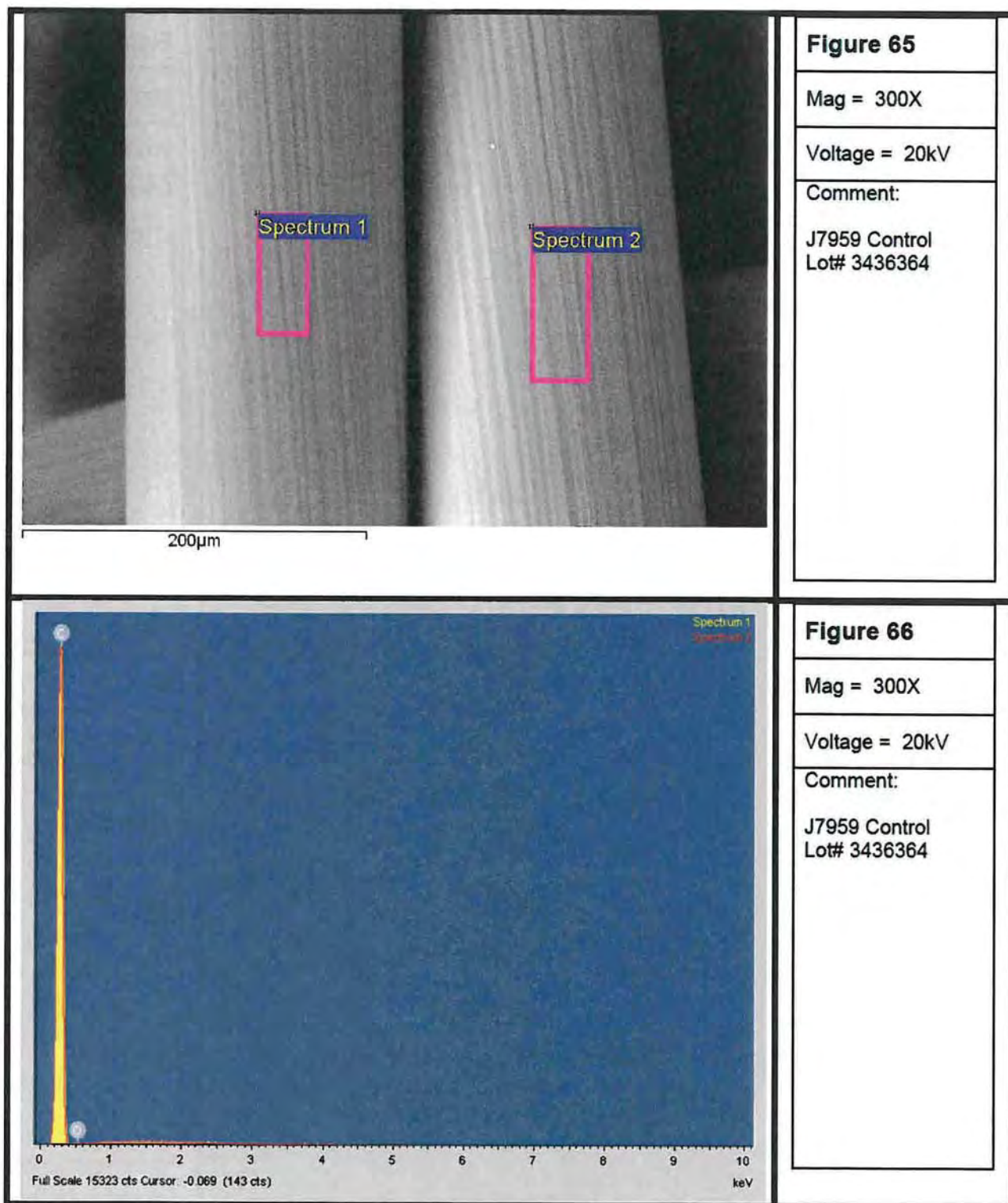
Based on my review of the scientific literature, my knowledge, experience and training, and my examination of the data, it is my opinion to a reasonable degree of scientific certainty that the data supports the contention that the cracked regions are not nitrogen containing and therefore not protein or other absorbed biological material.

It is further noted that distinct morphologies can be observed for material consistent with biological matrix, as opposed to cracked fiber surface. Spectra were taken from material suspected to be tissue adhering to the fibers in samples 13403 and 13408 to confirm that this material contained nitrogen (proteinaceous material contains nitrogen). The presence of nitrogen was confirmed. A comparison of the morphology of the biological material (nitrogen containing) and the regions found to not contain nitrogen is shown in **Figures 67-68 and 69-70** (no nitrogen) and **71-72** (contains nitrogen). The difference in the texture of these two materials can be easily observed allowing them to be distinguished visually. The two different morphologies have been highlighted in **Figure 71** and labeled to show this distinction.

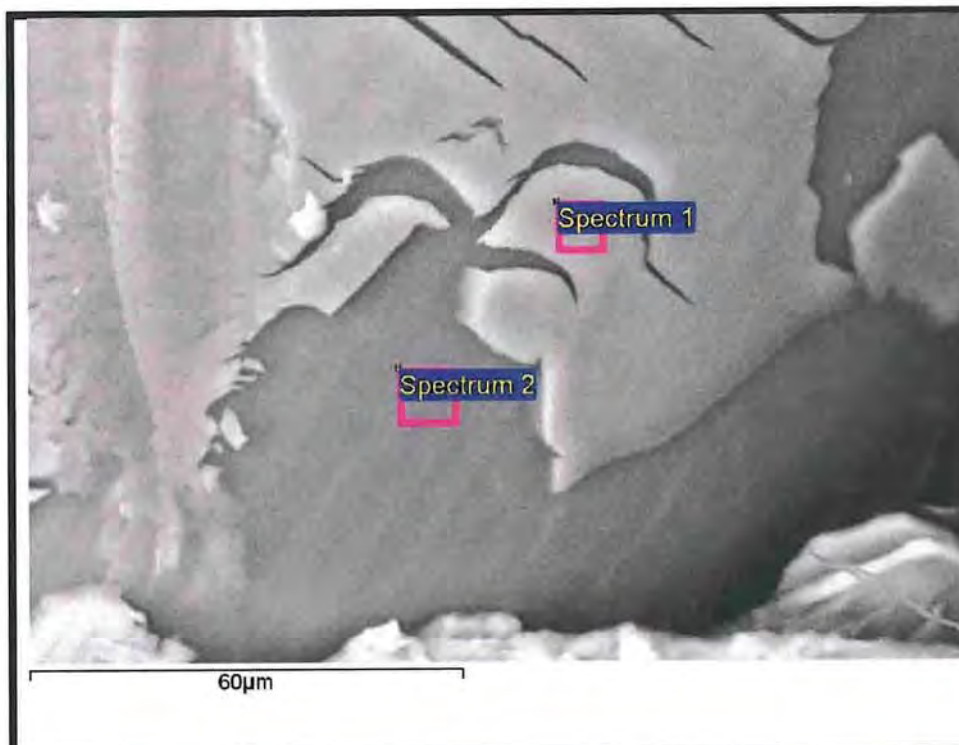
A significant increase is noted in the oxygen, sodium, sulfur and phosphorus content in the cracked regions as compared to the non-cracked regions. This increase in concentration is even more significant when comparing the cracked regions and the control samples. This indicates that the cracked regions have an increased extent of oxidation as compared to the non-cracked regions. The presence of phosphorous and sulfur, is most probably due to either sulfate and phosphate or increased oxidation of the polymer. In either case, it is noted that these components accumulate predominately in the cracked regions. Nonetheless, in some cases there is evidence of excess oxygen in the non-cracked regions of the explant samples even though no P (Sample # 13403, 13408 and 13418) and S (Sample # 13403 and 13408) are detected. This suggests that there is an increase in oxygen even if no sulfate and phosphate are present. This is evident from **Figures 65-66** (Control) and **71-72** (Sample 13403). As seen from **Figures 65-66 and 71-72**, the relative amounts of oxygen observed is greater in both the cracked and non-cracked regions of Sample 13403 relative to the control thereby indicating oxidation. Therefore, it is my opinion, to a reasonable degree of scientific certainty that the explant samples demonstrate evidence of oxidation/degradation.

In order to rule out whether the formalin contributed to increased oxidation, formalin treated fibers were tested and found to be indistinguishable from the control. Thus, it is my opinion, to a reasonable degree of scientific certainty, that the formalin did not cause any oxidation of the fibers. A modest number of white spots are observed on formalin treated fibers (**Figure 77**), which are easily distinguished from the cracked fiber morphology. These white spots are consistent with salt deposits (NaCl).

Control Sample



Explant Samples

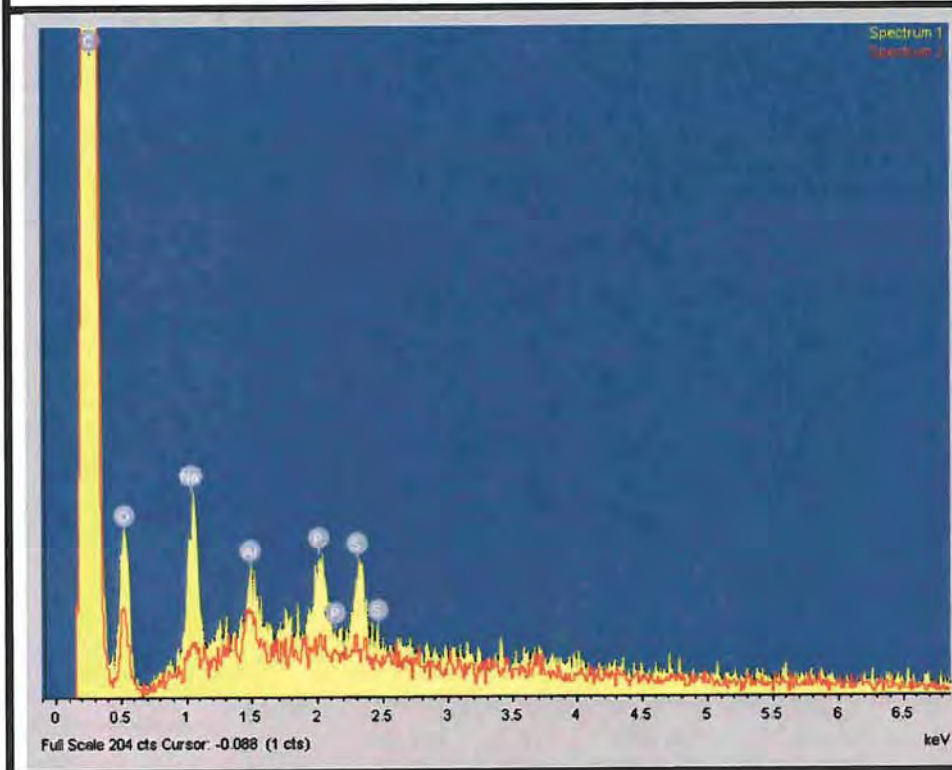
**Figure 67**

Mag = 1kX

Voltage = 20kV

Comment:

J7959 13400

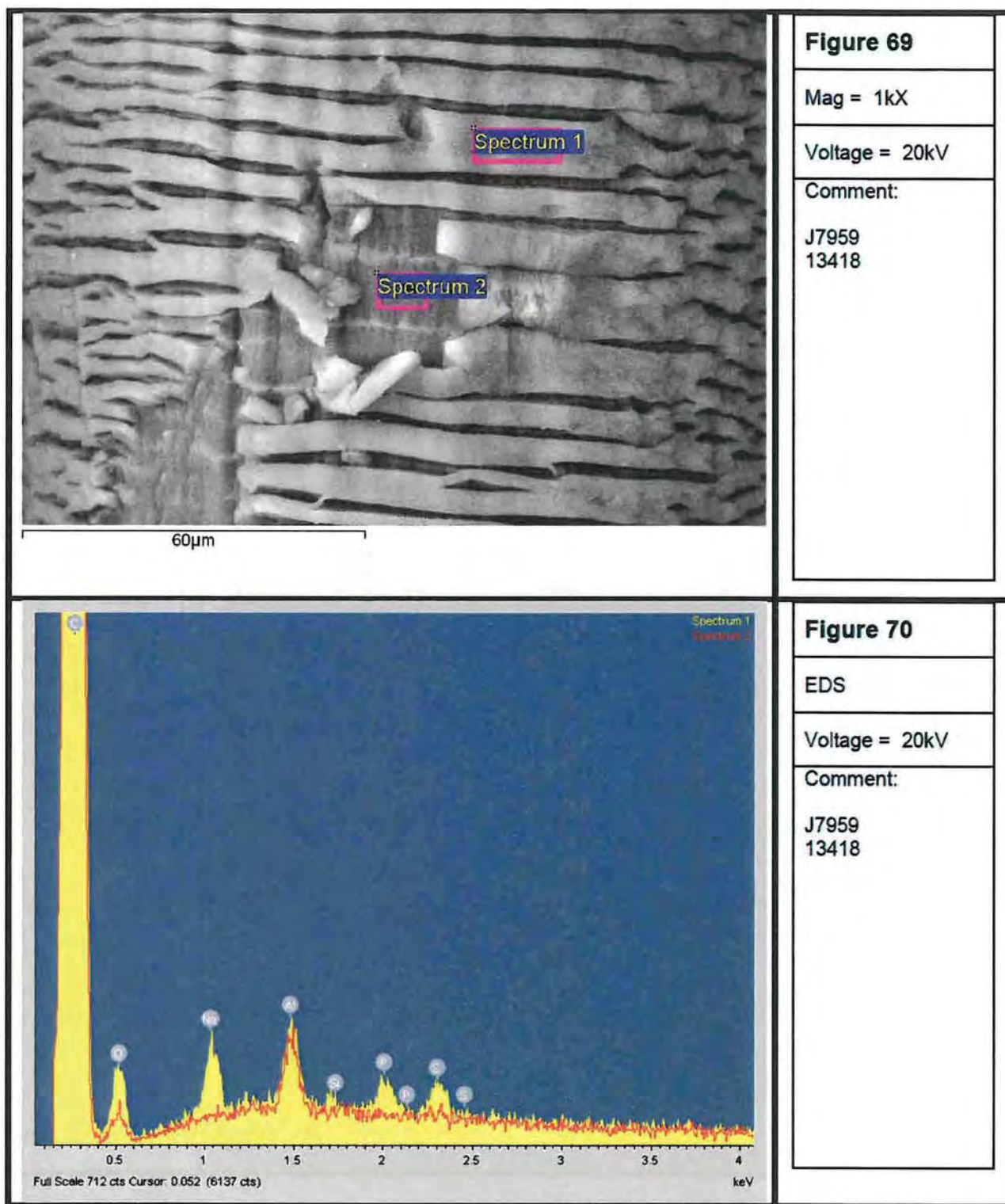
**Figure 68**

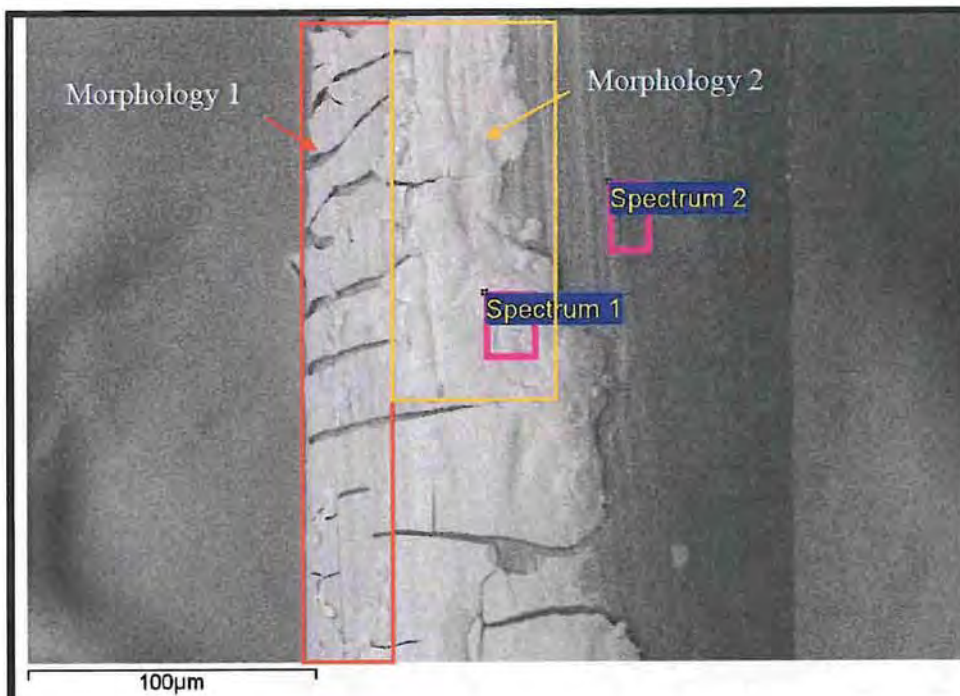
EDS

Voltage = 20kV

Comment:

J7959 13400

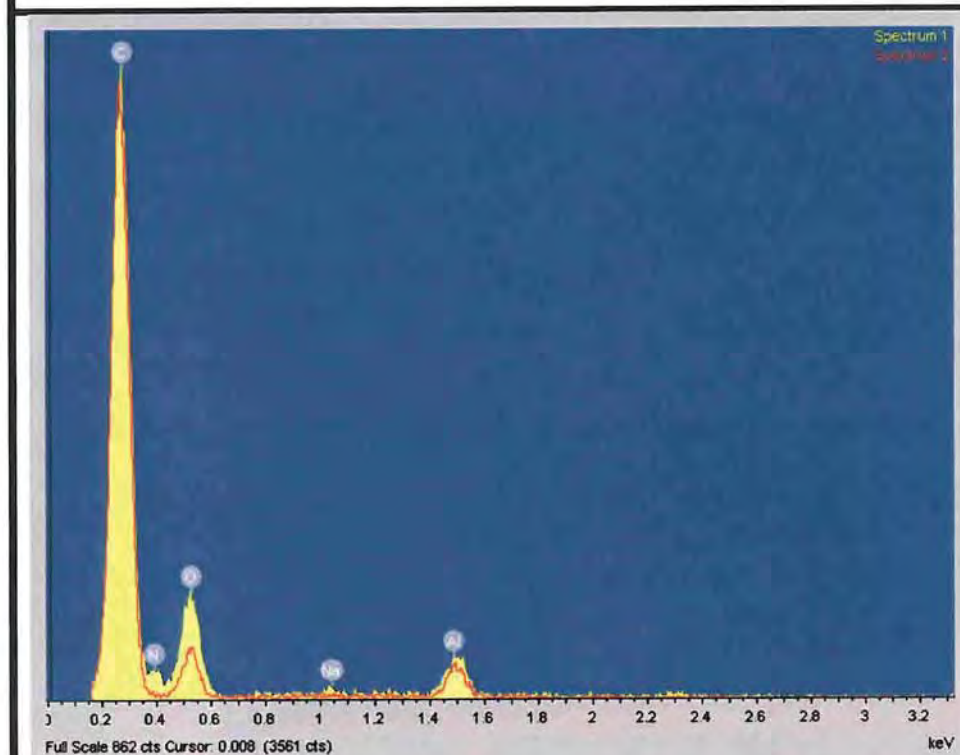


**Figure 71**

Mag = 400X

Voltage = 5kV

Comment:

J7959
13403**Figure 72**

EDS

Voltage = 5kV

Comment:

J7959
13403

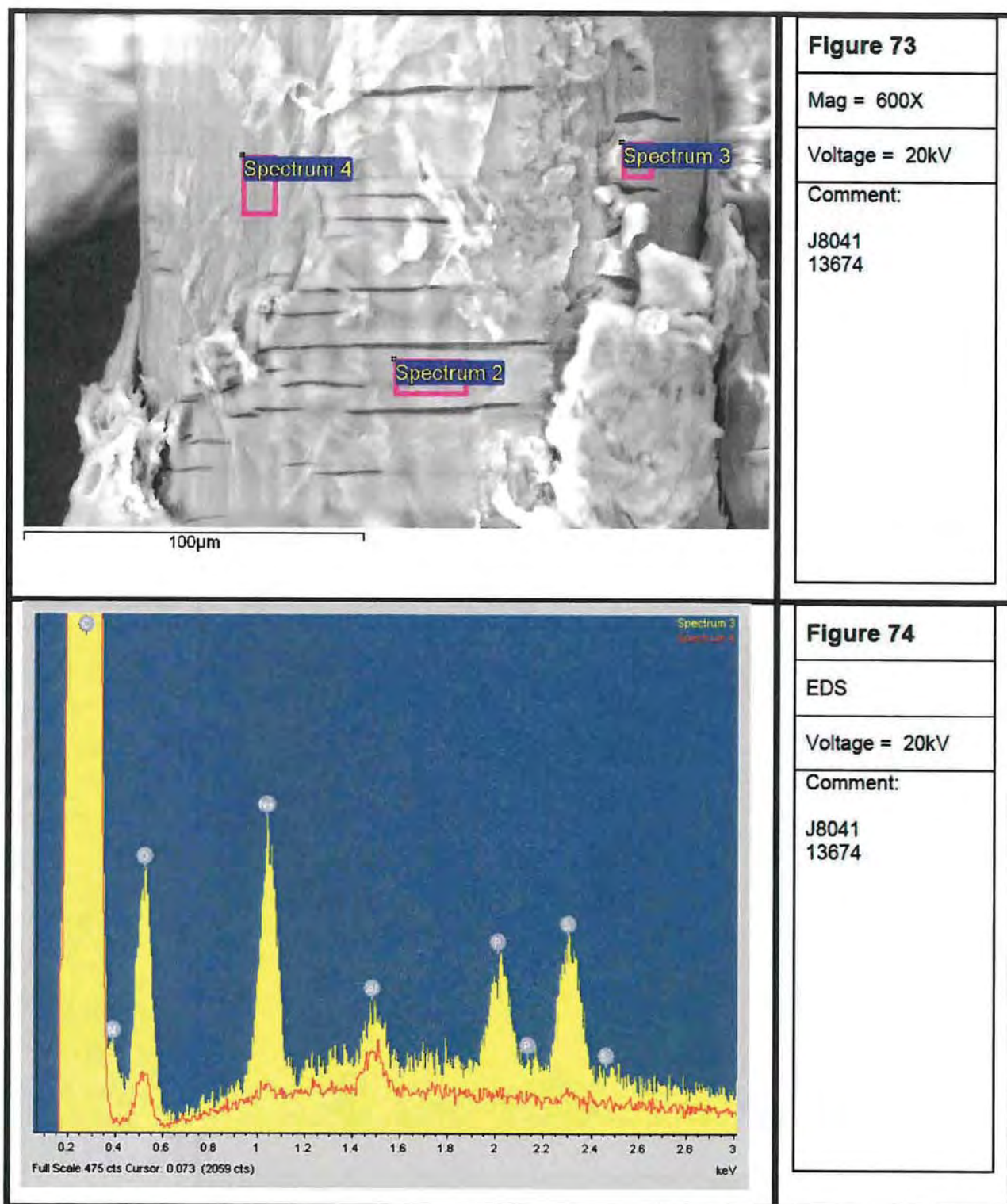


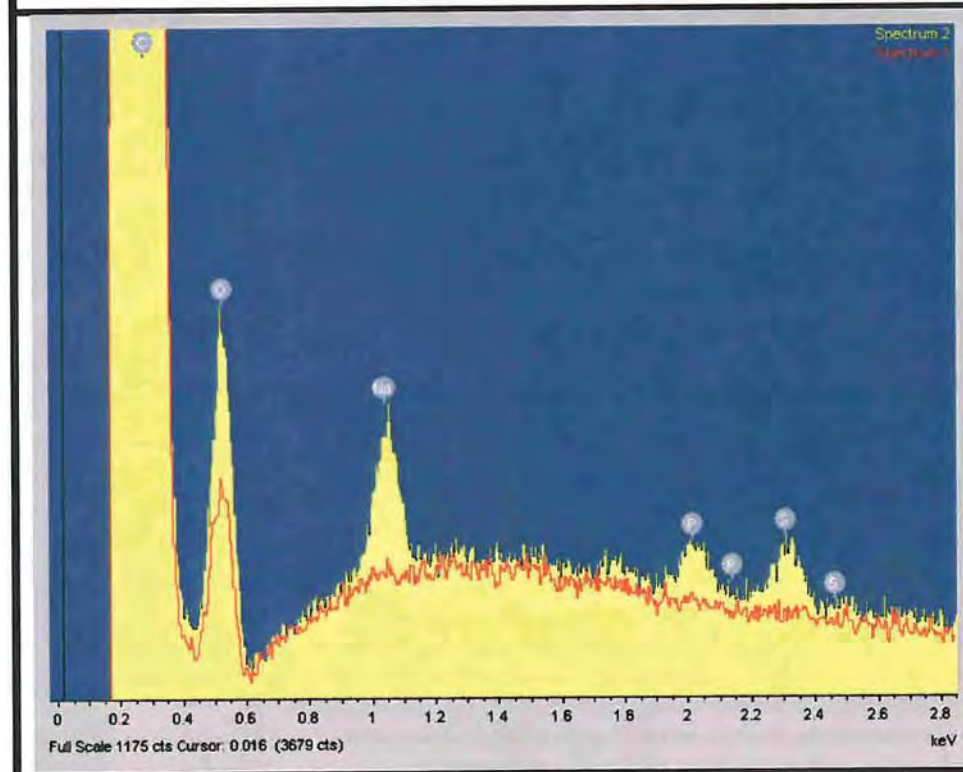
**Figure 75**

Mag = 400X

Voltage = 20kV

Comment:

J8041-13675

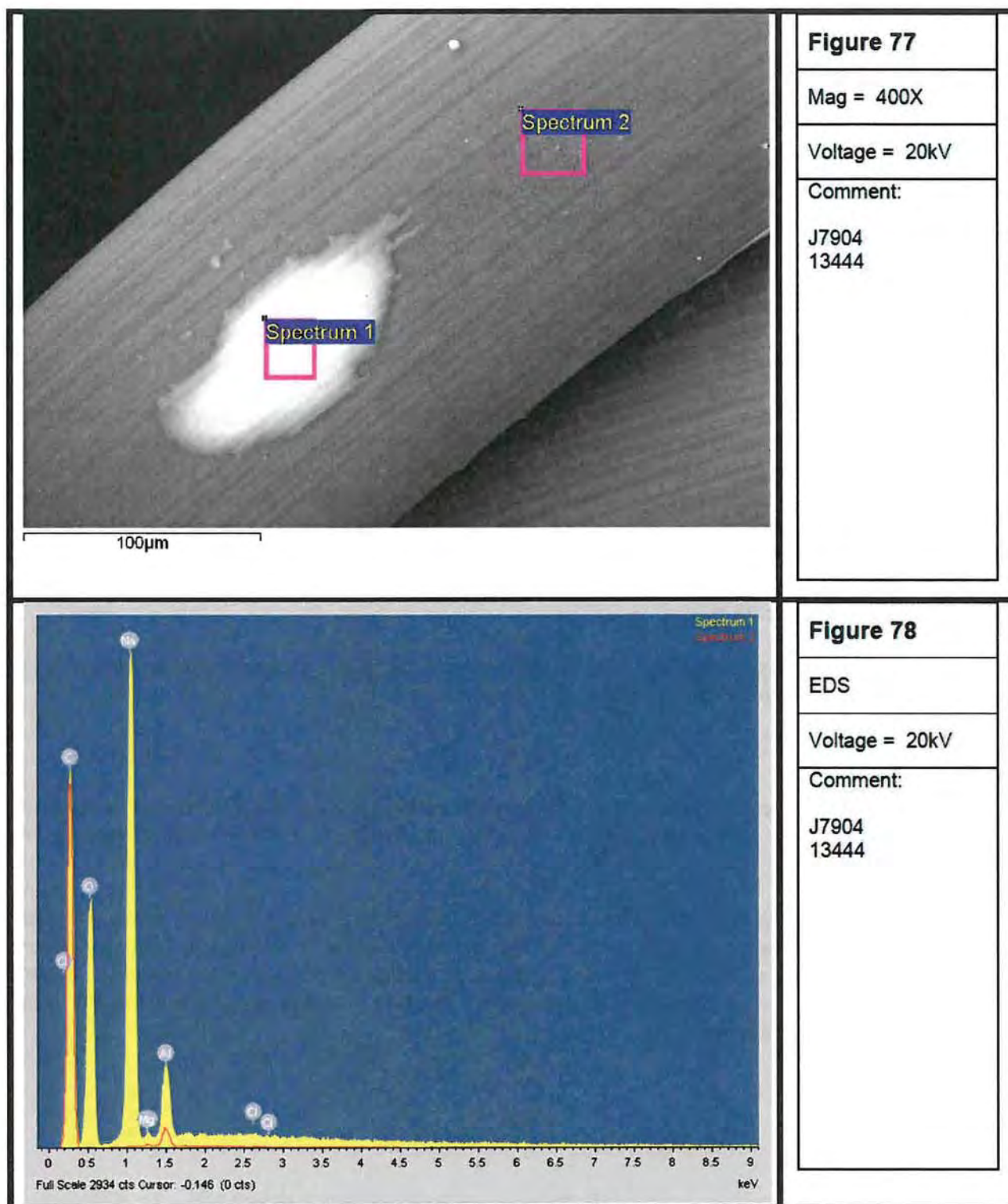
**Figure 76**

EDS

Voltage = 20kV

Comment:

J8041-13675



DSC

Background and Method

Differential Scanning Calorimetry (DSC)^{64,65,66} is a technique which measures the heat input required to achieve a change in sample temperature. It does this by heating the sample alongside a reference pan and measuring the difference in heat content required for the sample to achieve an equal increase in temperature as the reference.

DSC measures two key parameters for the purposes of this report, these are the enthalpy of fusion and the melt temperature. The enthalpy of fusion can be used to calculate the crystallinity present in the sample.

Changes in thermal history (exposure to heat and cold, processing temperatures) can affect the extent of crystallinity of a material. DSC uses multiple heat cycles to compare samples in their native state (1st heat cycle) and after a common thermal history is provided (2nd heat cycle). When comparing sample results, the 1st heating cycle is a measure of the heat history of a sample, while the 2nd heat is instructive as to differences in the chemistry of the samples which affect crystallization.

Sample Preparation

The fiber mesh was analyzed directly by DSC with no further sample treatment beyond what was described in the sample preparation sections.

Results

The samples were analyzed using a three-step heating program which consisted of the steps shown in Table 4. A control sample which was subjected to treatment with formalin was also analyzed.

The first heating cycle is representative of the samples in the state in which it was provided. The 2nd heating cycle is indicative of the polymer present in the sample after a common thermal history is provided. Figure 79 shows an example thermogram for one of the control samples and one of the explant samples. Data for the remaining samples is provided in the data section of this report.

⁶⁴ Edith A. Turi, *Thermal Characterization of Polymeric Materials* (Academic Press, New York), 1981.

⁶⁵ P. G. Laye, *Differential Thermal Analysis and Differential Scanning Calorimetry in Principles of Thermal Analysis and Calorimetry*, Ed. P. J. Haines, (The Royal Society of Chemistry, Cambridge, UK), 2002, 55-93.

⁶⁶ Nicholas P Cheremisinoff, *Thermal Analysis in Polymer Characterization Laboratory Techniques and Analysis* Nicholas P Cheremisinoff Ed. (Noyes Publications, Westwood, NJ, USA), 1996, 17-24.

Table 4 - DSC Heating Conditions			
Heating Cycle	1st Heat	Cooling Cycle	2nd Heat
Condition	-90°C to 200°C at 10°C/min	200°C to -90°C at 10°C/min	-90°C to 200°C at 10°C/min

The explant samples showed a single thermal transition (melt) at temperatures ranging from 158-166°C during the first heat analysis. The second heating pass also showed a single melt transition at temperatures ranging from 161-165°C. **Table 5** shows the calculated melt points and enthalpy of fusion values for the explant samples as obtained during the 1st and 2nd heating passes.

The control samples also showed a single thermal transition (melt) at temperatures ranging from 160-168°C during the first heat analysis. The second heating pass also showed a single melt transition at temperatures ranging from 163-164°C. **Table 6** shows the same values for the 2nd heating cycle.

Table 7 shows the average values obtained for the enthalpy of fusion with the data sorted based on their known extent of cracking (none, moderate, highly cracked) as determined in SEM. A general trend was observed in the data in that the extent of crystallinity went down as the extent of cracking went up. In the first heat cycle, the non-cracked explant samples were observed to show the highest average enthalpy of fusion (crystallinity) followed by the control lots, then the moderately cracked explant samples and the highly cracked samples which showed the lowest value.

In the second heat cycle, the control lots were observed to show the highest average enthalpy of fusion (crystallinity) followed by the non-cracked explant samples, moderately cracked explant samples and the highly cracked samples which showed the lowest value.

To aid in identifying the significance of the data, a control sample (Lot # 3405474) was analyzed five times to provide a measure of method precision. The sample was found to produce the values shown in **Table 8**. The standard deviations were found to be 2.6 J/g and 2.5 J/g for the 1st and second heat respectively.

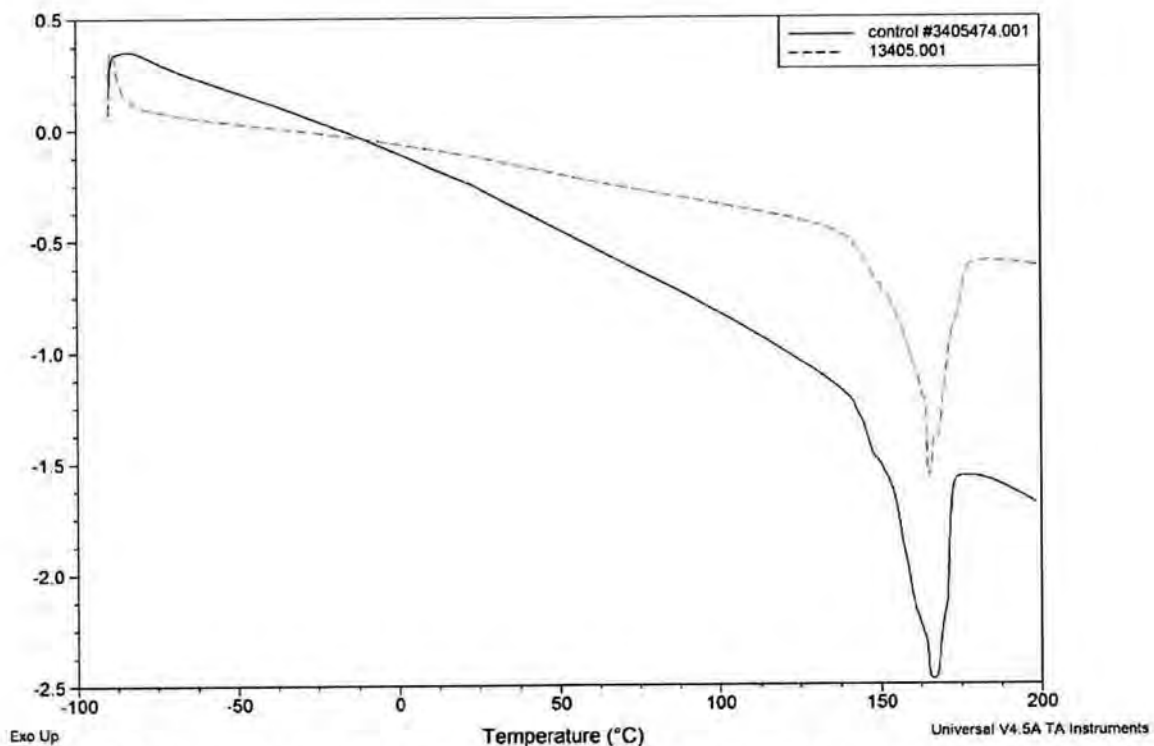


Figure 79: DSC overlay plot showing 1st heat cycle for control sample and explant sample. See legend in figure for sample identifications.

Table 5 DSC Results Explant Samples					
Sample ID	Mass (mg)	Tm (°C) 1st heat	Heat of Fusion for Tm (J/g) 1st heat	Tm (°C) 2nd heat	Heat of Fusion for Tm (J/g) 2nd heat
Not Cracked					
13419	1.014	165.90	88.90	163.16	74.14
13421	0.968	166.34	84.28	164.16	66.50
Moderately Cracked					
13401	1.004	162.25	83.25	162.95	72.75
13408	0.964	164.19	80.10	164.91	68.87
13411	1.048	165.64	73.87	163.74	62.65
13420	1.010	165.37	87.54	164.35	73.77
Highly Cracked					

Table 5 DSC Results Explant Samples					
Sample ID	Mass (mg)	Tm (°C) 1st heat	Heat of Fusion for Tm (J/g) 1st heat	Tm (°C) 2nd heat	Heat of Fusion for Tm (J/g) 2nd heat
13400	0.964	165.91	75.14	163.43	62.67
13402	1.002	164.44	63.29	161.64	59.83
13407	1.050	164.24	83.09	162.93	70.85
13409	0.968	165.42	80.83	163.57	69.34
13414	0.958	163.76	88.55	163.15	69.82
13415	0.980	158.11	77.74	164.37	63.37
13416	1.082	162.29	56.53	163.35	54.10
13418	1.040	162.96	80.98	163.02	66.67
13674	1.040	163.30	69.77	163.92	59.20
13675	0.9760	160.29	87.35	162.99	69.82

Table 6 DSC Results Control Samples						
Control ID	Run	Mass (mg)	Tm (°C) 1st heat	Heat of Fusion for Tm (J/g) 1st heat	Tm (°C) 2nd heat	Heat of Fusion for Tm (J/g) 2nd heat
3405405	1	0.968	160.28	93.41	163.85	71.78
	2	1.032	165.69	88.36	163.84	78.24
3436364	1	0.968	165.87	79.55	163.68	69.74
	2	0.974	165.70	90.43	163.63	75.06
3422128	1	0.978	167.59	79.09	164.17	69.22
	2	0.954	164.59	82.47	164.00	72.09
3398135	1	1.002	166.98	81.42	163.64	67.59
	2	1.018	166.91	73.58	163.87	68.96
3405474	1	1.008	165.88	86.15	163.92	73.91
	2	0.960	165.58	81.19	164.32	70.79
	3	0.984	168.07	81.37	163.71	77.65
	4	0.996	165.66	84.30	163.93	73.08
	5	1.020	164.85	86.84	164.07	73.46
3405460	1	0.986	166.65	75.46	163.35	69.53
	2	0.960	166.22	88.20	163.65	67.71
3422128 (formalin)	1	1.018	164.82	84.37	163.47	70.08
	2	0.970	166.84	80.75	163.62	74.64

Table 7 Average Enthalpy Values Sorted by Extent of Cracking		
Cracking Obs. in SEM	Average Enthalpy	Standard Deviation
1st Heat		
None	86.6	3.3
Moderate	81.2	5.8
Highly Cracked	76.3	9.8
Control Samples	83.5	5.5
2nd Heat		
None	70.3	5.4
Moderate	69.5	5.0
Highly Cracked	64.6	5.4
Control Samples	71.9	3.3

Table 8			
Replicate Analysis for Control Sample			
Lot# 3405474			
Sample ID	Mass (mg)	Tm (°C)	Heat of Fusion for Tm (J/g)
1st Heat			
3405474	1.008	165.88	86.15
	0.96	165.58	81.19
	0.984	168.07	81.37
	0.996	165.66	84.3
	1.02	164.85	86.84
Average Heat of Fusion		Standard Dev. Heat of Fusion	
84.0		2.6	
2nd heat			
3405474	1.008	163.92	73.91
	0.96	164.32	70.79
	0.984	163.71	77.65
	0.996	163.93	73.08
	1.02	164.07	73.46
Average Heat of Fusion		Standard Dev. Heat of Fusion	
73.8		2.5	

Scientific Opinion

Based on my review of the scientific literature, my knowledge, training and experience, and my examination of the data, it is my opinion to a reasonable degree of scientific certainty that the data supports the contention that the more highly cracked samples are showing a decrease in crystallinity as evidenced by the decreased average value for the enthalpy of fusion. This trend was observed in both the first and second heat analyses. The non-cracked and control lots also showed similar average enthalpy values. The spread in the data is relatively large (standard deviation) suggesting that a change in crystallinity is not a prerequisite for cracking but rather a general correlation.

As crystallinity (ordered polymer chains) decreases, the amount of amorphous material (disordered polymer chains) increases. The amorphous regions are well known to be more susceptible to degradation and chemical attack.^{67,68,69} This is a general phenomena which is true for polypropylene as well as other polymer types. Decreased crystallinity would also be expected to affect mechanical properties. Many examples exist in the literature showing that changes in polypropylene crystallinity effects material properties such as hardness and stiffness.⁷⁰

It was further observed that the average melt point for the samples (~165°C) was lower than the typical values expected for polypropylene (typical value ~175°C).^{71,72,73} The polymer melt point is a function not only of sample chemistry but also molecular weight and sample tacticity.

The observation of both a decrease in crystallinity and melt point demonstrates the mesh will be more susceptible to environmental stress cracking. As mentioned above, environmental stress cracking is the process whereby normal body chemicals such as cholesterol and fatty acids etc. enter the polymer chains causing them to expand and rupture the surface of the polymer. These initial cracks continue to grow until we see the large cracks in the SEM pictures.⁷⁴

Therefore, it is my opinion, to a reasonable degree of scientific certainty, that the levels of amorphous material as well as the observed decrease in the melt point demonstrate susceptibility of the explant fibers to environmental stress cracking (ESC).

⁶⁷ Wen Zaiqing, H.U. Xingzhou, Shen Deyan, The FTIR Studies Of Photo-Oxidative Degradation Of Polypropylene *Chinese Journal of Polymer Science* (1988) 6 285-288.

⁶⁸ Yutaka Tokiwa, Buenaventura P. Calabia, Charles U. Ugwu, Seiichi Aiba, *Int J Mol Sci.* 2009 September; 10(9): 3722-3742.

⁶⁹ T Labour, C Gauthier, R Séguéla, G Vigier, Y Bomal, G Orange, *Polymer, Volume 42, Issue 16, July 2001, Pages 7127-7135*

⁷⁰ Xiao Xun Zhang et al. (2011), *Advanced Materials Research*, 239-242, 2809

⁷¹ Cho, K., Li, F., Choi, J., "Crystallization and melting behavior of polypropylene and maleated polypropylene blends." *Polymer*, Vol. 40, pg. 1719-1729, 1999.

⁷² Moore, E., (1996) *Polypropylene Handbook, Polymerization, Characterization, Properties, Processing and Applications*, Hanser Publishing, New York.

⁷³ Brandrup, J., Immergut, E., Grulke, E., (1999) *Polymer Handbook*, John Wiley & Sons, Inc., New York.

⁷⁴ Arnaud Clave, Hanna Yahi, Jean-Claude Hammou, Suzelei Montanari, Pierre Gounon and Henri Clave, "Polypropylene as a reinforcement in pelvic surgery is not inert: comparative analysis of 100 explants" *International Urogynecology Journal and Pelvic Floor Dysfunction* 21 (2010) 261-270.

FTIR Microscopy

Background and Method

FTIR microscopy is a widely accepted tool in the chemical characterization and imaging of polymeric materials.^{75,76,77} FTIR works by irradiating the test samples with infrared radiation (4000 to 600 cm^{-1}). When exposed to infrared radiation, a molecule selectively absorbs infrared frequencies that match those of its allowed vibrational modes. Therefore, the infrared absorption spectrum of a material reveals which functional groups are present in its structure.

FTIR can be coupled with Optical Microscopy (OM) to allow for analysis of small sample particles. This combination is referred to as FTIR microscopy.

Sample Preparation

FTIR microscopy was performed on particulates which were removed from the surface of the fiber mesh directly. This was accomplished by placing a fiber onto an infrared transmitting substrate and rolling it, using a fresh disposable scalpel to lightly apply pressure to the fiber during the rolling process. The residue thus transferred was analyzed using the FTIR microscope in transmission mode.

Results

Control

A control sample was initially analyzed (lot 3422128). **Figure 80** shows the resulting FTIR spectra. The major absorption bands for polypropylene were observed. The FTIR results indicate that the polypropylene was isotactic as bands at 998 and 840 are only present in the isotactic form of polypropylene.⁷⁸ **Table 9** shows the band identifications for polypropylene.

Table 9	
Polypropylene bands	
IR Frequency	Functional Group
2948, 2916, 2876, 2836 cm^{-1}	C-H Stretch
1456 cm^{-1}	CH ₂ deformation
1376 cm^{-1}	CH ₃ deformation
1166 cm^{-1}	Isotactic
998 cm^{-1}	Isotactic
974 cm^{-1}	Isotactic
840 cm^{-1}	Isotactic

⁷⁵ Craver, C.D., Provder, T., *Polymer Characterization, Physical Properties, Spectroscopic, and Chromatographic Methods*, Advances in Chemical Series 227, ACS, Washington DC 1990, 333-356.

⁷⁶ Fawcett A.H., *Polymer Spectroscopy*, John Wiley and Son, 1996, New York, NY, 173-202.

⁷⁷ *The Infrared Spectra Atlas of Monomers and Polymers*, Sadtler Research Laboratories, Philadelphia, PA 1983.

⁷⁸ *The Infrared Spectra Atlas of Monomers and Polymers*, Sadtler Research Laboratories, Philadelphia, PA 1983.

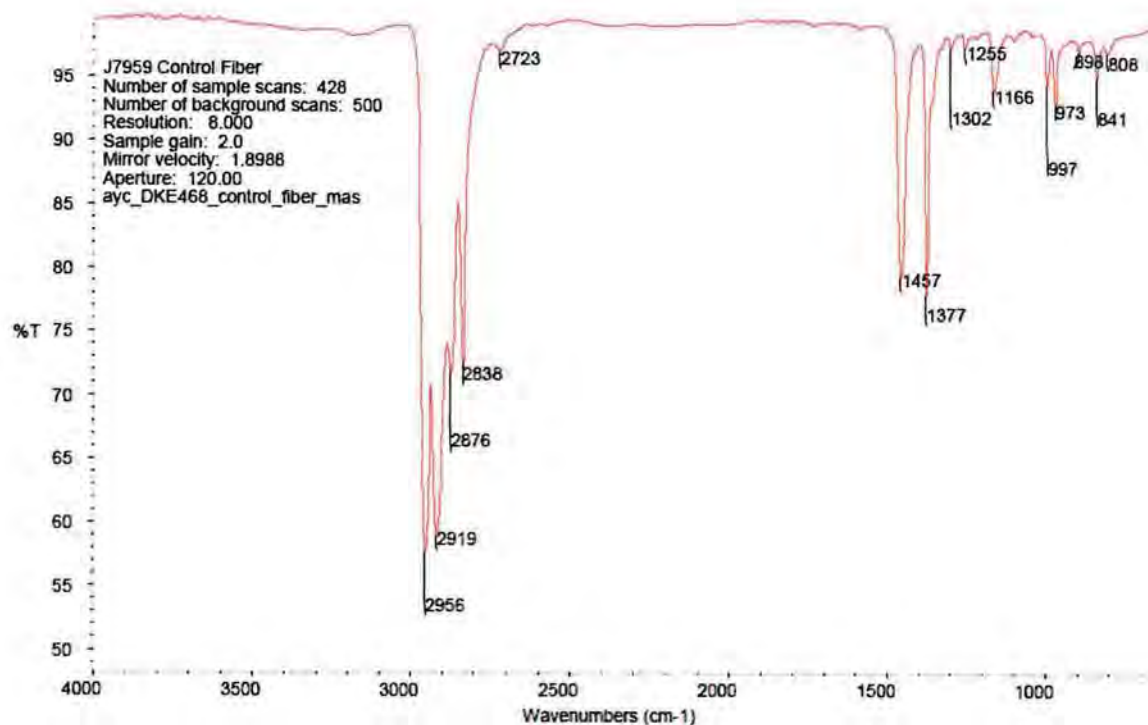


Figure 80: FTIR spectrum for control lot 3422128.

Explant Samples

The explant samples were found to produce a series of plate-like pieces or shards (particulates) when rolled on the FTIR substrate. **Figures 81, 83 and 85** show examples of several different particles or shards which were collected. **Figures 82, 84 and 86** show the corresponding FTIR spectrum taken of each shard. **Figure 87** shows an overlay of the spectrum for the shard sample collected from sample 13413 with the control sample lot# 3422128 and a reference spectrum for human albumin. Two bands were observed which were not present in the spectra of human albumin. These were observed at 1761 and 1044 cm^{-1} . A shoulder band was also observed at $\sim 1740 \text{ cm}^{-1}$ in most explant samples.

Scientific Opinion

Based on my review of the scientific literature, my knowledge, training and experience, and my examination of the data, it is my opinion to a reasonable degree of scientific certainty that the FTIR results demonstrate conclusively that the particulate matter released from the fibers contains a significant fraction of polypropylene. The shape of the particles can be compared with the SEM images and show a similar morphology to the cracked surface layer (See **Figure 81**). This demonstrates that particulate material from the fibers can be readily released following mechanical force. Thus, once the mesh in a woman's tissue begins to crack and peel, mechanical forces will cause these particulates to release from the surface of the fiber into surrounding tissue. SEM images of the cracked surface clearly showed very weak adhesion between the cracked surface layer and the remaining portions of the fiber.

Rolling of the cracked fibers on the infrared transparent substrate (after removal of the tissue) released the loosely held shards. Therefore, the shards observed in the FTIR microscopy of the explant samples are not an artifact of the sample cleaning method.

Strong evidence that the shards contain polypropylene is provided by the FTIR bands at 1457 and 1377 cm^{-1} . Additional bands at 997, 973 and 841 cm^{-1} increase the confidence of this identification. The strength of the FTIR absorbances indicates that the polypropylene is a significant fraction of the shards released from the explants. The molar absorptivity for alkyl bands is generally weak in comparison to other functional groups such as carbonyl groups and thus the strength of these bands suggests a high concentration.

Additional strong bands at 1654 and 1540 cm^{-1} are consistent with amide I and amide II bands (carbonyl bands). These bands are typical of proteinaceous material indicating that the particles also likely contain proteins or similar biological material.

Comparison of the spectrum for the explants shards with that for polypropylene and a human albumin reference material revealed two bands which were distinct from these materials (**Figure 87**). These bands would not be attributed to either polypropylene or the proteinaceous material. These were observed at 1761, ~1740 and 1044 cm^{-1} and are consistent with C=O and C-O-C functionality. The presence of these functional groups is consistent with oxidation of the polypropylene.

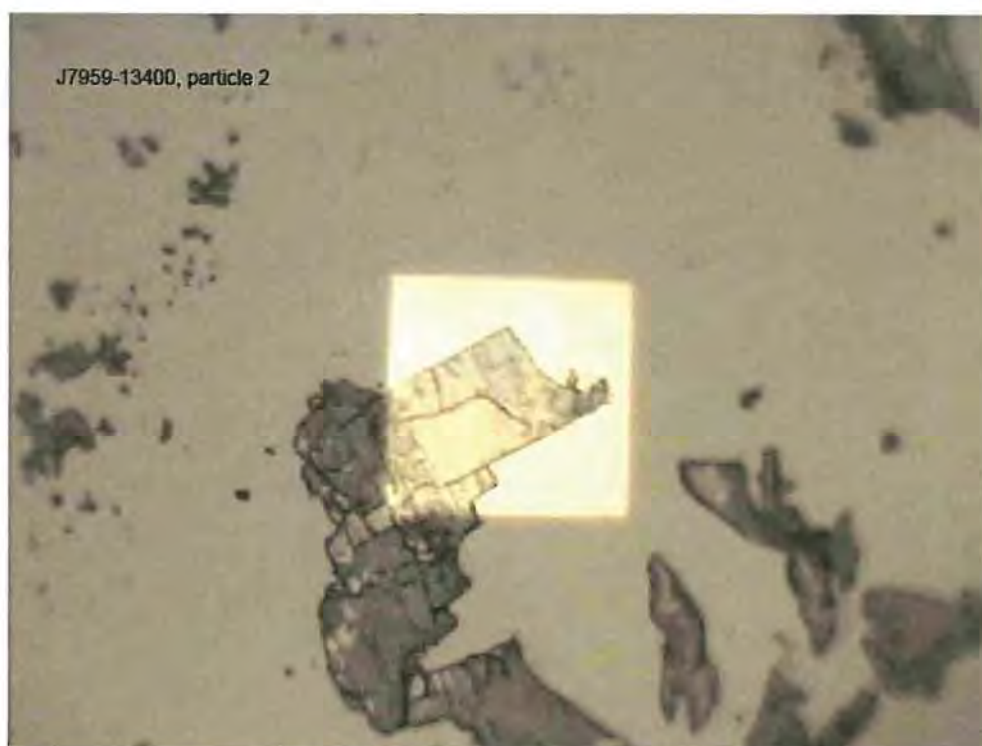


Figure 81: Microscopy images showing particles recovered from Explant sample 13400 (particle 2).

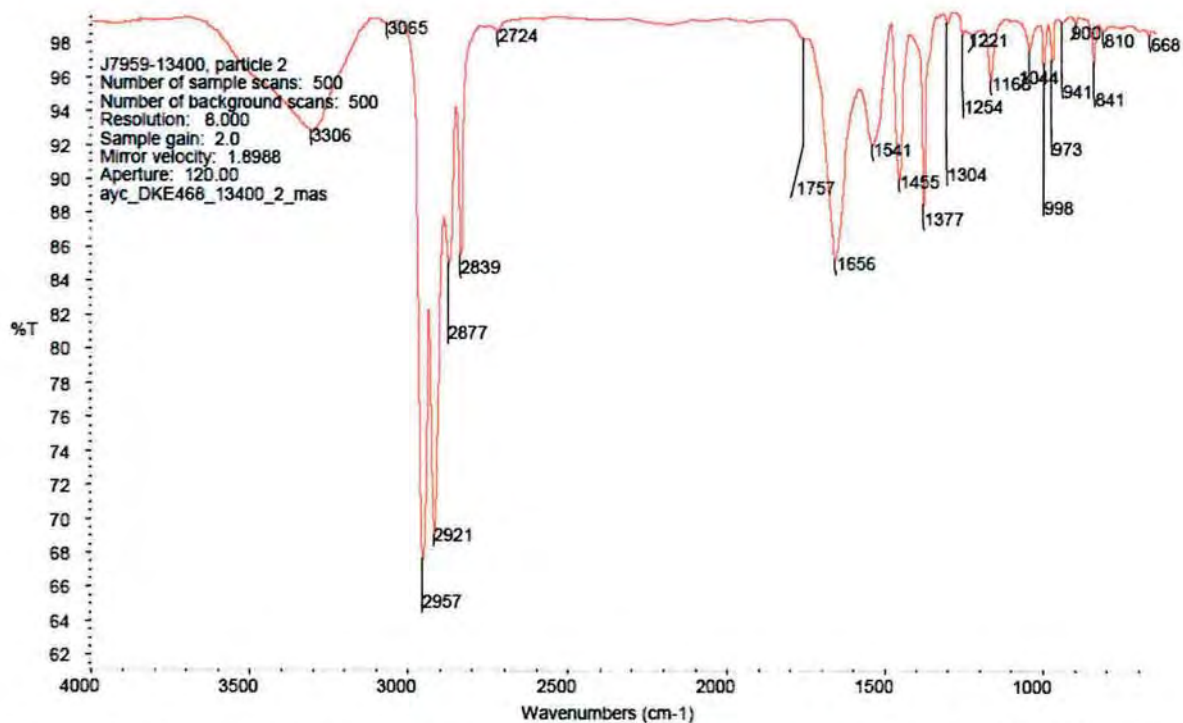


Figure 82: Example spectrum from particles collected from explant sample 13400 (particle 2).



Figure 83: Microscopy images showing particles recovered from Explant sample 13413 (particle 2).

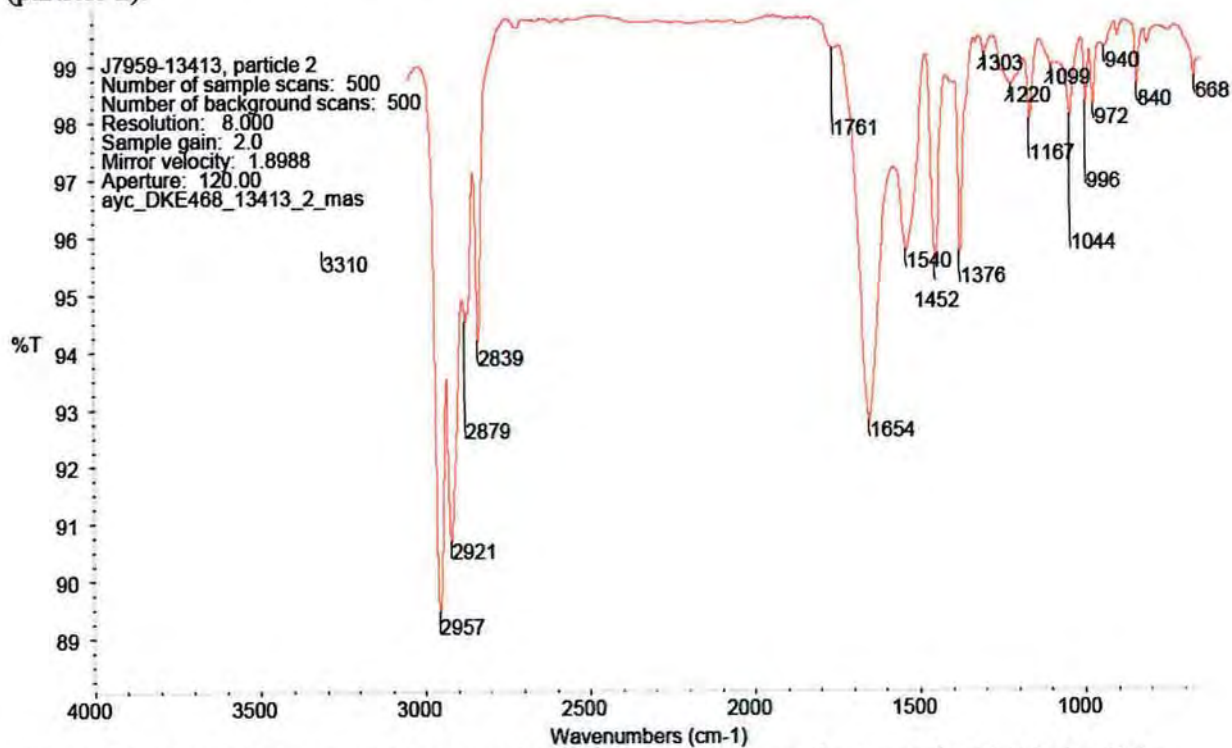


Figure 84: Example spectrum from particles collected from explant sample 13413 (particle 2).



Figure 85: Microscopy images showing particles recovered from Explant sample 13674 (particle 1).

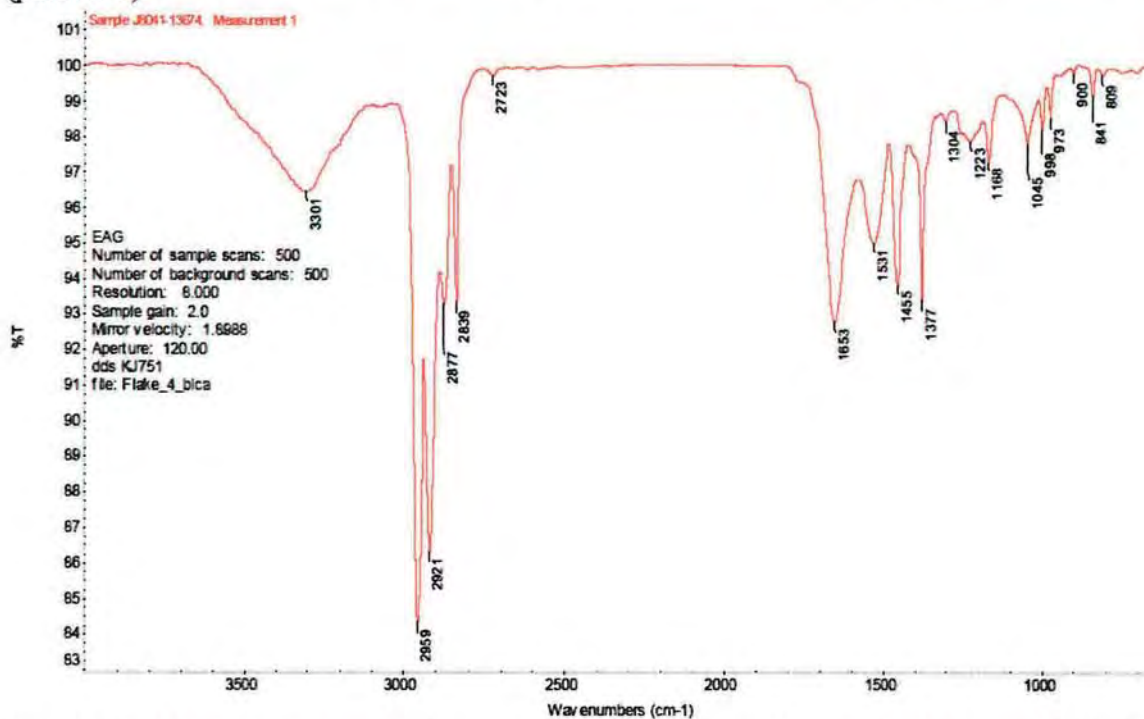


Figure 86: Microscopy images showing particles recovered from Explant sample 13674 (particle 1).

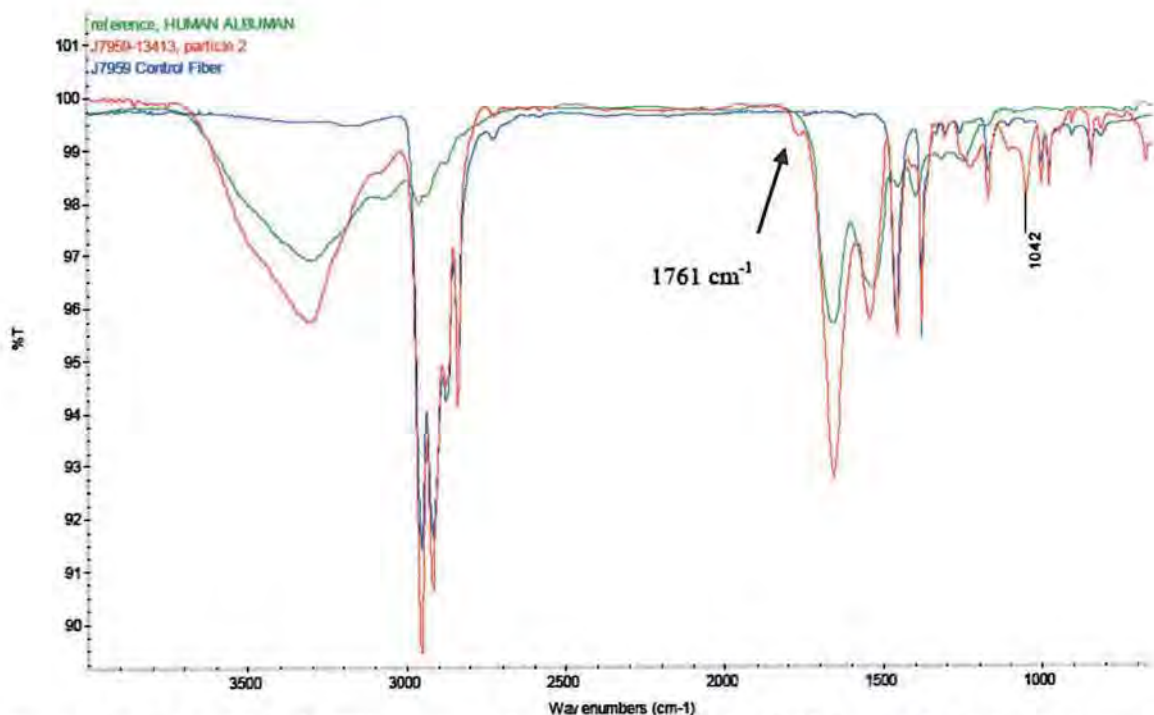


Figure 87: Overlay of FTIR spectra for explant sample 13413 particle 2 (red), human albumin (green) and control fiber lot 3422128 (blue).

GPC-HT

Background and Method

Molecular weight is often a crucial factor in determining material properties. Gel Permeation Chromatography (GPC)^{79,80,81,82} or Size-Exclusion Chromatography (SEC) provides information on the molecular size of the polymer components in the sample. In GPC, the sample is placed into a suitable solvent and passed through a GPC column. Sample components are separated based on molecular size. In Tetradection Gel Permeation Chromatography (GPC-HT), right angle light scattering, low angle light scattering, Viscometry, and refractive index detection are conducted on the sample as it exits from the column enabling the determination of the absolute molecular weight and intrinsic viscosity.^{83,84,85,86} GPC-HT is suitable for the determination of molecular weight of polyolefins including polypropylene.^{87,88,89}

⁷⁹ A. Handley, *Chromatographic Methods, in Polymer Characterization*, Eds. B. J. Hunt and M. I. James, (Blackie Academic & Professional, Glasgow, UK), 1993, 145-156.

⁸⁰ Chi-san Wu, *Column Handbook for Size Exclusion Chromatography*, (Academic Press, San Diego, USA) 1999.

⁸¹ Chi-san Wu, *Handbook of Size Exclusion Chromatography and Related Techniques*, (Merzel Dekker Inc.) 2004.

⁸² W. W. Yau, J. J. Kirkland and D. D. Bly, *Modern Size-Exclusion Liquid Chromatography: Practice of Gel Permeation and Gel Filtration Chromatography*, (John Wiley & Sons, New York, USA) 1979.

⁸³ André M. Striegel, Wallace W. Yau, Joseph J. Kirkland, Donald D. Bly, *Modern Size-Exclusion Liquid Chromatography*, 2nd Edition, Wiley, 2009.

⁸⁴ Wolfgang Schürdt, *Light Scattering from Polymer Solutions and Nanoparticle Dispersions*, Springer, 2007.

⁸⁵ Benjamin Chu, *Laser Light Scattering: Basic Principles and Practice*, 2nd Edition, Dover Publications, Inc. 2007.

Three different molecular weight averages are commonly used to provide information about polymers. These are the number average molecular weight (M_n), the weight average molecular weight (M_w), and the Z average molecular weight (M_z). M_n provides information about the lowest molecular weight portion of the sample. M_w is the average closest to the center of the peak, M_z represents the highest molecular weight portion of the sample. The different molecular weight averages have been related to specific polymer properties. As an example, the highest molecular weight portion of the sample is typically related to material toughness.

By comparing the different averages, it is possible to define a fourth parameter called the polydispersity index (PDI). This parameter gives an indication of how broad a range of molecular weights are in the sample.

Two other parameters were calculated during this analysis, the intrinsic viscosity (IV) and the radius of hydration (R_h). Intrinsic viscosity is the inverse molecular density and can be used as an indication of the extent of polymer branching and shape. R_h is a measure of the size of the polymer molecule.

Sample Preparation

The fiber mesh was analyzed by GPC-HT following dissolution. Samples were dissolved in 1,2,4-trichlorobenzene (TCB) with 0.5 mg/mL 2,6-di-*tert*-butyl-4-methylphenol (BHT) to a final concentration of ~ 2.5 mg/mL.

Results

The GPC-HT results have been summarized in Table 10.

Table 10 Summary of GPC Results		
Sample Group	Average	Std Dev
Not Cracked	*395658	N/A
Moderately Cracked	*394444	N/A
Cracked	389383	10680
Control	384809	5720
Formalin Treated	393764	4846

Note: For samples identification in each group see SEM analysis results.

Note: * only a single sample was analyzed which fell into this group.

N/A: not applicable

⁸⁶ Pavel Kratochvíl, *Classical Light Scattering from Polymer Solutions*, Elsevier, 1987

⁸⁷ Nicolai Aust, " Application of size-exclusion chromatography to polymers of ultra-high molar mass" *J. Biochem. Biophys. Methods* 56 (2003) 323-334.

⁸⁸ Immaculada Suárez, Baudilio Coto, " Determination of long chain branching in PE samples by GPC-MALS and GPC-VIS: Comparison and uncertainties" *European Polymer Journal*, 49(2013) 492-498.

⁸⁹ V. Grinshpun and A. Rudin, " High temperature GPC of polypropylene" *Journal of Applied Polymer Science*, 30 (1985) 2413-2418.

A series of standards were analyzed to demonstrate proper instrument function. The results for these samples are presented in Table 11.

Table 11. Reference Standards

Calibration Standard Analysis (GPC-T)
(PS 104,286)

Sample	Mn	Mw	Mz	Mw/Mn	IV	Rh
2013-09-12_09:54:02_ps105_104286_01.vdt	100,614	103,883	107,721	1.032	0.3301	8.13

ID	dn/dc	Conc
ps105_104286	0.0520	2.8080

Reference Standard Analysis (GPC-T)
(PS 233,008)

Sample	Mn	Mw	Mz	Mw/Mn	IV	Rh
2013-09-09_16:20:52_ps235k_233009_01.vdt	110,066	226,300	394,194	2.056	0.5390	11.82
2013-09-10_13:20:05_ps235k_233009_01.vdt	105,712	226,709	392,410	2.145	0.5382	11.82
2013-09-11_12:29:24_ps235k_233009_01.vdt	111,432	225,134	398,341	2.020	0.5406	11.81
2013-09-12_04:27:39_ps235k_233009_02.vdt	109,473	226,788	391,738	2.072	0.5325	11.79

ID	dn/dc	Conc
ps235k_233009	0.0524	6.1780
ps235k_233009	0.0527	6.1780
ps235k_233009	0.0526	6.1780
ps235k_233009	0.0515	6.1780

Control

The control samples were then analyzed to determine their molecular weights. The results are presented in Table 12.

Table 12. Control Sample Results

Lot# 3398135

Sample	Mn	Mw	Mz	Mw/Mn	IV	Rh
2013-09-10_15:55:20_3398135_1mL_01.vdt	85,691	381,313	955,643	4.450	1.2584	17.79

ID	dn/dc	Conc
3398135_1mL	0.0930	1.8366

Lot# 3405405

Sample	Mn	Mw	Mz	Mw/Mn	IV	Rh
2013-09-11_09;34;12_B_3405405_01.vdt	92,054	385,825	909,214	4.191	1.2902	18.10
ID		dn/dc	Conc			
B_3405405		0.0930	2.6503			

Lot# 3405460

Sample	Mn	Mw	Mz	Mw/Mn	IV	Rh
2013-09-11_10;35;57_C_3405460_01.vdt	86,170	395,925	951,052	4.595	1.3026	18.39
ID		dn/dc	Conc			
C_3405460		0.0930	2.5685			

Lot# 3405474

Sample	Mn	Mw	Mz	Mw/Mn	IV	Rh
2013-09-11_11;37;42_D_3405474_01.vdt	98,801	383,005	918,849	3.877	1.2760	18.03
ID		dn/dc	Conc			
D_3405474		0.0930	3.0531			

Lot# 3422128

Sample	Mn	Mw	Mz	Mw/Mn	IV	Rh
2013-09-11_13;21;07_E_3422128_01.vdt	83,985	381,714	931,335	4.545	1.2894	18.06
ID		dn/dc	Conc			
E_3422128		0.0930	2.8246			

Lot# 3436364

Sample	Mn	Mw	Mz	Mw/Mn	IV	Rh
2013-09-11_14;12;51_F_3436364_01.vdt	98,946	381,072	942,175	3.851	1.2730	17.94
ID		dn/dc	Conc			
F_3436364		0.0930	2.6876			

Explant Samples

The explant samples were then analyzed to determine their molecular weights. The results are presented in **Table 13**.

Table 13. Explant Sample Results13411

Sample	Mn	Mw	Mz	Mw/Mn	IV	Rh
2013-09-11_15;26;34_G_13411_01.vdt	108,078	398,558	969,093	3.688	1.3231	18.47
ID		dn/dc	Conc			
G_13411		0.0930	2.1794			

13407

Sample	Mn	Mw	Mz	Mw/Mn	IV	Rh
2013-09-11_18;06;49_H_13407_01.vdt	82,322	405,514	1.058 e 6	4.926	1.3183	18.48
ID		dn/dc	Conc			
H_13407		0.0930	1.7629			

13418

Sample	Mn	Mw	Mz	Mw/Mn	IV	Rh
2013-09-11_18;58;34_I_13418_01.vdt	19,158	371,484	946,492	19.390	1.3203	17.45
ID		dn/dc	Conc			
I_13418		0.0930	1.9147			

13400

Sample	Mn	Mw	Mz	Mw/Mn	IV	Rh
2013-09-11_19;50;18_J_13400_01.vdt	74,635	385,636	920,751	5.167	1.2450	17.83
ID		dn/dc	Conc			
J_13400		0.0930	2.3681			

13421

Sample	Mn	Mw	Mz	Mw/Mn	IV	Rh
2013-09-11_20;42;02_K_13421_01.vdt	98,698	395,658	987,760	4.009	1.2774	18.21
ID		dn/dc	Conc			
K_13421		0.0930	2.1204			

13404

Sample	Mn	Mw	Mz	Mw/Mn	IV	Rh
2013-09-11_21;33;47_L_13404_01.vdt	68,597	388,455	925,338	5.663	1.3338	18.32
ID		dn/dc	Conc			
L_13404		0.0930	2.7501			

13402

Sample	Mn	Mw	Mz	Mw/Mn	IV	Rh
2013-09-11_22;25;33_M_13402_01.vdt	27,720	371,411	965,128	13.398	1.1816	16.90
ID		dn/dc	Conc			
M_13402		0.0930	1.4691			

13415

Sample	Mn	Mw	Mz	Mw/Mn	IV	Rh
2013-09-11_23;17;19_N_13415_01.vdt	40,886	385,981	974,148	9.440	1.2699	17.83
ID		dn/dc	Conc			
N_13415		0.0930	2.5351			

13409

Sample	Mn	Mw	Mz	Mw/Mn	IV	Rh
2013-09-12_00;09;03_O_13409_01.vdt	105,170	393,038	978,492	3.737	1.3183	18.32
ID		dn/dc	Conc			
O_13409		0.0930	2.4101			

13416

Sample	Mn	Mw	Mz	Mw/Mn	IV	Rh
2013-09-12_01;00;48_P_13416_01.vdt	83,961	388,493	933,067	4.627	1.2624	17.99
ID		dn/dc	Conc			
P_13416		0.0930	2.4849			

13413

Sample	Mn	Mw	Mz	Mw/Mn	IV	Rh
2013-09-12_10;47;33_Q_13413_01.vdt	104,404	387,403	984,430	3.711	1.2652	18.03
ID		dn/dc	Conc			
Q_13413		0.0930	2.4058			

13414

Sample	Mn	Mw	Mz	Mw/Mn	IV	Rh
2013-09-12_12;24;37_R_13414_01.vdt	95,846	399,764	944,750	4.171	1.2967	18.41
ID		dn/dc	Conc			
R_13414		0.0930	2.4518			

13412

Sample	Mn	Mw	Mz	Mw/Mn	IV	Rh
2013-09-12_15;14;18_S_13412_01.vdt	56,727	393,031	970,985	6.928	1.2963	18.21
ID		dn/dc	Conc			
S_13412		0.0930	2.5938			

13410

Sample	Mn	Mw	Mz	Mw/Mn	IV	Rh
2013-09-12_16;20;59_T_13410_01.vdt	112,443	398,633	983,036	3.545	1.2775	18.27
ID		dn/dc	Conc			
T_13410		0.0930	2.0949			

13675

Sample	Mn	Mw	Mz	Mw/Mn	IV	Rh
2013-10-23_17;13;34_sample13675_lcms_01.vdt	99,271	403,867	993,583	4.068	1.3201	18.50
ID		dn/dc	Conc			
sample13675_lcms		0.0930	1.7720			

Control Samples - Formalin Treated

The Formalin treated control samples were analyzed to determine their molecular weights. The results are presented in Table 14.

Table 14. Formalin Treated Control SamplesLot# 3405460 – Formalin Treated

Sample	Mn	Mw	Mz	Mw/Mn	IV	Rh
2013-09-12_20;13;01_u_3405460_formalin_01.vdt	97,747	385,600	959,735	3.945	1.3283	18.19
ID		dn/dc	Conc			
u_3405460_formalin		0.0930	2.7704			

Lot# 3422128 – Formalin Treated

Sample	Mn	Mw	Mz	Mw/Mn	IV	Rh
2013-09-12_21;04;45_v_3422128_formalin_01.vdt	98,569	397,087	984,135	4.028	1.2980	18.32
ID		dn/dc	Conc			
v_3422128_formalin		0.0930	2.4274			

Lot# 3405474 – Formalin Treated

Sample	Mn	Mw	Mz	Mw/Mn	IV	Rh
2013-09-12_22;48;15_x_3405474_formalin_01.vdt	89,506	399,842	993,937	4.467	1.3108	18.45
ID		dn/dc	Conc			
x_3405474_formalin		0.0930	2.3818			

Lot# 3405405 – Formalin Treated

Sample	Mn	Mw	Mz	Mw/Mn	IV	Rh
2013-09-13_00;31;44_z_3405405_formalin_01.vdt	81,271	393,292	994,437	4.839	1.3015	18.29

ID	dn/dc	Conc
z_3405405_formalin	0.0930	2.5268

Lot# 3398135 – Formalin Treated

Sample	Mn	Mw	Mz	Mw/Mn	IV	Rh
2013-09-12_23;40;00_y_3398135_formalin_01.vdt	77,286	394,444	1.011 e 6	5.104	1.2908	18.17
ID	dn/dc	Conc				
y_3398135_formalin	0.0930	2.1820				

Lot# 3436364 – Formalin Treated

Sample	Mn	Mw	Mz	Mw/Mn	IV	Rh
2013-09-12_21;56;29_w_3436364_formalin_01.vdt	94,918	392,318	960,773	4.133	1.3145	18.29
ID	dn/dc	Conc				
w_3436364_formalin	0.0930	2.5559				

Lot# 3405474 – 10 mL prep to confirm small volume preps

Sample	Mn	Mw	Mz	Mw/Mn	IV	Rh
2013-09-13_01;23;29_aa_3405474_10_01.vdt	88,500	392,234	962,856	4.432	1.2879	18.19
ID	dn/dc	Conc				
aa_3405474_10	0.0930	2.3821				

Lot# 3436364 – 10 mL prep to confirm small volume preps

Sample	Mn	Mw	Mz	Mw/Mn	IV	Rh
2013-09-13_02;15;14_bb_3436364_10_01.vdt	100,750	392,413	913,854	3.895	1.2839	18.23
ID	dn/dc	Conc				
bb_3436364_10	0.0930	2.3021				

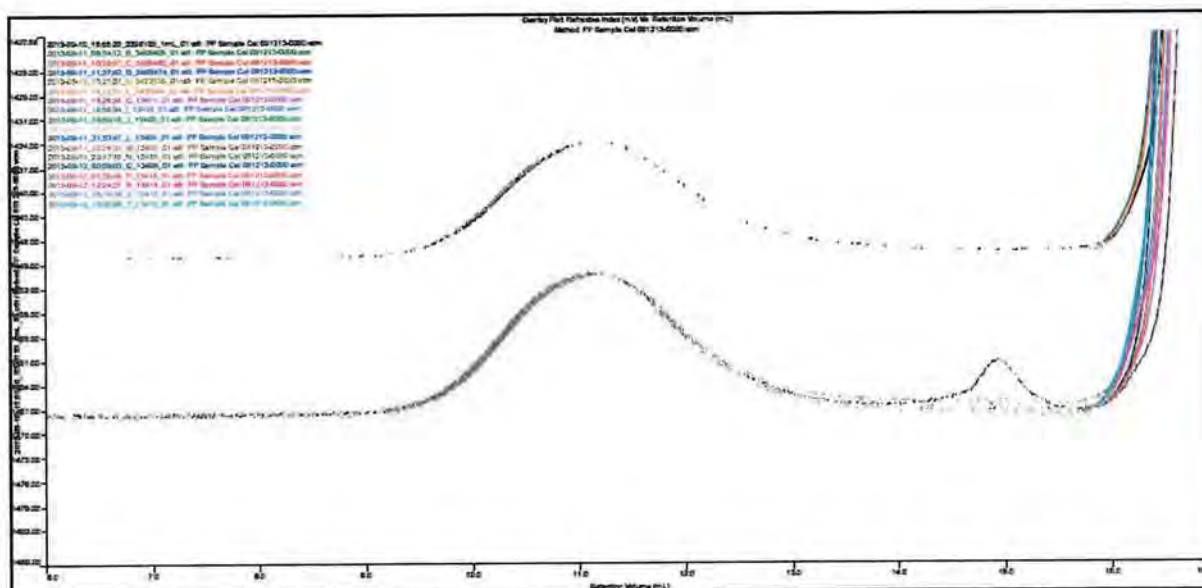


Figure 88: Normalized overlay of refractive index chromatogram for the explant (bottom) and control samples (top).

Scientific Opinion

The control and explant samples do not show a significant difference in molecular weight. It is evident from the SEM data that ~3um of the surface is cracked which is less than 2% of the fiber diameter. Thus it is expected that the GPC-HT will not show any large variation in the molecular weight. Because GPC-HT is a bulk technique (entire fiber is dissolved), changes in molecular weight may not be detectable given that the majority of the degradation is a surface phenomenon. Furthermore, the environmental stress cracking mechanism does not require a decrease in molecular weight. Therefore, based on my review of the scientific literature, my knowledge, training and experience as polymer scientists, and the examination of the data, it is my opinion, to a reasonable degree of scientific certainty, that given the previous results from SEM and DSC analyses (consistent with environmental stress cracking), and SEM-EDX and FTIR-microscopy analyses (consistent with oxidation), that the observed cracking in the explant samples is due to a combination of environmental stress cracking and oxidation.

PYMS

Background and Method

The characterization of the chemical structure of polymeric materials including polypropylene and its additives by PYMS is a well-established analytical technique.^{90,91,92}

⁹⁰ Hanton D.D., Mass Spectrometry of Polymers and Polymer Surfaces *Chemical Review*, 101 (2001) 527-569.

⁹¹ Vouras P., Wronka J., *Polymer Characterization using Mass Spectrometry in Modern Methods of Polymer Characterization*, Eds. Howard G. Barth, Jimmy W. Mays (John Wiley and Sons, Inc. 1991, New York, NY) 495-555.

PYMS uses high temperature to pyrolyze or desorb chemical species and to break down polymer molecules. After these fragments are produced, they are transferred into a capillary column and separated. The components are then analyzed by the mass spectrometer which generates a fingerprint (mass spectrum) of the compound. The fingerprint which is diagnostic of the chemical can then be readily compared to the NIST/EPA/NIH mass spectral library for identification. PYMS is especially useful for characterizing polymer additives.

Ethicon's Additives Package for it's Prolene Mesh

According to Ethicon internal documents, it's Prolene mesh manufacturing has changed little since 1968. Apparently, the current additives are as follows:⁹³

- Calcium Stearate 0.25-0.35% A lubricant to help reduce tissue drag and promote tissue passage.
- Dilaurelthiodipropionate (DLTDP) - 0.40-0.60% - An antioxidant to improve long-term storage of the resin and the fiber and to reduce the potential oxidative reaction with ultraviolet light.
- Santonox R - 0.10-0.30% - An antioxidant to promote stability during compounding and extrusion.
- Procol LA - 0.25-0.35% - A lubricant to help reduce tissue drag and promote tissue passage.
- CPC Pigment - 0.55% Max. - A colorant to enhance visibility.

Of these five ingredients, the two additives that stabilize the polypropylene meshes are Santonox R and Dilaurelthiodipropionate both of which are antioxidants.

Sample Preparation

The fiber mesh was analyzed directly by PYMS with no further sample treatment beyond what was described in the sample preparation sections.

Results

PYMS chromatograms of the control and explant samples are shown in **Figures 89 and 90**. The main features of the chromatograms included monomer and some volatile polypropylene pyrolysis products.

The control samples were found to contain a unique component at 14.0 minutes. This peak was not observed in any of the explant samples. The mass spectrum for this component showed ions at m/z 143, 168 and 178. A search of the mass spectral library produced only poor quality matches. To confirm the identity of this component a dilaurelthiodipropionate reference material was analyzed under the same conditions. The standard was found to show a strong fragment at the same retention time (14.0 minutes).

⁹² Bolgar, M., Hubball, J., Groeger J., and Meronek, S. editors, *Handbook for The Chemical Analysis of Plastic and Polymer Additives*, CRC Press, 2008, Boca Raton, FL.

⁹³ ETH.MESH.02268619 – Prolene Resin Manufacturing Specifications

When these ions were examined in both the control and explant samples, it was observed that these ions were present in the six controls, but were not detected in any of the explant samples.

A peak was observed at a retention time of 11.5 minutes. This compound produced a mass spectra with strong ions at 358 amu and 343 amu. A search of the NIST mass spectral library produced a best match for Santonox R. This component was observed in both the control and explant samples.

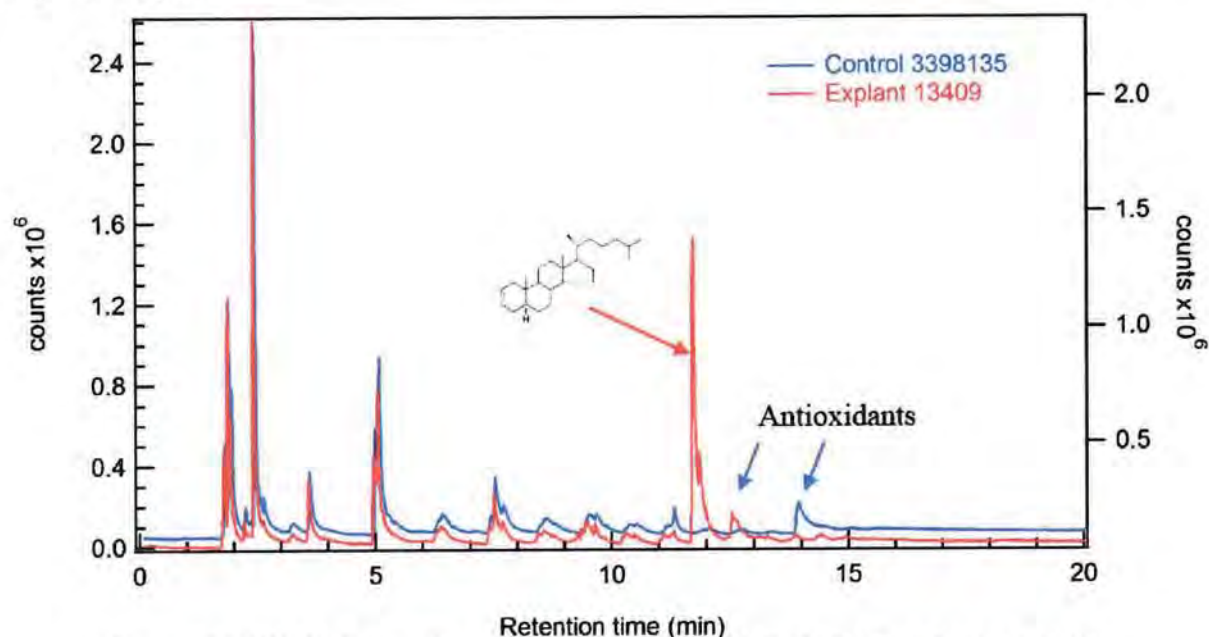


Figure 89: PYMS chromatogram overlay of Control 3398135 and Explant 13409

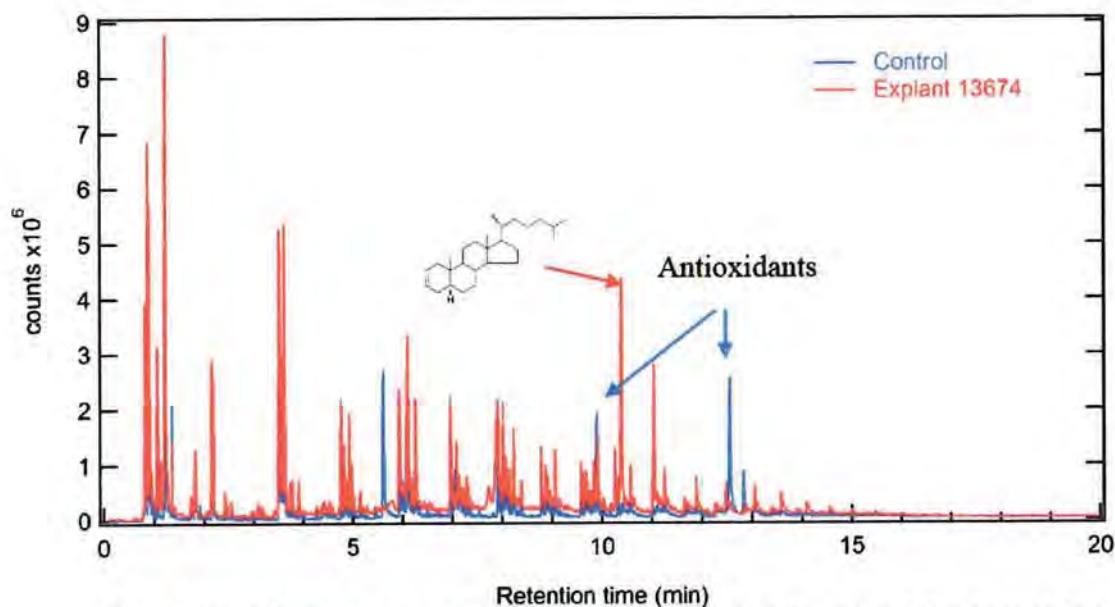


Figure 90: PYMS chromatogram overlay of Control 3422128 and Explant 13674

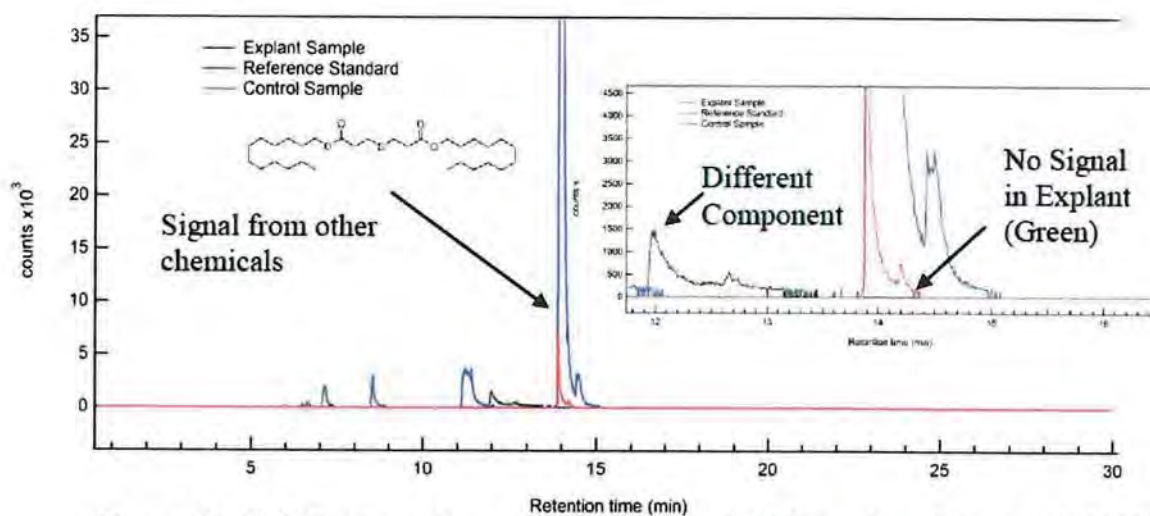


Figure 91: PYMS extracted ion chromatogram (m/z 143) overlay of Control 3422128 (red) Explant 13400 (green) with dilaurylthiodipropionate reference standard (blue).

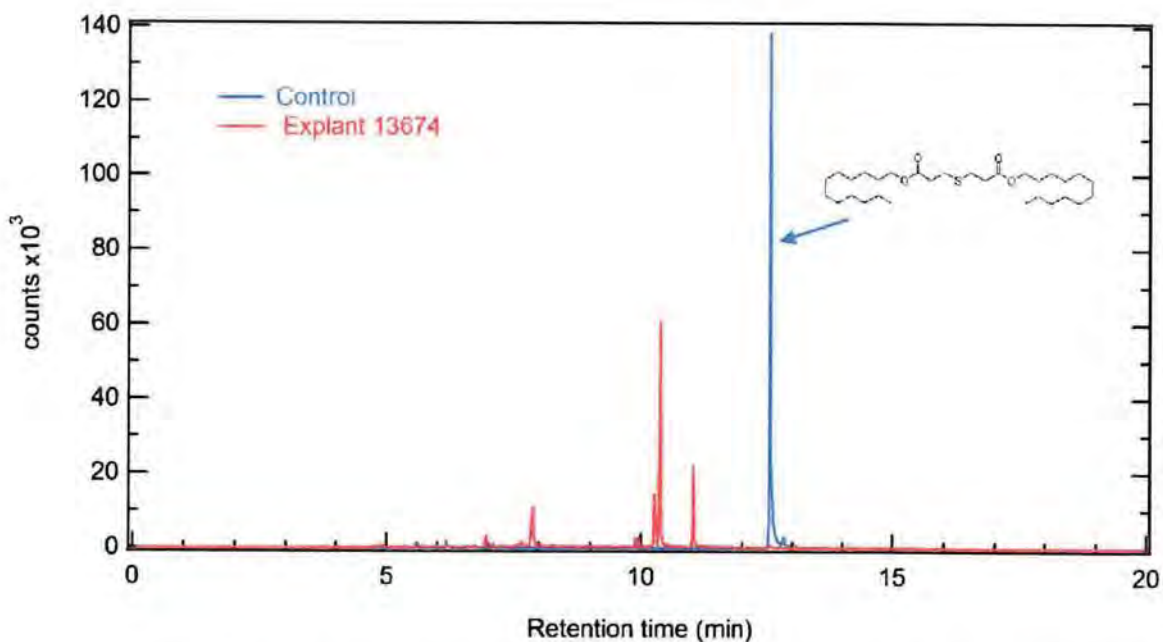


Figure 92: PYMS extracted ion chromatogram (m/z 143) overlay of Control 3422128 (blue) and Explant 13674 (red) showing detection of antioxidant dilaurylthiodipropionate (peak at 12.6 min) in the control but not in the explant sample.

Scientific Opinion

Based on the PYMS data collected, it is my opinion to a reasonable degree of scientific certainty that the control samples contain two antioxidants. They are dilaurylthiodipropionate and Santonox R. While PYMS is not strictly quantitative, the data demonstrates that a higher concentration of dilaurylthiodipropionate is found in the controls as this component was not detected at all in the explant samples. LCMS is more sensitive than PYMS explaining why this method was capable of detecting this component. Therefore, given that the purpose of adding antioxidants to the Prolene mesh in TVT is to prevent degradation and oxidation, without those antioxidants remaining on the surface of the mesh, the mesh is at higher risk of degradation and oxidation.

Liebert et al. studied oxidation of polypropylene filaments with and without antioxidants, which were explanted from hamsters.⁹⁴ Explanted samples without an antioxidant showed in vivo oxidation of polypropylene; which was evident from the carbonyl band in the IR spectra; which resulted in loss of mechanical properties. The oxidation process is effectively retarded using an antioxidant. This study conducted over 40 years ago demonstrates the same effect that we have observed in the current study.

Therefore, based on my review of the scientific literature, my review of Ethicon's internal documents, my knowledge, training and experience as polymer scientists, and the review of my data, it is my opinion to a reasonable degree of scientific certainty that the antioxidants added to the Prolene mesh by Ethicon leach away from the surface of the polypropylene fiber in vivo leaving the mesh fibers extremely vulnerable to oxidation/degradation.

Cholesterol, cholesterol-like molecules and stearic acid were also observed in the PYMS chromatograms of the explant samples. As mentioned on Page 8 of this report, molecules like esterified fatty acids or cholesterol are consistent with diffusion into the polypropylene fibers and thus are consistent with environmental stress cracking.⁹⁵

LCMS

Background and Method

Liquid Chromatography Mass spectrometry (LCMS) is a highly-regarded and well-established analytical technique in the characterization of polymers and their additives and degradants.^{96,97,98} Quadrupole Time of Flight LCMS (QTOF-LCMS) combines high mass

⁹⁴ Timothy C Liebert, Richard P. Chertoff, Stanley L. Cosgrove and Roberts S. McCuskey *Journal of Biomedical Materials Research* 10 (1976) 939-951.

⁹⁵ Arnaud Clave, Hanna Yahi, Jean-Claude Hammou, Suzelei Montanari, Pierre Gounon and Henri Clave, "Polypropylene as a reinforcement in pelvic surgery is not inert: comparative analysis of 100 explants" *International Urogynecology Journal and Pelvic Floor Dysfunction* 21 (2010) 261-270.

⁹⁶ Pasch, H. "Analysis of complex polymers by multidimensional techniques" *Phys. Chem. Chem. Phys* 1 (1999), 3879-3890.

⁹⁷ Arpino P.J., Hass P., "Recent developments in supercritical fluid chromatography-mass spectrometry coupling" *J. Chromatography A*, 703 (1995), 479-488.

⁹⁸ Fenn, J.B., Mann M., Meng K., Wong S.F., Whitehouse C.M., "Electrospray ionization for mass spectrometry of large biomolecules" *Science*, 246 (1989), 64.

accuracy time of flight mass spectroscopy with a liquid chromatography separation to provide detailed information about the elemental composition of unknowns.

LCMS requires that the molecule of interest be ionized. Thus, data is typically plotted in positive and negative modes indicating the charge on the ions. Ion formation is accomplished through the formation of a molecular adduct using a charge carrying species. Typical charge carriers in positive ion mode include H^+ , Na^+ , K^+ , NH_4^+ . Thus the observed mass is typically the mass of the compound plus the mass of the charge carrier. In negative ion, the loss of hydrogen is generally observed which results in the loss of one mass unit (1.0078 amu). It is also common to observe negative adducts with the addition of chlorine (Cl^-), formate (COO^-), or trifluoroacetate (CF_3COO^-).

A number of plots are used to aid in interpreting QTOF-LCMS data. This includes Base Peak Chromatograms (BPC), Extracted Ion Chromatograms (EIC), Mass spectra (MS) and Product Ion Spectra (MS/MS). A BPC is formed by plotting the most intense ion at a given retention time. This spectrum is particularly useful for identifying the retention time of unknowns. EICs are formed by plotting a single mass at all retention times. This could be considered a plot of peak intensity for a single compound (and its isomers) versus retention time.

All structures and identifications indicated represent best estimates based on the data observed. In most cases the MS/MS fragmentation spectra have been consulted to aid in identification of possible structures.

Sample Preparation

Analytical solutions of the control samples were prepared by extracting the provided mesh in the extraction solvent, 80/20 (v/v) methanol-isopropanol. A portion of each sample weighing approximately 50 mg was submerged in one (1) ml of the extraction solvent. The extraction was allowed to continue for 2 hours at 80°C. Following the heating procedure the extracts were allowed to cool and the extract solution was decanted into an LCMS sampling vial. The extracts were analyzed with no further preparation.

Table 15 Sample Preparation	
Sample	Mass Extracted (mg)
Lot 3405460	50.118
Lot 3422128	50.246
Lot 3436364	50.982
Lot 3405474	50.214
Lot 3398135	50.014
Lot 3405405	50.340

Additional extracts were prepared for the controls and the explant samples using approximately 2 mg and 100µl of 80/20 (v/v) methanol-isopropanol. The extraction was performed at 65°C and was allowed to continue for 2 hours. A lower extraction temperature was used to ensure significant solvent loss did not occur. The mass of the extraction vessels was measured before and after the extraction. Similar masses were observed, indicating that there was no significant solvent evaporation during the extraction.

Table 16			
Sample Preparation			
Sample	Mass (mg)	Extraction Vessel Mass (mg)	
		Before Extraction	After Extraction
Explant Samples			
13674	2.000	2648.646	2648.038
13675	2.036	2630.108	2615.391
13400	2.182	2615.568	2608.838
13401	2.084	2637.604	2634.924
13402	2.138	2634.880	2624.206
13405	2.062	2587.280	2568.782
13407	2.098	2623.218	2610.130
13408	1.998	2593.358	2585.534
13409	2.002	2649.766	2646.816
13410	2.028	2603.446	2600.234
13411	2.038	2564.772	2564.324
13412	2.004	2606.922	2606.224
13413	2.020	2627.808	2625.710
13414	2.014	2591.110	2583.298
13415	2.156	2632.816	2628.254
13416	2.100	2642.108	2639.306
13418	2.104	2610.950	2595.010
13421	2.012	2614.526	2612.642
Control Samples			
Lot 3398135	2.180	2586.358	2583.272
Lot 3405405	2.170	2620.602	2615.002
Lot 3405460	2.278	2638.486	2637.678
Lot 3405474	2.228	2650.752	2646.174
Lot 3422128	2.272	2586.184	2581.106
Lot 3436364	2.108	2635.652	2629.238
Lot 3422128 (Duplicate 1)	1.996	2594.194	2593.172
Lot 3422128 (Duplicate 2)	2.052	2624.278	2599.530
Formalin Treated Control Samples			
Lot 3405405 (Formalin Control)	2.219	2622.522	2605.506
Lot 3422128 (Formalin Control)	2.032	2595.486	2591.152

A limit of detection study was performed for the two antioxidants identified. To perform this experiment standard solutions were prepared containing dilauryl thiodipropionate (10.6 mg) and 4,4'-thiobis(6-tert-butyl-3-cresol) (10.3 mg) each with 10 ml of 80/20 v/v methanol/isopropanol. A stock solution containing both standards was prepared by adding 100µl of each of the standard solutions prepared to 9.8 ml of 80/20 v/v methanol/isopropanol (10 µg/ml). A series of further dilutions (1 µg/ml, 100 ng/ml, and 10 ng/ml) were then prepared from this stock solution.

Results

Table 17 includes a summary of the masses of the compounds detected. The compounds shown were observed in all of the control sample extracts. The provided data is representative of the extract collected from the control sample labeled Lot 3398135. The

data for the remaining control samples were similar and are provided in the data section of this report.

Table 17 Summary of LCMS Results Compounds detected in all samples							
<i>RT</i>	<i>Positive m/z</i>	<i>Negative m/z</i>	<i>Mass</i>	<i>Best Match</i>	<i>Score</i>	<i>Diff.</i>	<i>Possible ID</i>
7.0	207.0668		206.0595	C ₈ H ₁₄ O ₄ S	82.86	8.67	Dimethyl thiodipropionate
10.7	375.198		374.1907	C ₂₂ H ₃₀ O ₃ S	93.66	2.27	
11.7		357.1893	358.1965	C ₂₂ H ₃₀ O ₂ S	99.59	0.31	4,4'-thiobis(6-tert- butyl-3-cresol) (Santnox-R)
11.7	468.3893		450.3555	C ₂₄ H ₅₀ O ₇	98.6	0.33	Ethoxylated dodecanol
	512.4129		494.3791	C ₂₆ H ₅₄ O ₈	80.1	5.54	
	556.439		538.4052	C ₂₈ H ₅₈ O ₉	83.09	5.28	
	600.4657		582.432	C ₃₀ H ₆₂ O ₁₀	84.59	3.87	
	644.4933		626.4596	C ₃₂ H ₆₆ O ₁₁	96.08	1.48	
	688.5214		670.4875	C ₃₄ H ₇₀ O ₁₂	97.56	-1.17	
12.1	584.4716		566.4379	C ₃₀ H ₆₂ O ₉	91.75	2.59	Ethoxylated tetradecanol
	628.4965		610.4628	C ₃₂ H ₆₆ O ₁₀	84.11	4.64	
	672.5222		654.4886	C ₃₄ H ₇₀ O ₁₁	80.54	4.97	
	716.5502		698.5165	C ₃₆ H ₇₄ O ₁₂	95.12	2.19	
12.4	361.2385		360.2312	C ₁₉ H ₃₆ O ₄ S	75.61	6.08	Methyl lauryl thiodipropionate
12.4	568.4784		550.4445	C ₃₀ H ₆₂ O ₈	94.51	-0.07	Ethoxylated hexadecanol
	612.5048		594.471	C ₃₂ H ₆₆ O ₉	95.73	-0.45	
	656.5304		638.4965	C ₃₄ H ₇₀ O ₁₀	96.65	0.59	
	700.5553		682.5215	C ₃₆ H ₇₄ O ₁₁	91.68	2.39	
12.6		519.2949	520.3021	C ₃₃ H ₄₄ O ₃ S	97.61	-1.97	
12.6		665.2598	666.267	C ₃₇ H ₄₆ O ₇ S ₂	95.84	2.17	
12.8	338.341		337.3337	C ₂₂ H ₄₃ N O	97.92	2.24	Erucylamide
12.8		713.3722	714.3794	C ₄₄ H ₅₈ O ₄ S ₂	95.6	-2.46	
13.1	487.3818		486.3745	C ₂₈ H ₅₄ O ₄ S	98.43	-0.46	Decyl dodecyl thiodipropionate
13.3	532.438		514.4041	C ₃₀ H ₅₈ O ₄ S	93.01	2.84	Dilauryl thiodipropionate

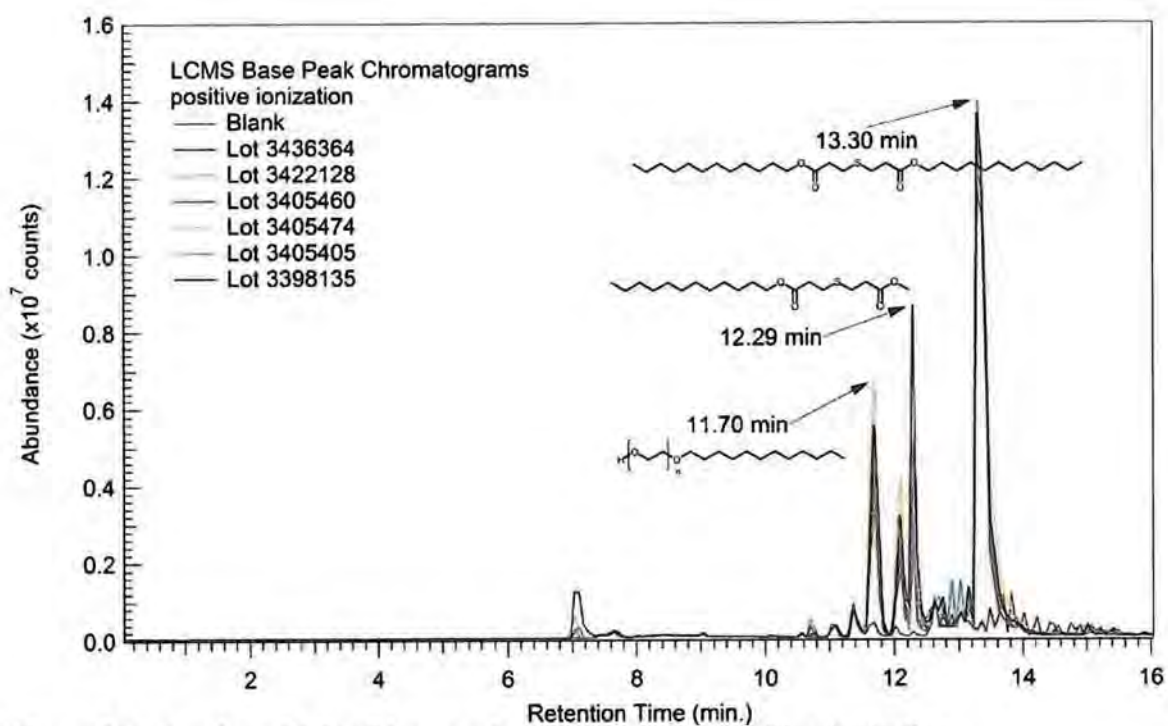


Figure 93 - Overlay of LCMS base peak chromatograms, positive ionization.

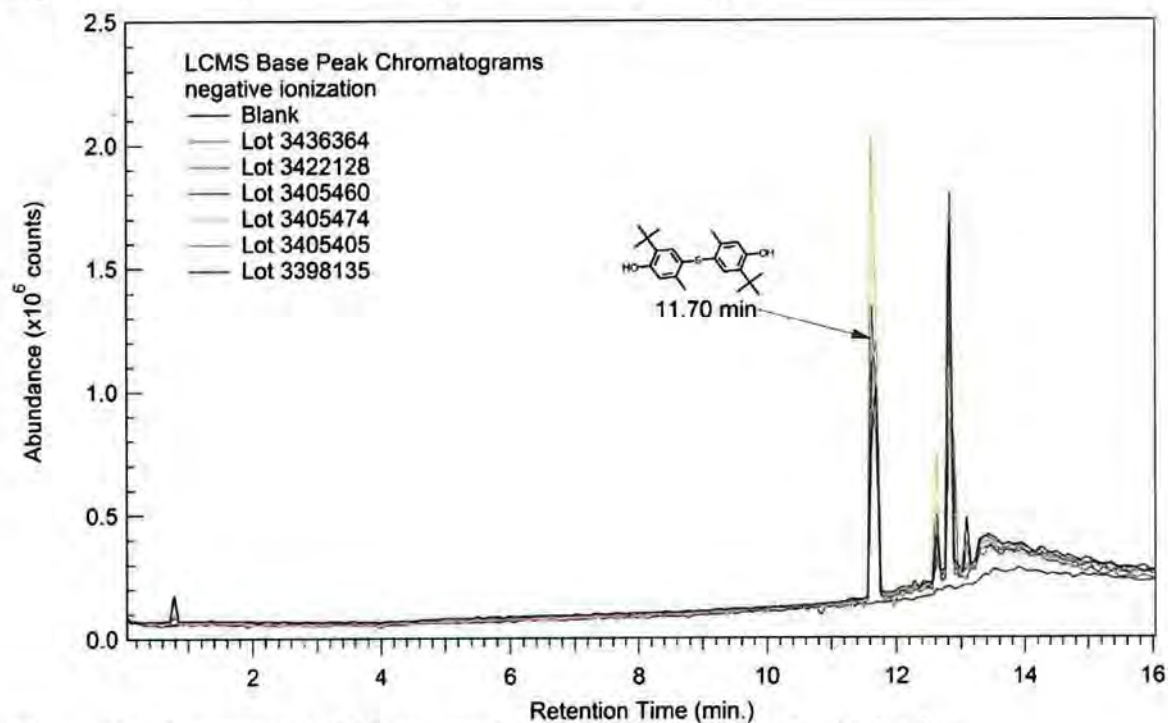


Figure 94 - Overlay of LCMS base peak chromatograms, negative ionization.

The relative concentration of the compound identified as dilauryl thiodipropionate was compared for the control samples analyzed. Resulting peak areas are shown in **Table 18**. **Figures 95-99** include an overlay of extracted ion chromatograms (EICs) for 532.4380 Da, the mass of the ion $(M+NH_4)^+$ observed for this compound.

Control lots 3398135, 3405405, 3405460, 3405474, 3422128 and 3436364 were run at the same time as all the explant samples other than samples 13674 and 13675. Sample 13674 was run at the same time as Control Lot 3422128 (Duplicate 1) while the sample 13675 was run at the same time as Control Lot 3422128 (Duplicate 2). These two explant samples were analyzed at later dates. Due to changes in detector ionization efficiency over time, the duplicate control base peak chromatograms showed some variation in peak area. The variation in the peak area is within the expected range suggested by the manufacturer. A replicate analysis of a control was included with each sample to account for this variation.

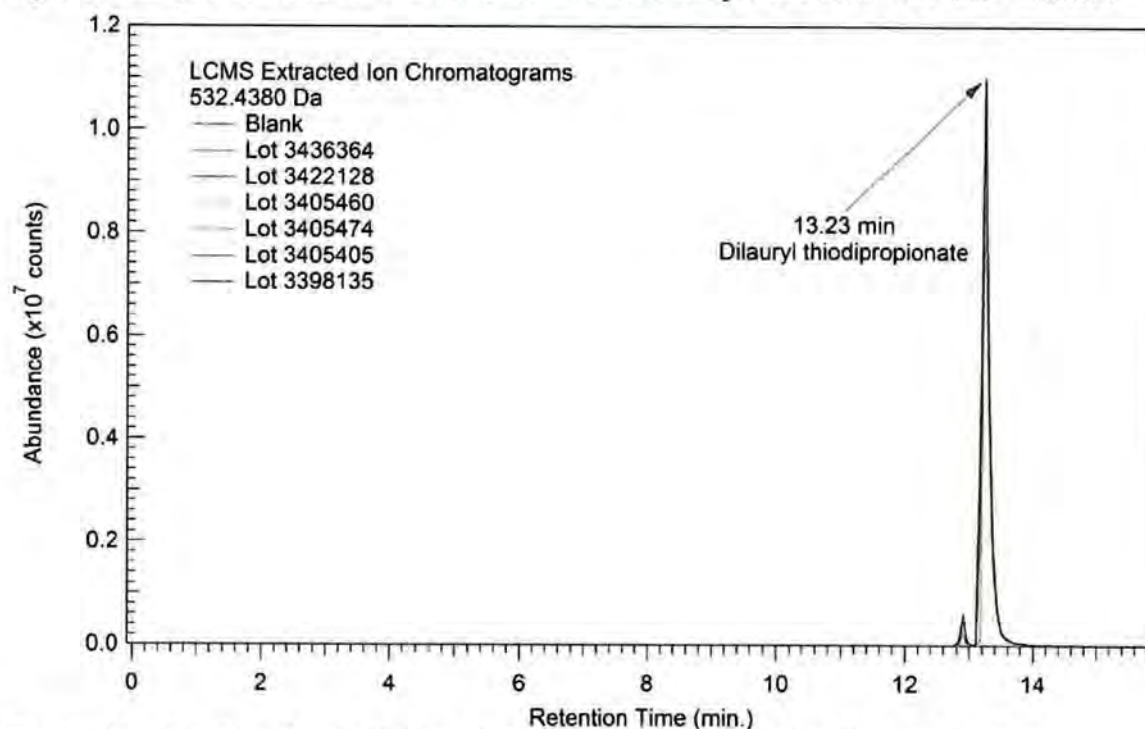


Figure 95 - Overlay of extracted ion chromatograms, 532.4380 Da, Control Extracts.

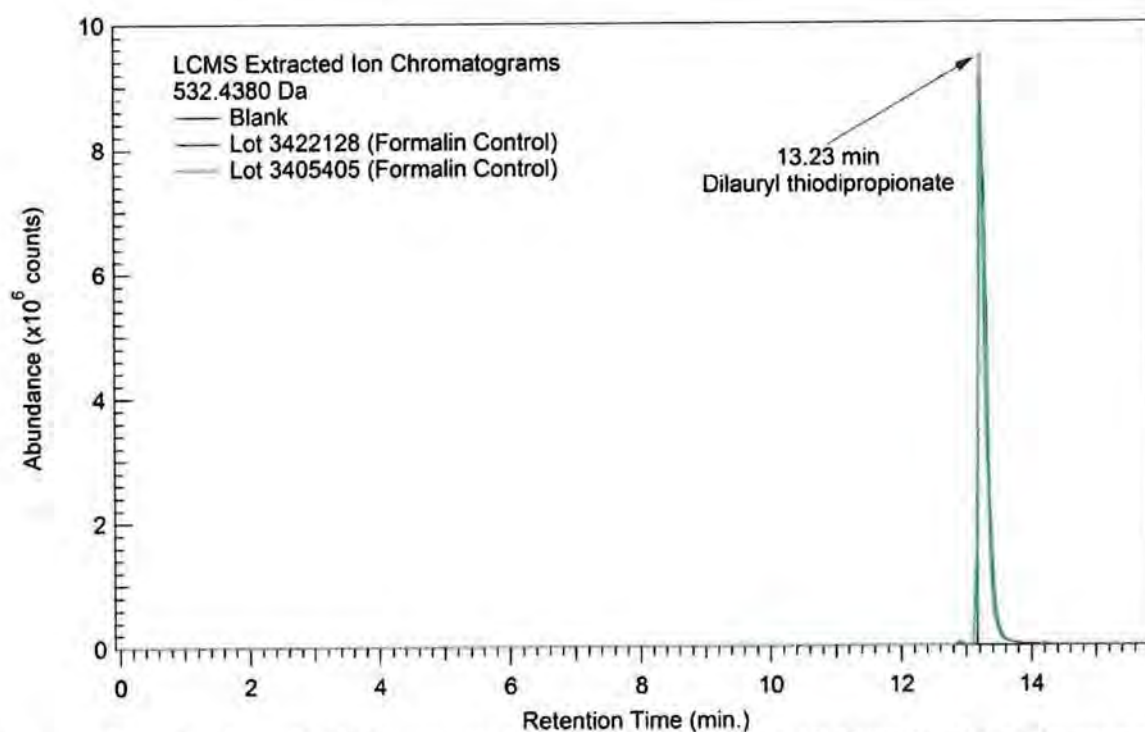


Figure 96 - Overlay of LCMS extracted ion chromatograms, 532.4380 Da, formalin control extract.

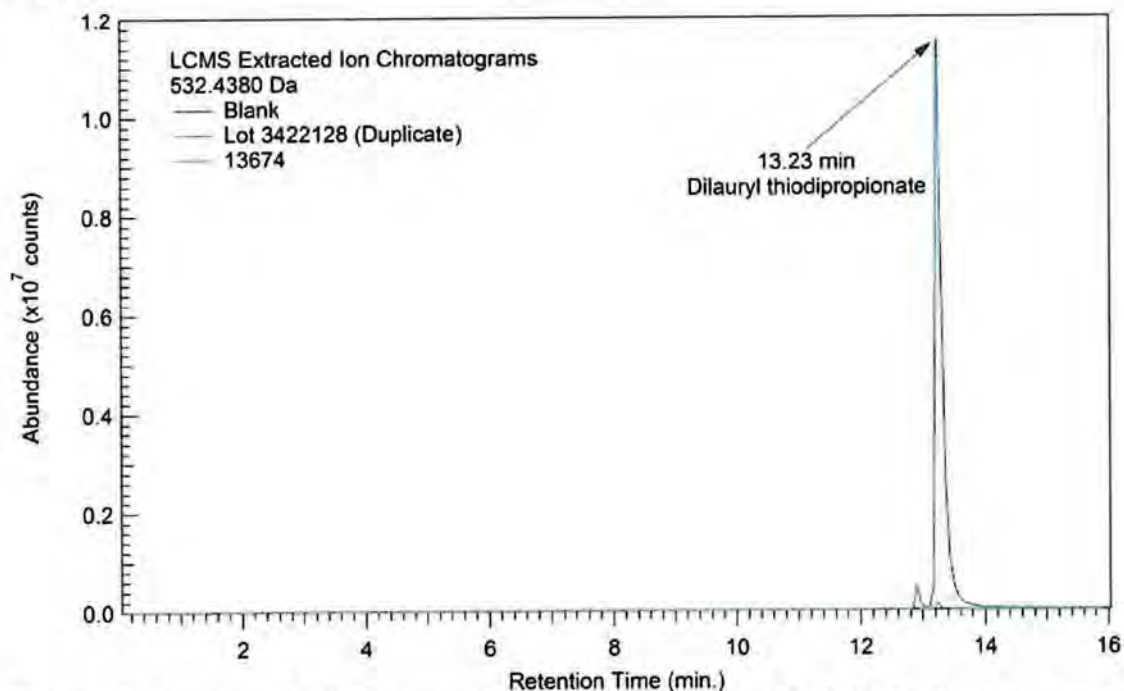


Figure 97 - Overlay of LCMS extracted ion chromatograms, 532.4380 Da, Explant sample 13674 and control sample from Lot 3422128.

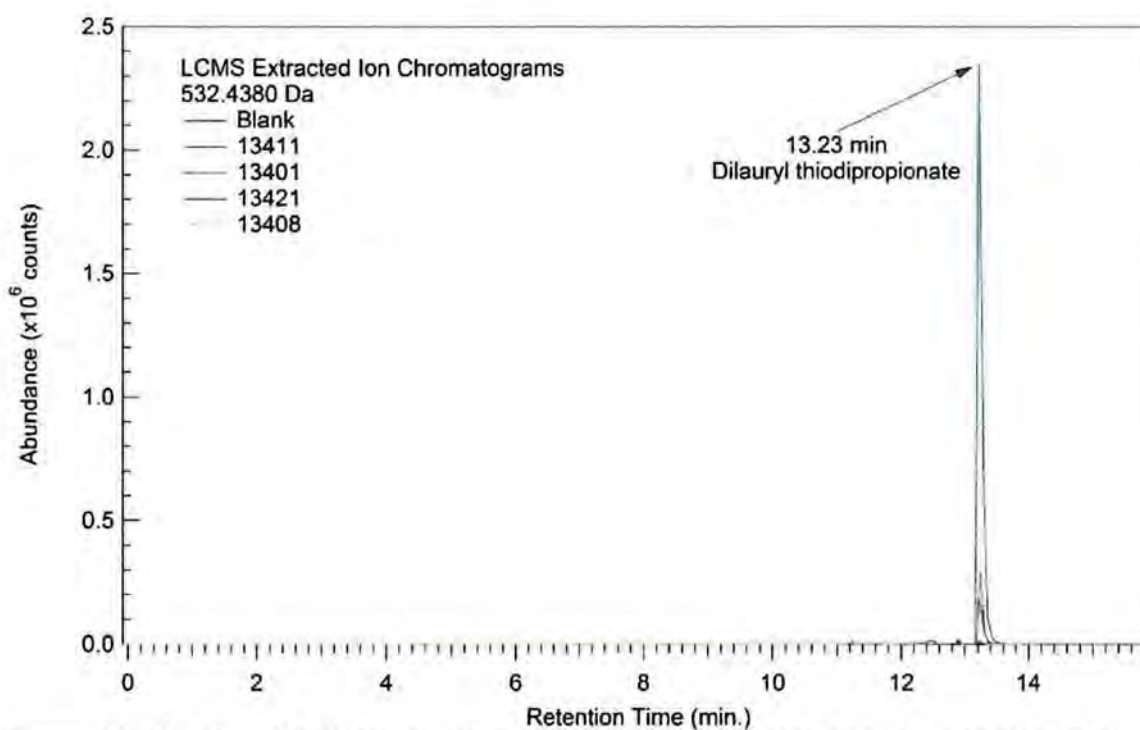


Figure 98 - Overlay of LCMS extracted ion chromatograms, 532.4380 Da, explant extracts showing a relatively low amount of cracking.

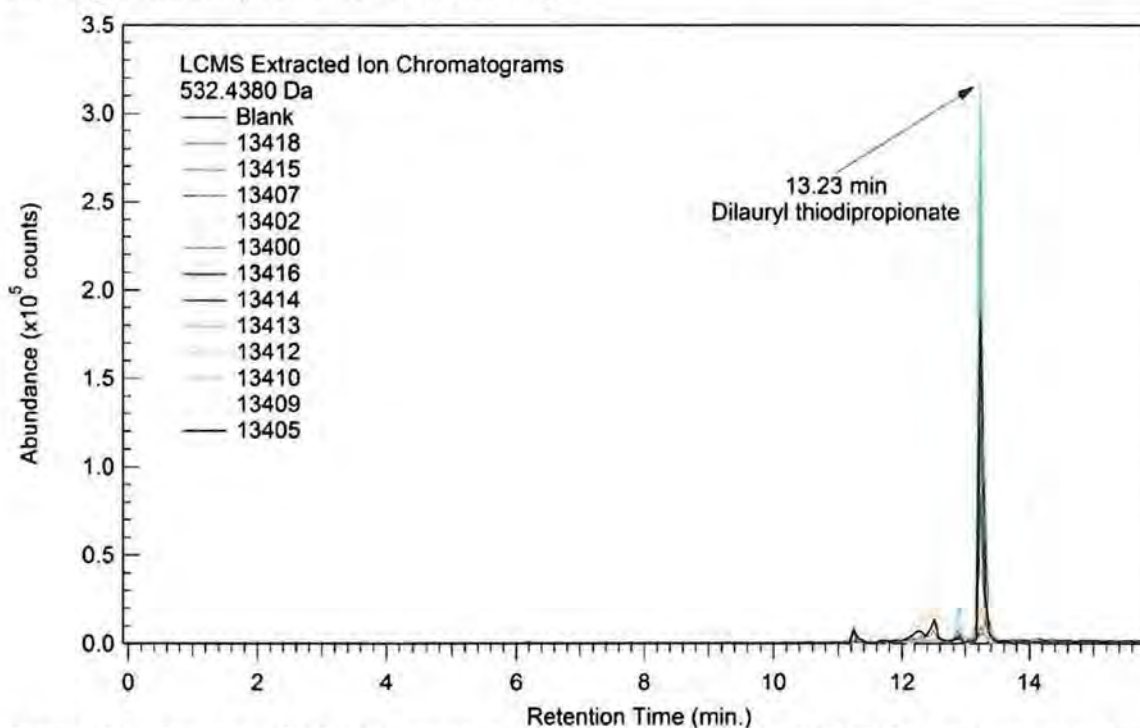


Figure 99 - Overlay of LCMS extracted ion chromatograms, 532.4380 Da, explants samples showing a relatively high amount of cracking.

Table 18	
Relative Quantitation - Dilauryl thiodipropionate	
Sample	Peak Area (532.4380 Da) Dilauryl thiodipropionate
Explant Samples	
13674	611,478
13675	896,468
13400	1,261,148
13401	965,120
13402	91,648
13405	887,017
13407	972,021
13408	88,744
13409	284,304
13410	1,300,680
13411	12,217,785
13412	1,549,404
13413	854,714
13414	437,861
13415	69,239
13416	1,011,756
13418	658,043
13421	1,381,045
Control Samples	
Lot 3398135	92,337,425
Lot 3405405	79,048,701
Lot 3405460	73,376,876
Lot 3405474	87,296,861
Lot 3422128	71,633,460
Lot 3436364	81,867,107
Lot 3422128 (Duplicate 1)	96,522,909
Lot 3422128 (Duplicate 2)	82,091,505
Formalin Treated Control Samples	
Lot 3405405 (Formalin Control)	69,954,022
Lot 3422128 (Formalin Control)	79,568,168

The relative peak intensity of the compound identified as Santonox R was also compared for the extracts analyzed. Resulting peak areas are shown in **Table 19**. Similarly, this was done through investigation of extracted ion chromatograms at 357.1893 Da, Santonox R (M-H)⁻. **Figures 100-104** include overlays of LCMS extracted ion chromatograms collected.

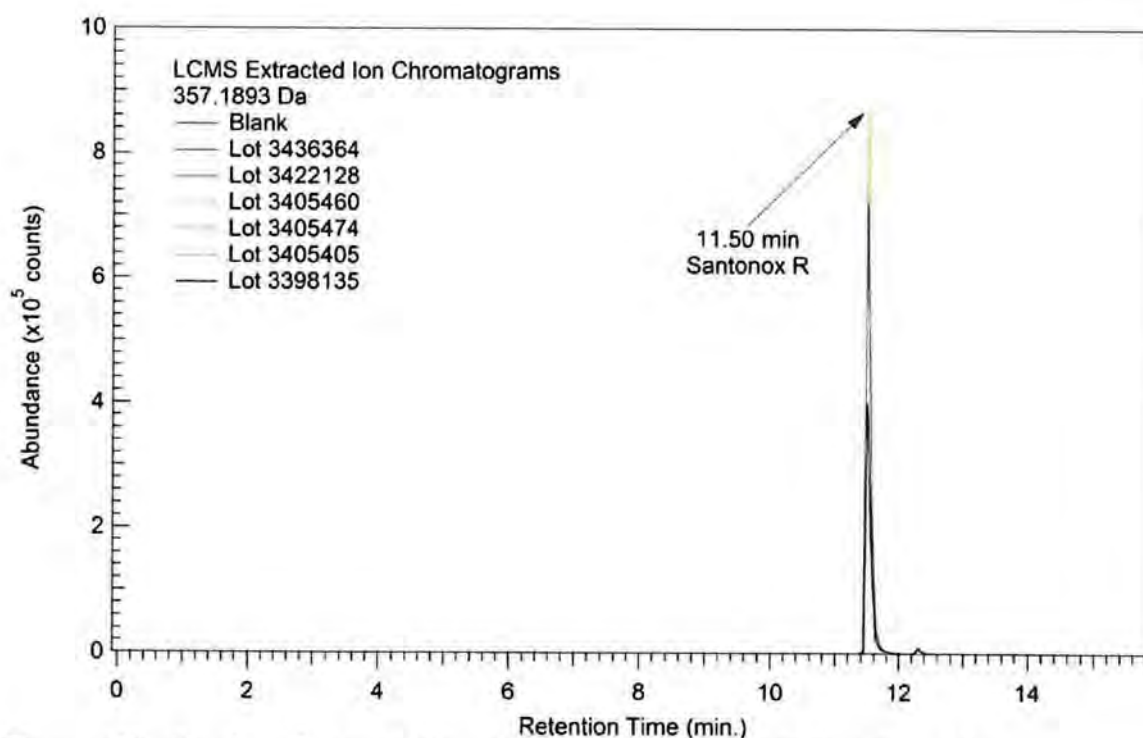


Figure 100 - Overlay of extracted ion chromatograms, 357.1893 Da, Control Extracts.

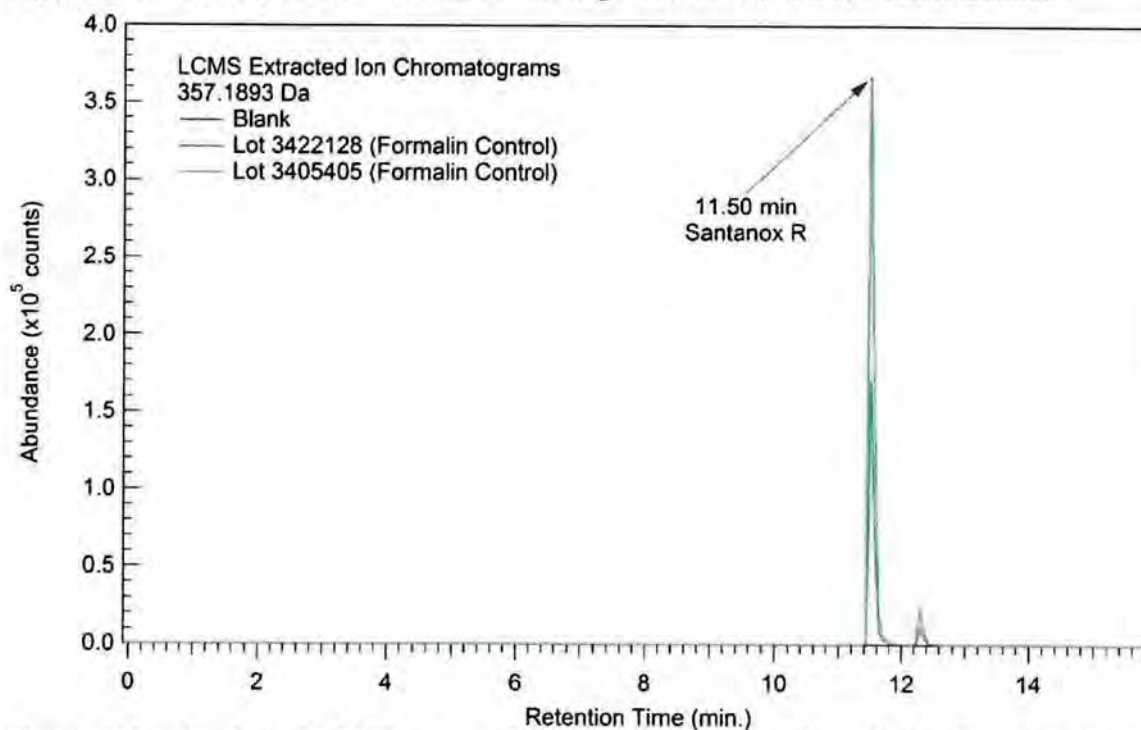


Figure 101 - Overlay of LCMS extracted ion chromatograms, 357.1893 Da, formalin control extracts.

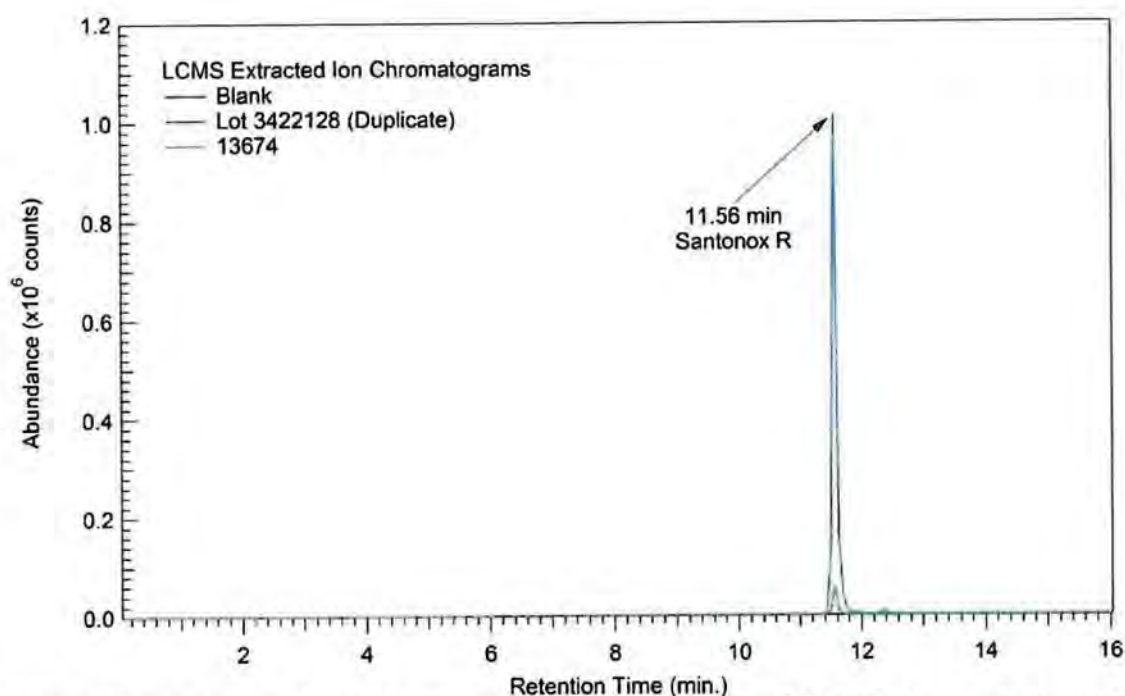


Figure 102 - Overlay of LCMS extracted ion chromatograms, 357.1893 Da, explant sample 13674 and control sample from Lot 3422128.

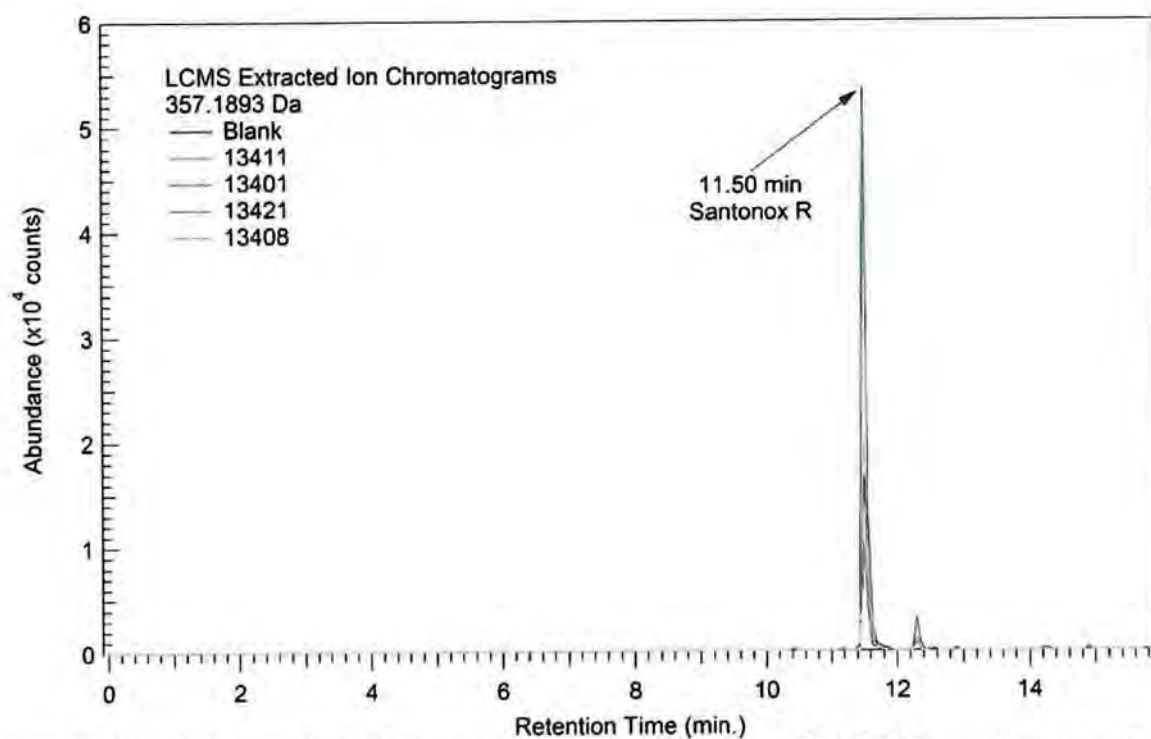


Figure 103 - Overlay of LCMS extracted ion chromatograms, 357.1893 Da, explant extracts showing a relatively low amount of cracking.

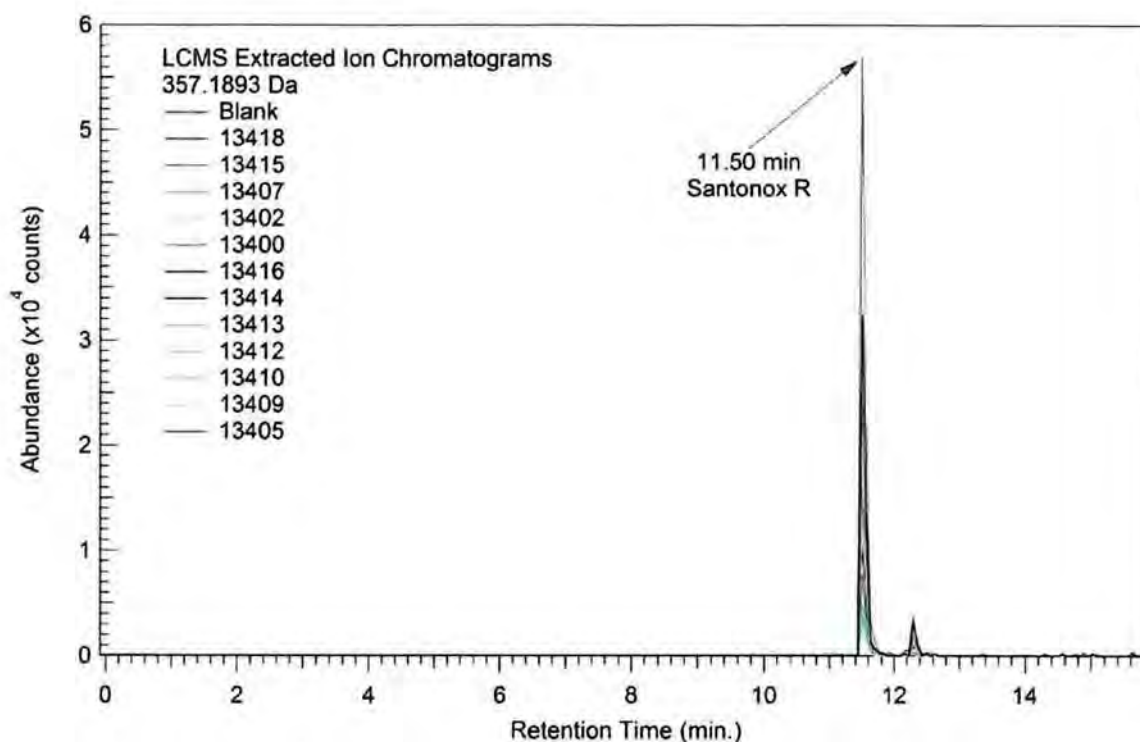


Figure 104 - Overlay of LCMS extracted ion chromatograms, 357.1893 Da, explant samples showing a relatively high amount of cracking.

The limit of detection was determined for each of the antioxidants detected using the prepared standard solutions. Both compounds were detected at a concentration of approximately 10 ng/ml. In both cases, the compound of interest could be correctly identified by the mass spectrum observed at this concentration.

Table 19 Santonox R - Relative Quantitation	
Sample	Peak Area (357.1893 Da) Santonox R
Explant Samples	
13674	315,246
13675	35,155
13400	339,859
13401	68,206
13402	177,039
13405	191,898
13407	89,043
13408	126,646
13409	79,308
13410	143,134
13411	274,743
13412	26,999
13413	140,968
13414	27,266

Table 19	
Santonox R - Relative Quantitation	
Sample	Peak Area (357.1893 Da) Santonox R
13415	43,899
13416	67,013
13418	66,716
13421	98,511
Control Samples	
Lot 3398135	2,324,899
Lot 3405405	4,012,675
Lot 3405460	4,876,273
Lot 3405474	4,343,419
Lot 3422128	4,550,748
Lot 3436364	4,135,490
Lot 3422128 (Duplicate1)	5,418,177
Lot 3422128 (Duplicate2)	4,430,284
Formalin Treated Control Samples	
Lot 3405405 (Formalin Control)	2,216,989
Lot 3422128 (Formalin Control)	1,019,604

Scientific Opinion

Based on my review of the scientific literature, my review of Ethicon's internal documents, my knowledge, training and experience as polymer scientists, and the LCMS data collected, it is my opinion to a reasonable degree of scientific certainty that the explant samples show clear evidence of decreased antioxidant as compared to the control samples. Two antioxidants were detected in the samples. The identity of the compounds was confirmed to be consistent with dilaurylthiodipropionate and Santonox-R based on their exact mass, isotope patterns, isotope spacing and ionization modes.

A large decrease in signal strength was observed in the extracts collected from the explant samples as compared to the extracts collected from the control samples. The average peak area for dilauryl thiodipropionate was 80,926,738 in the control lots and only 1,501,908 in the explant samples (1.8% of the control lot value). The signal for Santonox-R was 4,040,584 in the control lots and only 122,578 in the explant samples (3.0% of the control lot value).

From the comparison of the Formalin Treated Controls and the untreated Controls 3405405 and 3422128, it appears that formalin is able to partially extract Santonox R. It is possible that Santonox R in the explant samples was partially extracted during their storage in 10% formalin solution after explantation from the patients. Nevertheless, the relative quantitative data presented in **Table 19** clearly shows that the levels of Santonox R in the explant samples were significantly lower than that of the formalin treated controls. This indicates that Santonox R was at least in part extracted from the Prolene mesh while in vivo. Based on the data presented in **Table 18**, there is no evidence of extraction of DLTDP in formalin indicating that all of the lost DLTDP was extracted in vivo. The variation in the area counts of DLTDP

and Santonox R in duplicate runs for the controls is within the specification provided by the instrument manufacturer.

As referenced earlier in this report, the purpose of Ethicon adding antioxidants to the Prolene mesh in the TVT products is to prevent degradation, and it is expected that if absent, polymer degradation will result over time.⁹⁹

Therefore, it is my opinion, to a reasonable degree of scientific certainty that based on PYMS and LCMS data, the loss of Ethicon's two antioxidant additives to its Prolene mesh rendered it virtually defenseless to oxidation/degradation.

Analysis Conditions

Optical Microscopy

Optical micrographs were acquired using an Olympus SZ61 UC30 Optical Microscope with Highlight 3100 light source and Stream Basic software by Olympus. Additional images were acquired using a Nikon Stereoscope, Model SMZ010. A range of magnifications were used as indicated on each image.

SEM-EDX

The samples were analyzed in accordance with Standard Operating Procedure (SOP) SOP06 and Work instructions F-1 and F-14. The analysis was performed using a Hitachi S-3400N Scanning Electron Microscope with an Oxford Inca X-act Silicon Drift Detector. The instrument was operated with a beam voltage of 20kV and no sample tilt. Samples were analyzed in variable pressure mode at a chamber pressure of 50-60Pa. All images were acquired using the backscattering detector. A range of magnifications were used as indicated on each image. The samples were mounted on 12 mm diameter Al stubs that was partially covered with carbon tape. In order to avoid any cracking during mounting, the samples were laid down gently onto the C tape without pressing them on. Samples were not coated.

DSC

Samples were analyzed in accordance with method SOP P7.1.1.8 Rev C. Sample analyses were performed using a TA Q2000 Differential Scanning Calorimeter in combination with TA Universal Analysis software. Approximately 1 mg of the sample was weighed into an aluminum T-zero Hermetic pan and sealed. Samples were heated under nitrogen atmosphere from -90°C to 200°C at 10°C/min for the first heating pass, followed by cooling from 200°C to -90°C at 10°C/min and heated again from -90°C to 200°C at 10°C/min for the second heating pass. Specific operating conditions are summarized on the enclosed charts.

⁹⁹ Timothy C Liebert, Richard P. Chartoff, Stanley L. Cosgrove and Roberts S. McCuskey *Journal of Biomedical Materials Research* 10 (1976) 939-951.

FTIR Microscopy

The samples were tested according to method SOP03. Samples were prepared by placing a fiber onto an infrared transmitting substrate and rolling it, using a fresh disposable scalpel to lightly apply pressure to the fiber during the rolling process. The residue thus transferred was analyzed using the FTIR microscope in transmission mode. The analytical spot size was approximately 135 microns x 135 microns. The analysis was performed on a Thermo-Nicolet 6700 FTIR Spectrometer with a Continuum microscope.

A piece of the control fiber itself was also analyzed by FTIR microscopy, after thinning sufficiently to transmit IR light. Optical photographs were acquired on the FTIR microscope at a magnification of 150x.

GPC-HT

Samples were analyzing according to method SOP P7.1.1.48 Rev B and monitored using a HT-GPC Module 350A detector array by VISCOTEK. Data acquisition and handling were made with VISCOTEK software.

Data were obtained under the following conditions:

<i>SOLVENT</i>	Trichlorobenzene (TCB)/0.5 mg/mL BHT
<i>FLOW RATE</i>	1.0 mL/min
<i>INJECTION VOLUME</i>	200 µL
<i>COLUMN TEMP.</i>	140°C
<i>DISSOLUTION TEMP.</i>	120°C
<i>DISSOLUTION TIME</i>	100 Minutes
<i>CONCENTRATION</i>	~2.5 mg/mL
<i>COLUMN</i>	Two Agilent PLGel Mixed-B LS 300 x 7.5mm
<i>RUN TIME</i>	60 Minutes
<i>INTEGRATION METHOD</i>	Known dn/dc

PYMS Additives Mode

Samples were analyzed in accordance with Method SOP P7.1.1.16 Rev C. Solid samples were analyzed using a Hewlet 6890 gas chromatograph in conjunction with a 5975B mass selective detector using a Frontier Laboratories double shot Pyrolyzer model PY2020ID. Data acquisition was accomplished using chemstation software. Sample peaks were compared with over 796,613 reference compounds using the NIST/EPA/NIH mass spectral search program.

The following run conditions were applied for Gas Chromatographic analysis:

Sample Size = ~1mg

Initial Delay = 2.0 minutes
Initial Temperature: 50°C
Final Temperature: 350°C
Temperature Ramp Rate 1: 20°C per minute
Hold Time: 15 minutes
Pyrolysis Temperature: 1st pass = 100-425°C
Detector Temperature: 315°C
Injector Split = 30:1
Mass Range: Low Mass = 30 High Mass = 700
Column = Ultra Alloy –PBDE

PYMS

Solid samples were analyzed using an Agilent 6890 gas chromatograph in conjunction with a 5975B mass selective detector using a Frontier Laboratories double shot Pyrolyzer model PY2020ID. Data acquisition was accomplished using chemstation software. Sample peaks were compared with over 796,613 reference compounds using the NIST/EPA/NIH mass spectral search program.

The following run conditions were applied for Gas Chromatographic analysis:

Sample Size = ~1.1 to 1.2 mg
Initial Delay = 2.0 minutes
Initial Temperature: 100°C
Final Temperature: 350°C
Temperature Ramp Rate 1: 20°C per minute
Hold Time: 15 minutes
Pyrolysis Temperature: 1st pass = 100-425
Detector Temperature: 315°C
Injector Split = 30:1
Mass Range: Low Mass = 30 High Mass = 700
Column = Ultra Alloy –PBDE

LCMS

QTOF-LCMS was performed in accordance with Method SOP P7.1.1.64 Rev A. The following conditions were used for the qualitative QTOF-LCMS analysis:

Instrument: Agilent 6520 QTOF LCMS with Agilent 1200 HPLC system
Source: Dual ESI Source
Flow Rate: 0.4 ml/min
Temperature: 40°C
Column: Agilent Zorbax Eclipse Plus C-8, 3.5µm, 2.1 x 100mm

Gradient Conditions

Solvent A: 0.05% aqueous formic acid / 0.03% ammonium hydroxide / 5% methanol

Solvent B: Methanol/IPA 80/20

Run time = 16 minutes

Post Time = 6.5 minutes

Time (min)	% composition Solvent A	% Composition Solvent B
0	100	0
10	0	100
16	0	100

Detector Settings:

Gas Temp: 325°C

Drying Gas: 8 L/min

Nebulizer: 40 psi

VCap: 3500

Fragmentor Voltage: 150

Skimmer: 65

OCT 1 RF VPP: 750

Ionization Mode: ESI

Ion Polarity: positive & negative, separately

Mass Range: 80-3000 scan mode; 50-3000 MSMS mode

VIII. Alternative Design

Our review of Ethicon's internal documents as well as the scientific literature provides additional support for my opinions and findings herein. A study carried out by Ethicon in 1982 (sixteen years before TVT was marketed) of explanted Prolene sutures sizes 4-0, 5-0 and 10-0 showed that Prolene degrades with crack depth up to 4.5 microns.¹⁰⁰ Ethicon scientists also found degradation of Prolene explants in a 1987 study and concluded that "The material scraped from the 8 year sample showed IR bands indicative of oxidation. The same material exhibited a melting range of 147-156 °C which had been earlier assigned to oxidatively degraded polypropylene."¹⁰¹ In 1992, Ethicon scientists reported the data from their 7 year dog study concluding that "degradation in PROLENE is still increasing and PVDF, even though a few cracks were found, is still by far the most surface resistant in-house made suture in terms of cracking." A study published in 1998, the same year Ethicon began marketing TVT, also found that PVDF was more inert than Prolene in the long term.¹⁰² Other studies have consistently found that polypropylene can degrade¹⁰³ and

¹⁰⁰ ETH.MESH.12831405¹⁰¹ ETH.MESH.12831408¹⁰² ETH.MESH.05845592

Ethicon's scientist, Dieter Engel, wrote an email to his colleagues in 2007 titled "How inert is polypropylene" explaining that Ethicon would change the material of its mesh to Pronova, a PVDF co-polymer:

What is the future? We will change the material of my mesh and move to Pronova as the future material platform for mesh, starting with NG TSM. Pronova has a reduced foreign body reaction compared to Prolene, as shown in several animal studies, and will improve the perceived biocompatibility of my mesh. Besides, Pronova is much less susceptible to mechanical damage (as it is less stretched and a different chemical composition); it is much easier to process in the knitting machines, less quality issues.¹⁰⁴

Thus, Ethicon's own internal studies as well the scientific literature, provide additional support for my opinion that Prolene degrades *in vivo* and that Ethicon had an alternative polymer which was more inert than Prolene in the long term. Nevertheless, even though Ethicon had a safer alternative design, in terms of degradation, Ethicon continued to use Prolene which degrades while implanted in the body.

IX. Conclusion

In conclusion, based on my review of the scientific literature, my review of the Ethicon internal documents, including their own degradation studies, my knowledge, training and experience, and the review of the data discussed herein, it is my opinion to a reasonable degree of scientific certainty that the polypropylene Prolene mesh used in the TVT products degrades when implanted in the human body. The SEM and FTIR-microscopy data clearly show that the surface is cracked and that the cracked surface is mostly polypropylene. Polypropylene undergoes degradation by oxidation, enzyme attack, environmental stress cracking or a combination of these factors. The decrease in the levels of antioxidants as seen from LCMS and PYMS data, the carbonyl and C-O-C bands in FTIR microscopy and increased oxygen levels in the SEM-EDX are supportive of the contention that the mesh undergoes *in vivo* oxidation. Decreases in crystallinity as seen from the DSC data and the presence of cholesterol and fatty acids observed in PYMS data are consistent with Environmental Stress Cracking. Since evidence of oxidation and environmental stress cracking is seen in most samples, it is concluded that both these factors may be at play for degrading the polypropylene mesh. The various lines of evidence pointing in this direction would include, but not be limited to:

¹⁰³ See e.g., A.J. Wood et al., "Materials characterization and histological analysis of explanted polypropylene, PTFE, and PET hernia meshes from an individual patient" *J. Mater Sci: Mater Med* (2013) 24:1113-1122; Arnaud Clave, et al., "Polypropylene as a reinforcement in pelvic surgery is not inert: comparative analysis of 100 explants" *International Urogynecology Journal and Pelvic Floor Dysfunction* 21 (2010) 261-270.; C.R. Costello, et al., "Characterization of Heavyweight and Lightweight Polypropylene Prosthetic Mesh Explants From a Single Patient" *Surgical Innovation* 14 (2007) 168-176; C. R. Costello, "Materials characterization of explanted polypropylene hernia meshes" *Journal of Biomedical Materials Research Part B: Applied Biomaterials* 83B (2007) 44-49.

¹⁰⁴ ETH.MESH.05588123

1. SEM images: 92% (22/24) of the SEM images of explanted Prolene mesh of the TVT products showed signs of degradation. The Ethicon Dog Study dated October 15, 1992 also revealed similar degradation of explanted suture materials.
2. SEM-EDX: SEM-EDX chemical analysis results on all the tested polypropylene explant samples revealed the presence of excess oxygen in the outer cracked and peeling particulates relative to the control sample which is consistent with oxidation.
3. FTIR: FTIR results revealed the presence of carbonyl bands which is also consistent with oxidation. Further, it was shown that these particulates are polypropylene.
4. PYMS, LCMS: Mass spectroscopy revealed significant reductions in the relative concentration of the antioxidants leaving the surface of the polypropylene mesh samples vulnerable to oxidation.
5. Thermal analysis: DSC of the tested explant samples revealed that the crystallinity went down implying an increase in the amount of amorphous material which would be more susceptible to environmental stress cracking.
6. Cumulative literature reports on polypropylene degradation: Many studies of polypropylene characterization explanted from living organisms conducted by independent researchers over a period from 1965 to the present over and over again stress that polypropylene is not inert and that it degrades.

Moreover, based on my review of the scientific literature, my review of Ethicon's internal documents, my knowledge, training and experience as polymer scientists, and the review of the data discussed herein, it is my opinion to a reasonable degree of scientific certainty that Ethicon had available to it an alternative polymer PVDF or Pronova which was more resistant to degradation and would have been a reasonable alternative design that would have reduced the level of degradation.

X. EXHIBITS

All exhibits that will be used to support my findings and opinions are included above and listed below in Exhibits "A - I".

Exhibit "A" contains a true and accurate description of my curriculum vitae
Exhibit "B" contains a grid of identifying information regarding explanted materials
Exhibit "C" contains SEM and OM Data
Exhibit "D" contains SEM-EDX Data
Exhibit "E" contains DSC testing Data
Exhibit "F" contains FTIR Microscopy Data
Exhibit "G" contains GPCHT Data
Exhibit "H" contains PYMS Data
Exhibit "I" contains LCMS Data

XI. RECENT TESTIMONY (HOWARD JORDI, PhD)

Deposition/trial testimony:

Diversified Biotech, Inc. vs. GA International, CA Provided service work, consultation, pre-trial preparation and appeared in court in April 2007. To the best of my recollection, we believe that the case was settled on that day. This contention is supported by White and Fudala LC.

Howmedica Osteonics Corp. vs. Zimmer, Inc., Centerpulse Orthopedics, Inc., Smith&Nephew, Inc. Deposed (2006). Case settled, never went to trial based on my records.

Unisource Worldwide, Inc. v. Stone Plastics, Inc., Global Manufacturing Packaging Solutions, LLC Deposed 2008, Testified 2008

Gary Lamoureux, World Wide Medical Technologies, LLC, Advanced Care Pharmacy, Inc., Advanced Care Pharmacy, LLC and Advanced Care Medical, Inc. vs. AnazaoHealth Corporation, F/K/A GENESIS PHARMACY SVC., INC., D/B/A CUSTOM CARE PHARMACY Deposed 2008

United States v Dennis Beetham and DB Western Inc., Testified June 2010

Hoffman Angelie

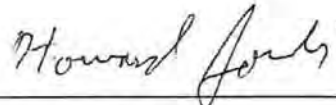
Carolyn Lewis v Ethicon, Testified by Deposition in Oct 2013 and Jan 2014 and Testified at Trial in Feb 2014

Linda Batiste v Ethicon, Testified at Trial in March 2014

XII. COMPENSATION

We are compensated for investigation, study and consultation in the case at the rate of \$350.00 per hour.

This 20th day of May, 2014

A handwritten signature in cursive script, appearing to read "Howard Jordi", is written above a horizontal line.

Howard Jordi, Ph.D.